The University Of Sheffield.

Augmenting Elderly Mobility with Lower Limb Assistive Exoskeleton

Thesis submitted to the University of Sheffield for the degree of
Doctor of Philosophy

by

Ghasaq Saeed Al Rezage

Department of Automatic Control and Systems Engineering
The University of Sheffield
Mappin Street,
Sheffield, S1 3JD
United Kingdom

October 2017

Abstract

Mobility is considered as one of the most essential acts of human being to stay independent and have good quality of life. Therefore, people who are faced with mobility impairment because of muscle weakness, illness, or injury, suffer from many health problems or become bedridden.

Recently, exoskeletons have emerged as a promising solution to augment the elderly people's lost physical strength though performing essential mobility functions. According to the technology advancement, the hardware size of most exoskeletons has reduced in order to keep the system portable with suitable sensors, actuators, and power supplies, and use of light and resistant material.

The current main challenge with robotic technology, is developing a device that has most of the required characteristics such as being safe, power sufficient, seamless, and affordable. Despite availability of many commercial devices for purchasing or renting, all these requirements are not adhered to and the cost is not affordable for all the people. The high costs are due to the advance of hardware, software, and costly material used in designing the prototypes. Developing sufficient controllers that are integrated with the user without adding weight or increasing energy consumption is one of the proposed solutions. Furthermore, software platform used plays significant role in evaluating the design and control techniques, and can save the cost and resources before building the prototype.

This research is focusing on development of modelling and design of control strategies for a multipurpose lower limb exoskeleton to assist the elderly people to move independently in the environment. The main aim of this research is aiding people who have physical weakness in their lower limbs.

A humanoid and exoskeleton models are developed within Visual Nastran 4D and Sim-

Wise virtual environments, to validate the controllers proposed in this research.

Various control methodologies are investigated in this research to drive the simulated humanoid and exoskeleton lower limb models. These include Proportional Integral Drivative (PID), PD fuzzy logic control (FLC) and fuzzy tuning PID. Moreover , two optimization algorithms , namely spiral dynamics and invasive weeds are used to improve the performance of the proposed controllers and an overall comparative performance assessment of the proposed strategies is carried out and relevant recommendations are given.

Acknowledgement

All praises be for Allah s.w.t, the beneficent, the merciful and the lord of the whole universe along with His mercy that have been awarded to the author.

I would like to express my appreciation and ultimate gratitude to my supervisor Dr. Osman Tokhi for his precious support, encouragement, motivation and many helpful advices and guidance through my research work during my PhD study period and doing research in his group in the University of Sheffield. With his enthusiastic supervision, logical thinking, comments, his idea and knowledge made my whole PhD journey clear, positive and enjoyable.

I am very thankful to all my research colleagues and staff in the department of Automatic Control and System Engineering for their help, advice and assistance, especially Normaniha Ghani, Siti Khadijah Ali, Daniela Miranda Linares, Norafizah Abas, Omar, Hyreil A Kasdirin, Nafri, Abdullah binomair, Ahmad Firdus, Abdullah Shati, Bukhari and all the people from 307.

Special thanks to my dearest husband, Asaad Alabdullah, for being my friend, and an amazing father. Without his moral support, sacrifice and understanding it would not have been possible to me to complete this project, to my dearest daughter Shams Alabdullah and my lovely son Ehab Alabdullah.

My love and most sincere gratitude to my beloved family members Father, Saeed Al Rezage, mother Hayfaa Aziz Aldoghachi , brothers : Mohammed and Haider, and sisters: Nabaa, Douaa and Zainab, thank you for your thoughtful prayer and your countless love, support, understanding and encouragement to chase my dreams.

Financial support provided by Higher Committee of Education Development Iraq (HCED). Thanks to the Higher Committee of Education Development Iraq (HCED) for sponsoring

my study as well as or supporting my family financially to join me during my study.

Contents

List of Figures

List of Tables

Acronyms

HCED Higher Committee of Education Development Iraq

LCL lateral collateral ligament

MCL medial collateral ligament

PCL posterior cruciate ligament

ACL anterior cruciate ligament

IPD Idiopathic Parkinson's Disease

CNS Central Nerve System

DM diabetes mellitus

PN peripheral neuropathy

OA Osteoarthritis

FCHP Fallon Community Health Plan

vN4D visual Nastran 4D

SDOA Spiral Dynamic Optimisation Algorithm

IWOA Invasive Weed Optimisation Algorithm

PID Proportional Integral Drivative

FLC fuzzy logic control

CAD computer aided design

DOF degrees of freedom

SCI spinal cord injury

FDA Food and Drug Administration

EMG electromyographic

SDA Spiral Dynamic Algorthim

IWA Invasive Weed Algorthim

Chapter 1

Introduction

1.1 Motivation

The world faces up to the challenge of the ageing population. The birth rate according to some statistics has rapidly decreased in all regions. Therefore, there are more elderly people than before due to decline in the number of young people to care for the elderly. Thus, much research is needed to address this problem from a technological perspective. The United Nations stated that the proportion of old people above 60 was 9.2% in 1990 , in 2013 has grown to an 11.7 percent and is expected to grow further to 21.1 percent by 2050. The absolute number of the elderly people is expected to be more than two billion by 2050, that is it will be doubled in the next three decades. The older population aged 80 years and above was 14 percent in 2013, and this is estimated to grow to 19 percent in 2050, that is there will be three times the number of people aged 80 years and over worldwide (Nations, 2013). Nearly, about two thirds of the world's elderly people live in the developing countries. By 2050, nearly eight in ten of the world's older population will live in the less developed regions.

Mobility is the human ability to move in the environment. It is one of the most common feature of human ability. Age can cause significant changes in mobility for elderly. It is estimated that around one third the elderly have mobility limitations. This means that globally about 219 million people above 65 years of age have some sort of mobility issue. Walking efficiency will decrease because of the loss of muscle strength due to reduced motor neuron, muscle fiber and aerobic capacity (Prince et al., 1997). It is estimated that

one third of the 65 years old and more tend to fall at least once a year (Moylan and Binder, 2007). This number grows even to one half for the 85 years old and more. As the situation is becoming more serious, new solutions are required to reduce this risk. Many types of assistive technology have been commonly used to help the elderly such as the classic crutches, wheelchair, walkers, standing frame and scooter but these are of limited benefit. The assistive technology is unable to solve the problem of ageing population; however, the elderly need to stay active and independent as long as possible. The elderly people need to be able to perform their daily living functions such as bathing, dressing, transferring, feeding, etc. For all these tasks having a decent mobility is crucial for both physical and psychological well-being.

A key development in addressing the problem of mobility could be the exoskeleton system. Recently, exoskeletons have constituted an important addition to assistive mobility technology. An exoskeleton is a wearable robotic system to support the motion of the user. It is a person-oriented robot worn to support the function of the limb or to substitute the missing limb (Pons, 2008). It is considered to integrate benefits of a range of common devices in one device.

1.2 The lower limb anatomy

The body is supported by the lower limbs; their main function is to carry the body's weight while expending minimum energy. The lower limb is divided into four parts, namely: the gluteal region, thigh, leg and foot. This is linked to the lower part of the trunk. The essential lower limb joints are, the ankle, knee and hip.

1.2.1 Hip Joint

The hip joint represents one of the significantly important powered joints in the human body. It enables one to carry out activities such as walking, jumping and running. It carries most of the human weight as well as the power of strong muscles of the hip and leg. It is very flexible and allows a significant range of motion than other parts of human

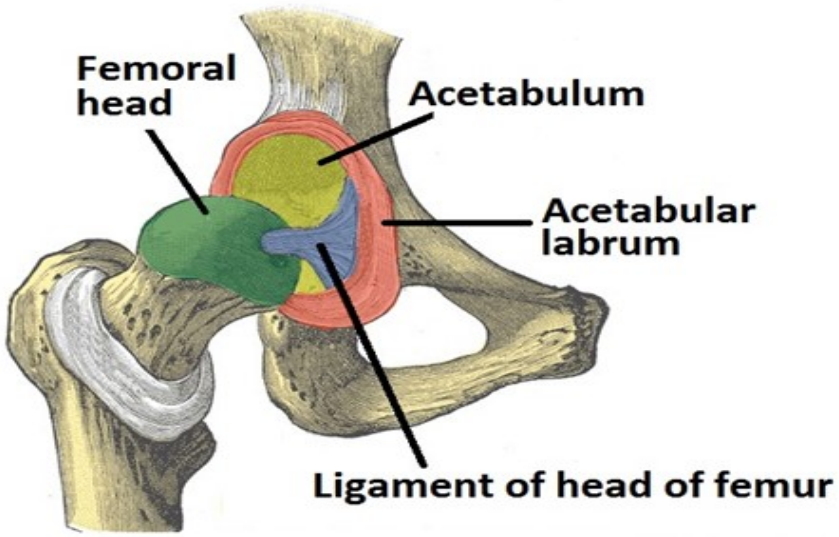

Figure 1.1: The anatomy of the hip joint
(Oliver Jones , 2014)

body except shoulder (Byrne et al., 2010). The structure of hip joint is a ball and socket, which is constrained between the head of femur and the acetabulum of the pelvic bone. The hip joint is multi axial, and thus can rotate in different planes allowing three degrees of freedom (3DOF). The significant function for hip is to provide stability and weight bearing in the gait cycle as shown in Figure 1.1. The movements of hip joint are: flexion-extension, adduction-abduction, medial and lateral rotation (Drake, 2009; Pons, 2008). It is surrounded by many robust ligaments that hinder the dislocation of the joint. The strong muscles also play a crucial role in holding the hip joint together and prevent slipping off. In the flexion motion the thigh moves forward and upward. The anterior part of the body includes most of the muscle that contribute to flexion rotation. These are: the iliopsoas, tensor fasciae latte, rectus remorse, pectins, and Sartorius and adductor muscles. The extension movement includes the following muscles: semitendinosus, gluteus Maximus, biceps femoris, semimembranosus, and adductor Magnus.

1.2.2 Knee Joint

The knee joint can be considered as the largest and strongest synovial joint in human extremity. Its major function is to allow the lower leg to move while supporting the body (weight bearing). It represents a synovial hinge located between the bones; the femur,

tibia and patella. It is blocked by strong muscle and ligament in order to protect it from any movement that may damage the knee joint . There are four essential ligations that play a major part in knee stability. These are: the lateral collateral ligament (LCL), the medial collateral ligament (MCL), and the posterior cruciate ligament (PCL), the anterior cruciate ligament (ACL), Figure 1.2 shows the anatomy of the knee joint. The ligaments connect the tibia to the femur crossing the knee joint. The main function of the MCL is to hinder the forces refereed to the lateral direction of the knee from changing the knee in an ordinary position. Likewise,LCL prevents forces applied to the medium side of the knee from moving the knee sideways. The cruciate cords play a vital part in preventing the extra extension or flexion movement of the knee and they are crucial for knee stability (Drake, 2009; Pons, 2008) . Functionally, the knee plays a massive role in walking and standing. As the knee is a hinge joint, its major task is permitting the extension and flexion of the leg relative to the thigh.

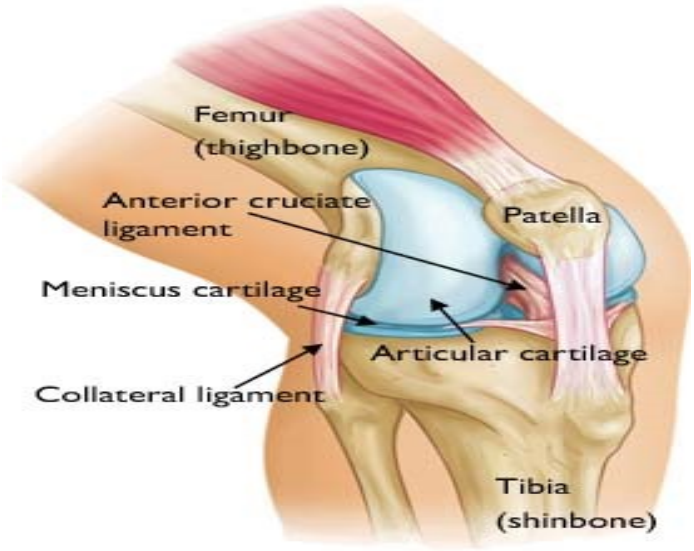

Figure 1.2: The anatomy of the knee joint
(American Academy of Orthopaedic Surgeons, 2014)

1.3 Elderly muscle weakness

Multiple diseases are responsible for disorders of balance and gait in elderly people; the aging process is related to loss of muscle mass and strength. The muscle mass reduction

has a direct effect on decreasing strength and power of the muscle, as well as the mobile functionality loss in the elderly. For elderly people over 90 years old, their muscle strength diminish by 50 percent and nearly around 20 and 40 percent for people between 70 and 80 years old (Garcia et al., 2011).

Schultz1995 reports that the decline in muscle strength is one third between ages 25 and 65. In addition, the isokinetic tests done for muscle strength and hip and knee power prove that the capacities of peak torque were around 35 per cent higher in a 65 to 69 years old group as compare to 80 years or over group (Garcia et al., 2011). Moreover, around one fourth of people between 70 to74 years old, and two thirds of 80 to 84 years old have gait disorder. Various symptoms identify the mobility impairments. These include imbalance, dyspnea, diminished strength, poor posture and limited range of motion (Salzman, 2010). Some scientists propose that maximum torque is not fully associated with motion impairments, since the torque needed to perform most mobility tasks is lower than existing torque. In contrast, the decrease in ability to develop joint torques rapidly is connected to age decline, for instance younger adults need 161 milliseconds less than older adults to produce 60 Nm of plantar flexor torque (Schultz, 1995).

1.4 Walking impairments in elderly

Theoretically and in the absence of disease, the gait patterns of elderly people are very similar to younger subjects when walking at the same speed. It has been reported that considering healthy and active seniors only, there is no significant difference with young people in terms of main gait parameters such as: cadence, stride length, and double support time (Blanke and Hageman, 1989; Chen and Sung, 2011; Hageman and Blanke, 1986; Jansen et al., 1982).The majority of elderly people have long reaction time,thus they have to consume higher energy during walking. The sway while standing increases with advancing age, therefore their attentional resources are required to recover (Brown et al., 1999; Sudarsky, 1990). It is thus evident that all these factors have direct impact on the elderly walking and the risk of fall. Furthermore, most elderly have to experience notable

difference in gait parameters. It is difficult to consider the elderly people as extremely heterogeneous, and many factors exist that cause the gait disorder.

1.4.1 Pathologies affecting gait

Various disease may directly affect the elderly walking ability. Weak muscles may result in due to different Pathologies. The cardiovascular diseases such as (Arrhythmias, Congestive heart failure, Coronary artery ,Orthostatic hypotension, Peripheral arterial, and Thromboembolic disease) have significant impact on the person effort and on the gait (Salzman, 2010). In addition, more than thousand muscles during walking are moved synchronously and over 200 bones rotate around hundred joints (Prince et al., 1997). The pathologies affecting the nerves and musculoskeletal system vitally have the most consequence on locomotion (Salzman, 2010). However, it is difficult to find precise data of different diseases and their relationship with gait impairment. Often more than one factor causes the gait disorder. Neurological and musculoskeletal diseases are the main causes of immobility.

1.4.1.1 Neurological pathologies

Stroke is one of the neurological diseases affecting the elderly, and the most common cause of gait disorder (Donnan et al., 2008) . This pathology is clinically known as Cerebrovascular accident (CVA). Stroke is a damage of brain action due to poor blood flow in the brain. The brain cells begin to destruct due to lack of blood to supply oxygen and nutrients (Sims and Muyderman, 2010). In fact the area of brain where cells are dead are no longer functioning properly. The affected person usually has one or more paralysed limbs on one side of the body. The rehabilitation process is an effective solution to roster the gait function to walk independently (Bortole, 2013).

Idiopathic Parkinson's Disease (IPD) is the second disease affecting the elderly that more frequently causes movement disorder. Stolze et al. (2005) have reported that about 93 % of people who are diagnosed with IPD experience gait impairment. IPD is a neurodegenerative disease affecting the central nerve system (CNS), and thus influencing the person's

movement. About 80% of the cases with IPD have shown slowness of gait sequence performance , which is the most common symptoms known as bradykinesia Morris (2000). Hypokinesia is a serious case of IPD when the movements are extremely restrained. People suffering from hypokinesia typically walk with short steps, diminished trunk rotation, and limited arm swing.

The most popular disease in elderly is a **myelopathy**. This pathology is a deficit affecting the spinal cord. People suffering from myelopathy have gait characterized as clumsy movement in their legs. Malone et al.(2012) have reported that the kinematic analysis of gait of people with myelopathy exhibits notable differences at the pelvis, hip , knee and ankle in terms of motion range. The kinetic parameters also show significant decrease. Some diversities are related to the slow pace but the differences at the knee and ankle remain the same even if matched with the walking speed.

The diabetes mellitus (DM) and **peripheral neuropathy (PN)** are causes of gait disorder. The DM constitutes a group of metabolic diseases and not directly a neurological disease (Richardson et al., 2004). However, DM may have an indirect effect on the Central Nerve System (CNS). The hyperglycaemia results from the impairment of insulin secretion, insulin action or both (Association et al., 2012). Massively PN is caused by DM even though other disease may be the cause, for example vitamin defection and drinking alcohol extensively. Chenamgere et al.(2015) reported that the falling rate in DM subjects with PN are 15 times than DM subjects without PN. Therefore PN can be considered as a serious cause of impairment for DM patients.

1.4.1.2 Musculoskeletal pathologies

The **Osteoarthritis (OA)** is a joint degenerative disease which involves the cartilage and tissue surrounding it (Litwic et al., 2013). The hip and knee joints are considered the most important articulations, due to the body weight bearing relying on them. The feet can also be subject to OA. Osteoarthritis can occur in any joint of the body, but most often it affects the knees, hips, hands and feet. According to Fallon Community Health Plan (FCHP) in Massachusetts (USA) the incidence rate was highest for knee, medium rate for hand and

least observed rate for hip but remain high as 17% of the population was affected. Many symptoms are associated with this disease such as: joint pain, stiffness and movement limitation. Litwic et al.(2013) have reported that about 50 % of people aged 75 and above suffer from OA. Zeni and Higginson(2009) contended that the walking speed is linked to the severity of the disease.The walking speed and the torque are decreased in sagittal plane at knee and ankle joins while the hip follows the inverse trend.

Sarcopenia is a very common condition affecting people. Baumgartner et al.(1998) have reported that approximately 30% of individuals over 60 and more than 50% of individuals over 80 suffer from sarcopenia. Sarcopenia is defined as a low relative muscle mass and is associated with metabolic, and functional changes in the elderly. Multiple factors cause loss of muscle strength, and some of the changes are part of biological system such as nerves and hormonal systems, where as other linked to Lifestyle pattern (Vandervoort, 2002). Tripping is a major cause of falls, especially in the elderly

1.4.2 Risk of falling

Falls during walking lead to cause a major health problem particularly in the ageing population. Many researchers have reported factors that lead to falls in the elderly (Ambrose et al., 2013). There are many important risk factors that lead to falls such as low muscle strength, decrease in vision , affected vestibular function , and gait and balance problems (Lord et al., 2007). It is estimated that 30% of the population aged 65 will fall once annually, and 50% of people over 80 (Ambrose et al., 2013). Twenty to thirty percent of patients who fall suffer from moderate to serious injuries such as broken bones,or head injury.Fall is the fifth cause leading to death in adult over 65(Ambrose et al., 2013; Moylan and Binder, 2007). Most of falls occur during walking and it is the main threat for the elderly when they are walking (Ambrose et al., 2013). Therefore, two main reasons may lead to falls. The first one is trip and the second is slip both occurring inside or outside the home (Lilley et al., 1995). Tripping plays a major role in falls, especially in the elderly (Pijnappels et al., 2005) . Pijnappels et al.(2005) have reported that the elderly people who could not regain from tripping have low ability and rapid decrease in torque at the lower

limb joints and lower peak ankle. Slipping is related to gait hazard. It has been reported that old people require more time than others to initiate slip response (Lord et al., 2007). Moreover their weak muscle strength does not enable them to provide high torque as young people do.

1.5 Research Objectives

This research aims to design and develop a lower limb exoskeleton as an assistive robotic device, which can help the elderly in their walking to be independent and to do their daily life activity. In order to achieve this goal successfully, the following research objectives are realised:

- Design humanoid model to mimic physical characteristics of a human using suitable software platform.
- Design an exoskeleton frame which can be attached to the humanoid body to enhance the lower limb during the walking cycle.
- Develop a PID controller to control the humanoid with exoskeleton to follow the predefined trajectory.
- Investigate development of fuzzy logic based control approaches to control the humanoid during walking cycle to follow predefined trajectory and further to control the humanoid with exoskeleton.
- Carry out a comparative assessment of different types of controller for the exoskeleton in assisting the humanoid during the walking cycle, and select the most suitable one for further investigation.
- Investigate adaptation techniques to further develop the control approach and test with the humanoid and the exoskeleton.
- Extend the exoskeleton system with a walking mechanism for sitting down- standing up regimes.

1.6 Publications and contributions of the thesis

Publications from this research are either accepted or in print are as listed below. There are also further publications being prepared for submission , and not listed here.

- **Al Rezage G.**, Alshatti A and Tokhi MO. PD-fuzzy control of lower limb exoskeleton for elderly mobility. Proceedings of 19 International Conference on Climbing and Walking Robots(CLAWAR 2016), London, Uk, 12-14 Sep. (pp. 823-831).

- Alshatti, A., Tokhi, M. and **Al Rezage G.**. Design and control of single leg exoskeleton for hemiplegia mobility. Proceedings of 19 International Conference on Climbing and Walking Robots (CLAWAR 2016), London, Uk, 12-14 Sep. (pp. 832-839).

- **Al Rezage G**, Kasdirin HA, Ali SK and Tokhi MO. Invasive weed optimization algorithm optimized fuzzy logic scaling parameters in controlling a lower limb exoskeleton. Proceeding of Methods and Models in Automation and Robotics, MMAR :21st International Conference on 2016 Aug 29 (pp. 1116-1121). IEEE.

- Ali SK, Firdaus AR, Tokhi MO and **Al Rezage, G**. Tracking human upper-limb movements with sliding mode control type-II fuzzy logic. Proceeding of Methods and Models in Automation and Robotics, MMAR :21st International Conference on 2016 Aug 29 (pp. 426-431). IEEE.

- **Al Rezage G.** and Tokhi MO. Fuzzy PID control of lower limb exoskeleton for elderly mobility. In Automation, Quality and Testing, Robotics (AQTR), 2016 IEEE International Conference on 2016 May 19 (pp. 1-6). IEEE.

- Miranda-Linares D, **Al Rezage G.** and Tokhi MO. Control of lower limb exoskeleton for elderly assistance on basic mobility tasks. In System Theory, Control and Computing (ICSTCC), 2015 19th International Conference on 2015 Oct 14 (pp. 441-446). IEEE.

- **Al Rezage G.** , Tokhi M and Ali SK. Design and control of exoskeleton for elderly mobility. Proceedings of the 18th International Conference on Climbing and Walking Robots (CLAWAR 2015).6-8 Sep (pp. 67-74).

- Ali SK, Tokhi M, Ishak AJ and **AL Rezage G.** . PID and adaptive spiral dynamic algorithm in controlling human arm movements. Proceedings of the 18th International Conference on Climbing and Walking Robots (CLAWAR 2015), 6-8 Sep (pp. 87-94).

- **AL Rezage, G.** and Tokhi, M.O. (2014). Desgin and control exoskeleton for elderly mobility. Poster session presented at Sheffield Centre for Robotics Symposium 2014. Pam Liversidge Building Sir Frederick Mapping Building Sheffield, The University of Sheffield, United Kingdom.

- **AL Rezage, G.** and Tokhi, M.O. (2014). Desgin and control exoskeleton for elderly mobility. Poster session presented at the ACSE PGR Symposium 2014. Department of Automatic Control and Systems Engineering, The University of Sheffield, United Kingdom.

1.7 Organisation of the thesis

A brief summary of the contents of the thesis is given as follows:

Chapter 1 : This chapter presents brief introduction to the subject with motivation to the research undertaken. Lower limb anatomy , walking impairments in elderly , aim and objective of the research and , list od publications and arising from the research are also included in this chapter.

Chapter 2 : This chapter contains brief overview of lower limb exoskeleton systems and their developments and applications. Moreover, hardware components such as mechanical structure, actuator, sensor, power supply and the control strategies are described.

Chapter 3 : In this chapter, the methodology used to develop the human body model and the lower limb exoskeleton model in visual Nastran 4D (vN4D) and SimWise software environments is presented. The (computer aided design (CAD)) models thus developed with Matlab/Simulink for development and evaluation of suitable controllers.

Chapter 4: This chapter provides a general description of the proposed control techniques considered for purpose of assisting elderly mobility for low level. The control approaches include Proportional Integral Drivative (PID) control, fuzzy logic control (FLC) and fuzzy PID control. Furthermore, Spiral Dynamic Algorthim (SDA) and Invasive Weed Algorthim (IWA) used in this research to tune the controller parameters are also described..

Chapter 5 : This chapter introduces the control mechanism for the assistive exoskeleton in walking manoeuvres.The investigations are carried out through simulation of a humanoid model combined with actuated lower limb exoskeleton using the vN4D and SimWise software platforms. PID control, FLC and fuzzy PID control are used for actuation of exoskeleton knee and hip joints. The Matlab/Simulink controllers are designed and implemented within and the motion visualised in graphic animation from vN4D or SimWise. A comparative assessment of the controllers are also provided in this chapter.

Chapter 6: This chapter introduces a control scheme of assistive exoskeleton for Sit to Stand mechanism. The study is carried out with a humanoid model combined with lower limb exoskeleton using the vN4D and SimWise software platforms. PID control, FLC

and fuzzy PID control are designed in Matlab/Simulink and tested with the exoskeleton in sit-to-stand manoeuvres. The results of system performance are presented and discussed.

Chapter 7: This chapter summarizes and concludes the overall work,and recommendations for future directions are given.

Chapter 2

Exoskeleton Systems

2.1 Lower limb exoskeletons for rehabilitation

Exoskeletons have been emerged over the years as assistive technology within the robotic sector. Significant number of researchers have engaged in development of assistive devices for empowering or rehabilitation purpose. The intention is to augment reduced power of the joint and carry part of the body weight or use as aid and substitute the human limb (Hong et al., 2013; Pons, 2008). A growing number of exoskeletons have been prosperously developed for rehabilitation with different purposes and functions. These exoskeleton systems are capable of guiding the joints of the lower limbs (Young and Ferris, 2016). The exoskeletons used for rehabilitation could be classified according to the method they act on the user. The categorisation used below is based on the driving action capabilities of exoskeletons.

2.1.1 Gait training exoskeletons with body-weight support

Rehabilitation fundamentally is a relearning process for disordered lower limb movement. Large number of training sessions are required for rehabilitating gait affected by diseases (Olivier, 2016). Mobile training is of significant importance for gait impairment patients such as paralysed and spinal cord injury (SCI) patients. Physiotherapists perform this task only, which is an exhaustive function and often requires more than one therapist to carry out movements. With recent advancement in robotics, rehabilitation robots have been designed for assisting the therapists, thus the robotic training has become very prominent

solution .There are two forms of training exoskeleton: treadmill-based and over ground.

2.1.1.1 Trade mill-based training exoskeleton

Earlier exoskeletons developed for gait rehabilitation were treadmill based gait devices. This type of system was originally designed to enable the patient to have gait training in rigid and confined regions (Díaz et al., 2011; Viteckova et al., 2013).

A system for body weight support was develop in treadmill, predetermined pattern for walking was introduced, normally variation was not allowed within the gait pattern. Sometimes, virtual reality environment was used, that may be both induce and power the patient to perform the movement actively.

However, manual rehabilitation training has some drawback especially for treadmill, because the training time is dedicated for each patient. Thus, the treatment process is not effective and the patient gait pattern is not restored. In addition, some cases require two or three therapists to support the patient such as in case of severe SCI patients. Moreover, the therapist may witness a physical force and bad ergonomic position. The demanding conditions, including physically massive effort, will make the therapist exhausted and affect the overall rehabilitation process (Chen et al., 2013) .

One of the most studied and commercialized device in this field is Lokomat developed by a Swiss company Hocoma. Lokomat is the most widely adopted exoskeleton for rehabilitation around the world. The Lokomat device is shown in Figure 2.1(a). The first version of Lokomat was limited in position control. But many developments have followed to increase the participation and motivation of the user (Colombo et al., 2000; Jezernik et al., 2003; Riener et al., 2005). Lokomat has four degrees of freedom (DOF) that allow hip and knee joints to move in sagittal plane. DC motor and ball screw actuate the hip and knee joints to provide assistive torque.The continuous torques provided by the system are limited to 50 Nm at hip joint and 30 Nm at knee joint. Force sensor is used to estimate the interaction force between the exoskeleton and lower limb (Low, 2011).

LOPES (lower extremity powered exoskeleton) is another gait rehabilitation device designed by university of Twente, see Figure 2.1(b). LOPES has three DOF two for hip

joint in sagittal and horizontal and one for knee joint in sagittal plane. The device aims to support the partially impaired patients by improving their walking ability. Force sensors are attached on each side of joints side to measure the joint torque (Veneman et al., 2005). Bowden cable derived series drive elastic actuators actuate the hip and knee joints. The maximum support torques provided by the system are approximately 65 Nm at hip and knee joints in sagittal plane while it is 35 Nm for hip in horizontal plane. Impedance control is used based on interaction control mechanism (Veneman et al., 2007).

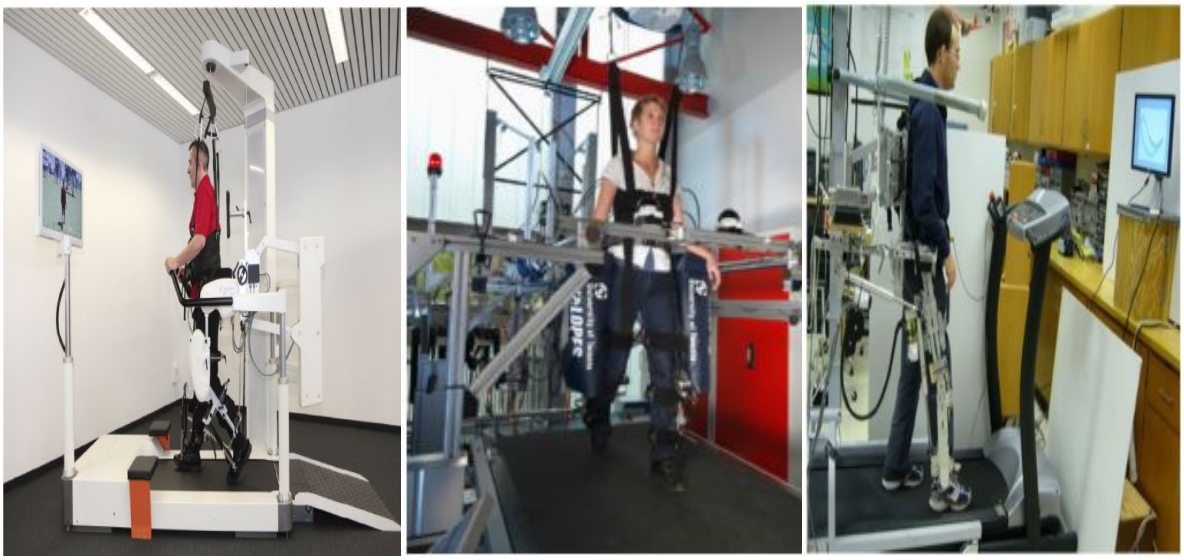

(a) Lokomat (Díaz et al., 2011) (b) LOPES Meng et al. (2015) (c) ALEX (Banala et al., 2007)

Figure 2.1: Examples of tread-mill gait training exoskeletons with body weight support

Another prominent treadmill based exoskeleton device is ALEX (Active Leg Exoskeleton) designed by the university of Delaware (USA) as shown in Figure 2.1(c). ALEX has seven DOF, three for waist joint , two for hip joint ,one for knee joint and one for ankle joint. Linear actuator is used to actuate the hip and knee joints, controlled by force-field controller which relay on assist as need strategy (Banala et al., 2007, 2009). The device is aimed for rehabilitating patients of gait disorder. In order to measure the force between wearer extremity and the exoskeleton a force-torque sensors are integrated. The modified version of ALEXII, uses rotary motor in order to control the hip and knee by replacing the linear actuator (Winfree et al., 2011). This rotary motor can address the range limitation problem, and the joint can achieve a wider range of motion. ALEX has been tested by

healthy people and stroke patients.

2.1.1.2 Over ground gait training exoskeletons

Overground gait training exoskeletons allow the patients to restore natural walking in more realistic conditions than the treadmill-based. Patient motivation can be increased and they can achieve actual locomotion. These devices follow the user intention and support the body weight.

(a) WalkTrainer
(Stauffer et al., 2009)

(b) NaTUre-gaits
(Wang et al., 2011a)

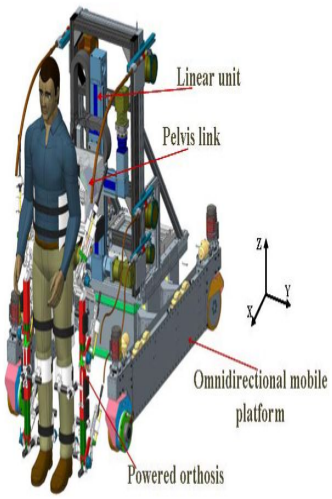

(c) CORBYOS
(Slavnic et al., 2014)

Figure 2.2: Examples of over ground gait training exoskeletons with body weight support

WalkTrainer is a walk rehabilitation robotic described in (Bouri et al., 2006) designed at the laboratory of System Robotics (LSRO) at the EPFL (Ecole Polytechnique Federale de Lausanne) for training SCI patients . The WalkTrainer actuates both legs in sagittal plan. The device illustrated in Figure 2.2(a) has 6 actuated DOF on pelvis. It contains position sensors to measure angles of hip, knee and ankle joints as well force sensors are implemented between the patient and exoskeleton for monitoring of interaction force (Allemand et al., 2009; Stauffer et al., 2009). DC brushless motors drive the actuated joints

The Nanyang Technological University has introduced an overground assistive device for gait rehabilitation, NaTUre-gaits (natural and tunable rehabilitation gait system). The device applies 5 actuated DoF on pelvis and actuate the hip, knee and ankle joints (Wang et al., 2011a,b) as depicted in Figure 2.2(b).

Another type of the overground training exoskeletons is the CORBYS (Slavnic et al., 2014) which consists of mobile platform and exoskeleton attached to it. The device has 6 DOF; three for hip; one for knee; and two for ankle. Figure 2.2(c) shows the device, and the associated features are implemented to enable physiological movement. Force and torque sensors are placed between the patient and the device within pelvis link.

2.1.2 Wearable mobility exoskeletons

The wearable exoskeletons are developed to assist the people who are unable to move their legs voluntarily. These overground training exoskeletons do not provide body-weight support, therefore balance becomes a critical factor that needs to be taken into consideration.

(a) ReWalk
(Díaz et al., 2011)

(b) REX Bionic
(Bogue, 2015)

Figure 2.3: Example of wearable exoskeletons with and without balancing

One of the main commercial devices without balance control is the ReWalk. ReWalk is a wearable robot designed for treating patients with SCI, actuating the hip and knee joints by DC motor (Esquenazi et al., 2012; Fineberg et al., 2013). The device designed by Argo medical technology, comprises lightweight brace for supporting the suit, rechargeable batteries,and an array of sensors and computer control system. Finite state machine is used in the control. Many type of sensors are used such as: ground force sensor, wireless tilt sensor and accelerometer. The device can perform many tasks such as standing, sitting

and normal walking (Goffer, 2006; Zeilig et al., 2012). The device cannot keep balancing control, so the user always needs to use crutches as can be seen in Figure 2.3(a). High cost about $\$70,000$. In 2014 the Food and Drug Administration (FDA) approved to use the ReWalk in the home and community.

Another commercial device produced by REX Bionics (Auckland, New Zealand); the REX. REX exoskeleton provides mobilization and balance. It has 6 DOF: three at hip, two at ankle and one at knee.The lower limb joints are actuated by DC motor (Bogue, 2015; Kilicarslan et al., 2013; Viteckova et al., 2013). Many researchers have experimented REX device by integrating the brain control using EEG.The limitation of the device is the bulk design and slow speed. High cost about $\$120,000$.

2.1.3 Wearable assistive exoskeleton

The assistive exoskeletons participate actively to help the users in their motion. Their major function is to follow the user's intention and augment the lower limb by providing a support torque. In 2004, the Roboknee device was introduced as first prototype to enhance and strengthen the wearer's muscle as Figure 2.4(a). PD controller and linear series elastic actuator was selected to produce low impedance and high force. Therefore, the main purpose of the roboknee is to enhance the torque of the human joint, but the roboknee supports the muscle strength not the bone strength because it depends on the bone to transfer the force to the ground, so the torque produced and the exoskeleton weight all affect the user's bone (Pratt et al., 2004).

Recently, has been interest in exoskeletons for the elderly. One of the most recognisable prototype on assisting old people is Exoskeleton for Power Assistive (EXPOS) to help elderly people and patients in their motion presented by the Sogang University in 2006. The purpose of the device is to minimize the weight and volume of the exoskeleton to be more convenient and suitable for walking and sitting. The device consists of wearable exoskeleton and smart walker. The wearable device is less than 3 kg weight, and applies the mechanically driven tendon and it has a motion detection sensors. The walker carries most of the heavy weight of the motor and the battery, and servo motor control. The wear-

able exoskeleton has potentiometer to measure the joint angle and pressure sensor in order to measure the movement of the muscle, which is proportional to joint torque (Kong and Jeon, 2006; Viteckova et al., 2013).

(a) Roboknee
(Low and Yin, 2006)

(b) HAL
Olivier (2016)

(c) WSE
(Onen et al., 2014)

Figure 2.4: Example of wearable assistive exoskeleton

Tsukuba University and Cyberdyne in Japan have developed a Hybrid Assistive Limb (HAL-3), as a wearable robot designed for different functions. The main goal is to help disordered and elderly people to enhance their walking performance. DC actuator is used to generate proper torque for both hip and knee joints. Force sensor is used in the sole of the foot to measure reaction force, while EMG is attached to skin surface of leg to estimate the muscle activity (Kawamoto et al., 2003; Kawamoto and Sankai, 2002; Sankai, 2010). High cost rent per month about £1, 300, Figure 2.4(b) shows HAL device.

Ikehara et al. (2010) have introduced a walking assistive device adopted based on a combination of worm gear and flexible shaft. Hybrid control is used for both knee and ankle joints (Ikehara et al., 2010). The device aims to help the elderly or impaired walking people. DC gears motor is used for actuation and placed in the backpack (Ikehara et al., 2011) .

In 2014, Necmttin Erbakan University (Turkey) developed (WSE) walking support exoskeleton for individuals who lost their lower extremity muscular activity partially or totally to support them in their daily activity such as walking, sitting and standing (Li

et al., 2015; Onen et al., 2014). Two DoF at hip and knee, DC servo motor used as actuator. Safety requirement adhered to with and maximum maneuverability and lightweight structure. The programmed position control (PCM) used because the conventional ones are poor when dealing with patients who lost limbs. Adaptive network-based fuzzy logic control (ANFLC) is used in the control ; prototype of WSE can be seen in Figure 2.4(c).

Honda Company has developed Stride Management Assist (SMA) lower limb robotic exoskeleton. The SMA robotic device intends to enhance mobility of elderly and gait disordered patients. SMA attaches with angle and current sensors to monitor the orientation and the torque of user's hip joints (Buesing et al., 2015). Brushless DC motor drives the hip joint actuator.

2.2 Hardware

Currently, most of the exoskeleton systems are consist of: mechanical frame, sensor, actuator, controller and power supply.

2.2.1 Sensor

The exoskeleton is equipped with sensors to know the system transitions every moment to provide the right control actuation (Walsh, 2006). The biomechanics data related to human motion can be classified into three types: kinematic data such as position, orientation, velocity, and acceleration, kinetic data such as the contact force between the wearer's foot and the ground and joint torque, and bioelectric data such as electromyographic (EMG) and brain signals (Chen et al., 2016). Different types of sensors are commonly instrumented to the lower limb exoskeleton system to measure these data. For example, potentiometers, encoders, goniometers, accelerometers, and gyroscopes are usually used to gauge the kinematics data, whereas the kinetics data are measured by force, torque sensors (Grimaldi and Manto, 2010).

Sankai and his group developed the fifth version of Hybrid Assistive Limb (HAL-5). The HAL-5 utilizes various types of sensors such as surface EMG electrode to detect the

wearer intention, potentiometer to monitor and measure the human joint angle, gyroscope and accelerometer to obtain trunk absolute angle , and semiconductor pressure sensor implemented in shoes (Sankai, 2010; Tsukahara et al., 2010). BLEEX employs angle sensor for hip and knee joints,and switches to obtain the centre of pressure location, and load disturbance sensor (Kazerooni, 2008; Kazerooni et al., 2005, 2006).

Lokomat is instrumented with force sensors to detect contact force between lower limb and exoskeleton and position sensors to read the joint angle (Jezernik et al., 2003). ReWalk uses various types of sensor such as: ground force sensor, wireless tilt sensor, and accelerometer.

EXPOS employs pressure sensors attached to thigh braces and shoes and potentiometer installed to the pulley of wearing part to read the joint angle and determine the joint velocity. A changing pressure in air bladder is calculated according to muscle contraction before motion is initiated to estimate the required torque, then the exoskeleton controls the action and drives the joints (Kong and Jeon, 2006).

The Chinese university in Hong Kong has introduced the CUHK-EXO , which is based on a multi sensory system. Inertia measurement units (IMUs) are placed on backpack to obtain the trunk position; pressure sensors are used in the exo soles and smart crutches to detect the contact force with ground. Using information from these sensors, the exo can estimate the user intention by calculating the change of motion data (Chen et al., 2015).

Hanyang University in South Korea has designed the lower limb exoskeleton (HEXAR) Hanyang Exoskeleton Assistive Robotic. The HEAXR exoskeleton is equipped with sensors to measure the expansion degree of muscle known as muscle stiffness sensor. These signals are important to detect the intention of the wearer's (Kim et al., 2014).

Due to the advancement in technology, various types of sensor are commercially available for exoskeleton application. Some of these sensors are already used in prototypes while some are wirelessly communicated with controller in order to keep the system portable.

2.2.2 Actuators

The actuators are usually located at the exoskeleton frame and their action is to generate the movement based on signals received from the controller. Many crucial elements have historically limited the practical realisation of exoskeleton systems. These include size, weight, and power efficiency of the motors. However, the technology is significantly advanced since early days and this has contributed to improved and highly functional portable devices (Chen et al., 2013; Huo et al., 2014; Li et al., 2015; Young and Ferris, 2016).

In this section, the actuation development of the lower extremity exoskeleton is summarized and classified according to their use in each device. The state of art of lower limb exoskeletons have indicated that 72% of devices are actuated by electric actuators while hydraulic and pneumatic actuators are less commonly used.

Electric actuators are the most commonly used in exoskeleton designs. REWALK (Fineberg et al., 2013), and WSE (Onen et al., 2014) both employ DC motors to actuate the hip and knee joints, whereas HAL exoskeleton actuates the hip and knee joints based on DC motors with harmonic drives (Kawamoto and Sankai, 2002). Many exoskeletons use brushless DC motors due to the advantages offered for wearable exoskeleton such as: high efficiency, high torque, increased reliability, reduced noise, long lifetime and electromagnetic reduction. Honda walking assist device uses two brushless DC motors to power the hip (Buesing et al., 2015), while Vanderbilt exoskeleton uses the same actuators to drive hip and knee joints (Farris et al., 2014).

However, Yamamoto et al. (2003) applied pneumatic actuator for his nurse assistance device to power hip and knee joints. Similarly Kawamura et al. (2013) initiated walking assistance device and used pneumatic actuator for hip joint. On the other hand, Pratt et al. (2004) have used linear series elastic actuator in Roboknee in order to produce low impedance and high force. Kazerooni et al. (2006) used hydraulic actuators for hip, knee and ankle in BLEEX.

2.2.3 Energy

Traditionally, power supply has constituted an important component in developing portable exoskeletons to allow autonomy and personal use. Almost all the commercialized exoskeletons use batteries, specifically lithium ion.

The Human Universal Load Carrier (HULC) is hydraulic actuated battery operated lower limb exoskeleton designed by Lockheed Martin. A fuel cell power supply, which can sustain up to 72 hours has been proposed as new energy source for the next prototype. Although fuel cell may be a promising alternative source, it will not be an optimum solution for exoskeleton energy unless there is appropriate hydrogen source available (Bogue, 2015; Kopp, 2011; Young and Ferris, 2016).

Sarcos XoS2 is an amplification full body exoskeleton presented by Raytheon for military application. It weighs about 95 kilogram and is able to lift 100 kilograms for prolong time. A new version utilises hydraulic actuation system, and many of sensors, controllers, and functional units. However, the requirement for tethered high-pressure hydraulic motor is becoming high demand. The following prototype is being suggested to use a fuel-carrying backpack with hydraulic servos to power the system up to 8 hours. Raytheon and Sarcos developing team reject lithium ion batteries to avoid the risk of burn and explosion (Kopp, 2011; Zhiqiang et al., 2014). Nowadays, due to their availability lithium ion batteries have become the most common and safest for civilian implementation such as ReWalk,Honda and BLEEX. It can provide up to 6 hours of continuing movement without charging. Definitely, in exoskeletons the energy efficiency requires a significant improvement to prolong the functional time. Therefore, researchers are interested in minimizing the weight and dimension of the exoskeleton to increase the efficiency.

2.2.4 Material

Mechanical design is a fundamental issue affecting the overall performance of a rehabilitation system. The mechanical frames are commonly attached to the human body as orthosis device. Exoskeleton frames offer many functions such as human machine interaction between exoskeleton and user, keep the motion in specific axis, and maintain the strength of the exoskeleton. Many significant design principles should be taken into account in system design process such as comfort for wearer, light weight, simple structure, easy to control, customized for different users and safety Onen et al. (2014). Metallic material is typically employed for the frame such as carbon steel, aluminum, titanium and its alloy. Whereas the aluminum alloy is mostly considered as the most important material employed in exoskeleton structure while titanium is less likely used. Other alternative materials considered as promising option often utilized in single degree of freedom design are Fiber Reinforced Polymers such as Carbon (CFRP) and Glass (GFRP) (Young and Ferris, 2016).

2.3 Control strategies

The major goal of the controller in the rehabilitation process is to match the patient's movement and provide assistance for his/her walking cycle. Different control strategies have been applied in exoskeleton application. The control strategy plays significant role in exoskeleton technology. In the first stage, a trajectory is obtained from selected healthy subject and then process to create a stranded reference to send to actuators; consequently, exoskeleton control mechanism has been open loop prior to inclusion of sensors in the system to enable feedback control capability and facilitated the user and the exoskeleton to communicate (Kwak et al., 2015).

A considerable amount of literature has been published on control methodologies of lower limb exoskeleton. Most of these studies have comprehensively focused on precise descriptions of hardware used, and the mechanical design.

According to the classification provided by Yan et al.(2015), the control strategies of full body exoskeleton and single joint may be classified into nine approaches.

Two assistive techniques are only implemented in single joint devices; muscle stiffness and proportional myoelectric control. The first approach is sensitivity amplification control predominantly applied for performance augmentation exoskeleton. Devices that use this strategy are the BLEEX and Naval Aeronautical Engineering Institute Exoskeleton Suit (NAEIES).

The second approach is predefined gait trajectory control. In this methodology, the desired joint trajectory references are record from selected healthy persons or from gait analysis like Clinical Gate Analysis (CGA). The literature shows that this procedure is significantly applied for subjects that have completely or partly lost voluntary movement. Several exoskeletons work based on this strategy such as ReWalk, ATLAS, ReWalk, IHMC ,sLEGS, walking assistance device by Ikehara, Vanderbilt lower-limb orthosis, Powered Knee Orthosis (PKO), MINDWALKER and Stance control knee–ankle–foot orthosis (SCK-AFOs) (Yan et al., 2015).

Another approach is model based control, under which the structure and required actuation of joints is computed according to a human-machine model. Frequently, they consider gravity compensation and Zero Moment Point (ZPM) for balance criteria. Many devices use this strategy such as HAL, ABLE, Body Extender (BE), Nurse Robot Suit, Wearable Walking Helper (WWH), Walking Power Assist Leg (WPAL), XoR, RoboKnee, Technische Universität Berlin Powered Lower Extremity Exoskeleton (TUPLEE). These devices are mainly assist the disabled and weak muscle people Yan et al. (2015).

An adaptive oscillator based control strategy aims to capture periodical locomotion related to signal feature in mobility rehabilitation exercise. Based on this strategy the required joint trajectory is determined. This technique is presented to diminish the exertion of healthy person. This scheme is widely applied in robotics, like LOPES and ALEX II (Yan et al., 2015).

Predefined action based gait patter control is essentially implemented for many applications such as load handling augmentation, healthy people enhancement and disabled or impaired mobility assistance. Some of the pioneer exoskeletons widely using these strategies include MIT exoskeleton, Soft Exosuit, knee extension assist device (KEA), MIT

knee exoskeleton, Belforte and MIT active ankle–foot orthosis (AAFO). In this technique, the system frequently tracks predefined trajectory such as pneumatic cylinder actuators or passive spring are actuated or unactuated according to the gait phase(Yan et al., 2015).

Fuzzy control approach is considered when it is sophisticated to formulate a precise dynamic model, for this reason, it is appropriate for the exoskeleton control and is typically used for the physically weak people. Despite of it being an effective way to control such devices, many variables need to be tuned. The literature shows that only two devices specifically using this control method they are EXPOS and Lower-limb motion assist exoskeleton by He and Kiguchi (Yan et al., 2015).

Hybrid assistive strategies attempt to apply different methods for different functions in the exoskeleton. An example of the exoskeleton incorporating this strategy is BLEEX which uses position controller for stance and force controller for swing and AIT leg exoskeleton which create predefine walking trajectory offline and subsequently apply fuzzy controller to adapt it online(Yan et al., 2015).

Eventually, muscle stiffness and proportional myoelectric in most applications depend on the muscle reference whereas the sensors measure the muscle action to drive motion of pneumatic actuator. The key difference between the two strategies is the type of sensor used for estimating the muscular action. Application of muscle stiffness control was introduced in the knee orthosis by Kim et al., (2010) while the proportional myoelectric control has been used in Powered Ankle–Foot Orthoses (PAFOs).

Tucker et al.(2015) have presented a review based on categorization of exoskeleton control schemes. They have classified the control strategies in a hierarchical manner and have considered the effect of environment in addition to the exoskeleton and user. Therefore the interaction between user, exoskeleton and environment are incorporated in the design. Figure 2.5 shows the proposed control structure classification for active lower limb exoskeletons.

The purpose of the high level controller is to perceive the locomotion intent of the user through a combination of activity recognition mode and direct voluntary control and to detect the current locomotive state such as walking, standing, position, velocity and torque

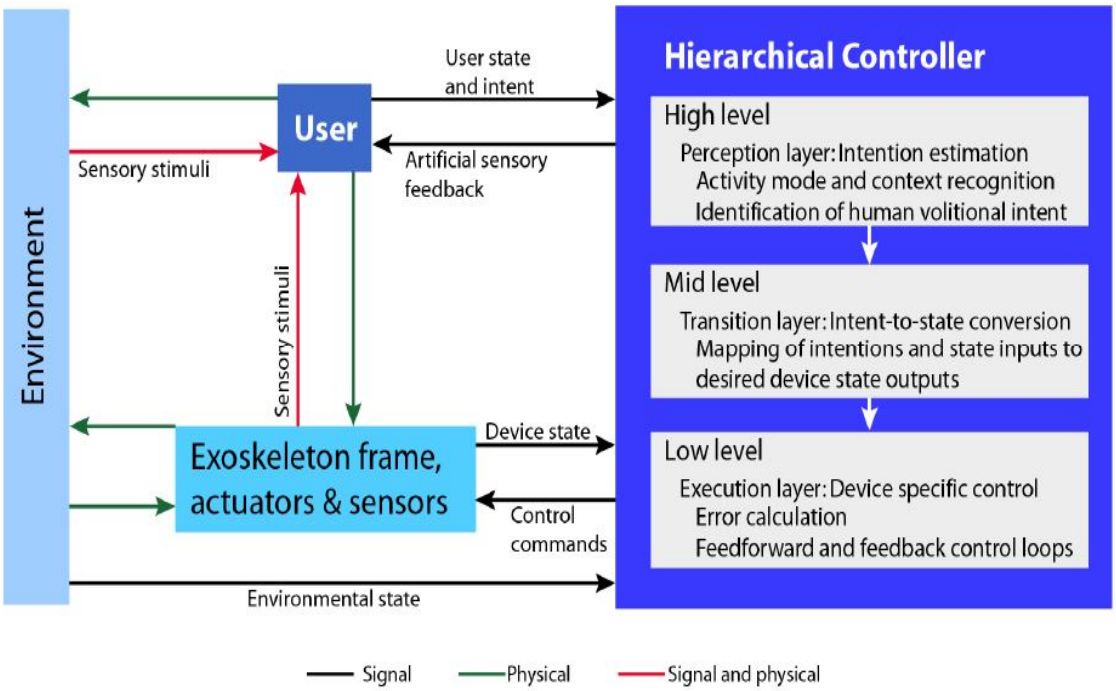

Figure 2.5: Lower limb exoskeleton control structure
Tucker et al. (2015)

as well for devices and the environment.

The mid-level control is responsible of translating the estimated motion intention output from the high level controller for use by low level controller. The low level controller or execution layer drives the actuator in order to minimize the error between the current and desired device states.

2.4 Summary

A literature review of various types of exoskeletons and their applications, hardware structures, control techniques applied has been carried out. Gaps in facilities of software used in early stage of design have been identified. Moreover, it is found that most of the works on lower limb exoskeleton devices have focused on prototype construction. Only few works describe virtual environments to evaluate early stages of designs; thus, it is possible that these have not been executed. Moreover, the literatures shows that most of the published work on developing exoskeletons have intensively considered paraplegic and disabled peo-

ple for assisting or restoring walking task. Additionally, there is a low quantity of papers regarding low level exoskeleton control strategies, for standing-up and sitting-down motions, particularly for elderly assistance. Furthermore, few works consider the combination of intelligent algorithms and PID control to improve the system performance by integrating their advantages and eliminating their disadvantages.There are some advantages of using fuzzy logic such as: it is easy to understand, simple to implement, the development cost is inexpensive for hardware and software and it is suitable for complex systems. However, its drawbacks are that it cannot be analyzed in a close loop system, the performance relies on the designer perception, and its manual tuning is time consuming in industrial applications (Albertos and Sala, 1998).

As a result, the essential aim of this project is to consider exoskeletons for elderly assistance for walking and sit to stand function. The current computational tools allow integration of complex physical and mathematical systems in a virtual environment. The advantages of available software facilities are thus exploited in this research to develop and evaluate control schemes via a virtual visualization of the human and exoskeleton. Furthermore, the research investigates the development of adaptive fuzzy PID controller with fuzzy logic controller to tune the PID controller parameter online to improve the system efficiency, while little work has been done in these areas in context of exoskeletons for elderly.

Chapter 3

Modelling of Humanoid and Exoskeleton

3.1 Introduction

In many scientific fields choosing the right model to represent the dynamics of the system accurately is the major issue to simulate and control the system's operation. The additional information about the real system specification, has a valuable effect on the modelling accuracy and therefore better simulation and control performance.

This chapter describes the process of modelling a multi purpose exoskeleton system and humanoid model to carry out multi functions such as walking, sit to stand, and stand to sit. Simulation environment and models can provide a great facility to test and control the system. Therefore, the purpose behind developing a humanoid and exoskeleton model in simulation, is to avoid the complexity and costs when building prototype, as well as to test the developed controllers. A humanoid and exoskeleton were modelled through computer aided design (CAD) since the mathematical model will be significantly complex. It is important to involve exoskeleton mechanics and electric components, and further nonlinear complex system dynamics , in addition to full system kinematics.

CAD models need to be created as close to the mechanical characteristics as the real prototype. Thus, one of the possible methods is to ensure that their behaviour is realistic by selecting appropriate features found in a virtual environment such as material type, properties, dimensions, masses, friction and gravity factor.

Therefore a humanoid and exoskeleton models are first developed using Solidworks

software then each part exported separately using SimWise software, which is a virtual environment where the parts will assemble according to the features previously mentioned. Moreover, SimWise links to MATLAB/SIMULINK to evaluate and develop the devised control strategy.

3.2 SolidWorks

SolidWorks is CAD software and delivers 3D robust design capability performance. The user can create 3D detailed parts , assemblies, complex surfaces based on 2D sketches , in addition to numerous features that software provide (Dassault Systèmes SolidWorks , 2016). This software can easily export the complex parts generated to other softwares. It was selected in this project to develop realistic limbs and segments of the human body based on (Winter, 2009), according to the parameters of height and weight as well as keeping them simple to simulate in virtual environment. The exoskeleton is also designed using solid work software and attached to the humanoid to support the lower limbs.

3.3 SimWise

SimWise 4D is a virtual software developed by MSC Software Corporation for design and engineering and allows assembling of 3D parts. It has various properties allowing realistic reaction to external physical forces such as contact and gravity forces with other items. It allows simulating the kinematic and dynamic of a system. These applications vary from virtual preliminary prototype to optimized performance in the design strategy (Design Simulation Technologies, 2016)

It would be necessary to test the designed behaviour under realistic conditions within a simulation platform before implementing a physical prototype to save cost and reduce downtime. The software provides different types of material that designers can specify in the design process based on the requirement to perform a real performance as shown in Figure 3.1. However, these properties help the user to modify and adjust own material by editing the database block to fit the system demand. A list of elements for material

adjustment and the preference to adjust material is given in Figure 3.2. .

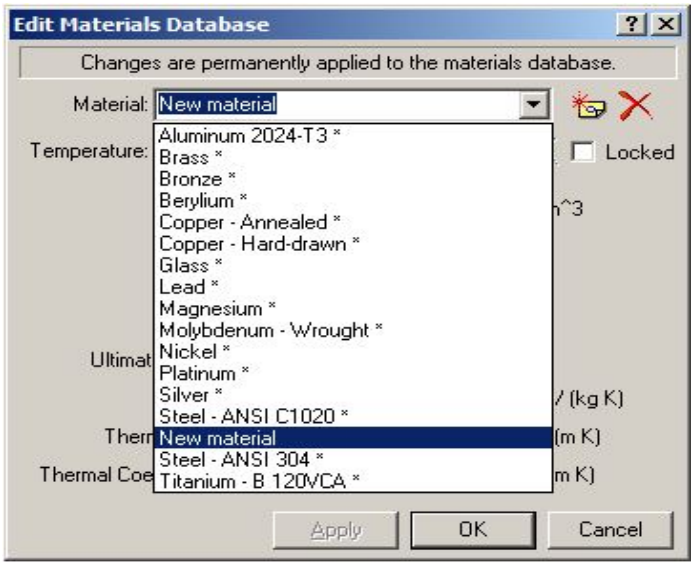

Figure 3.1: Material properties

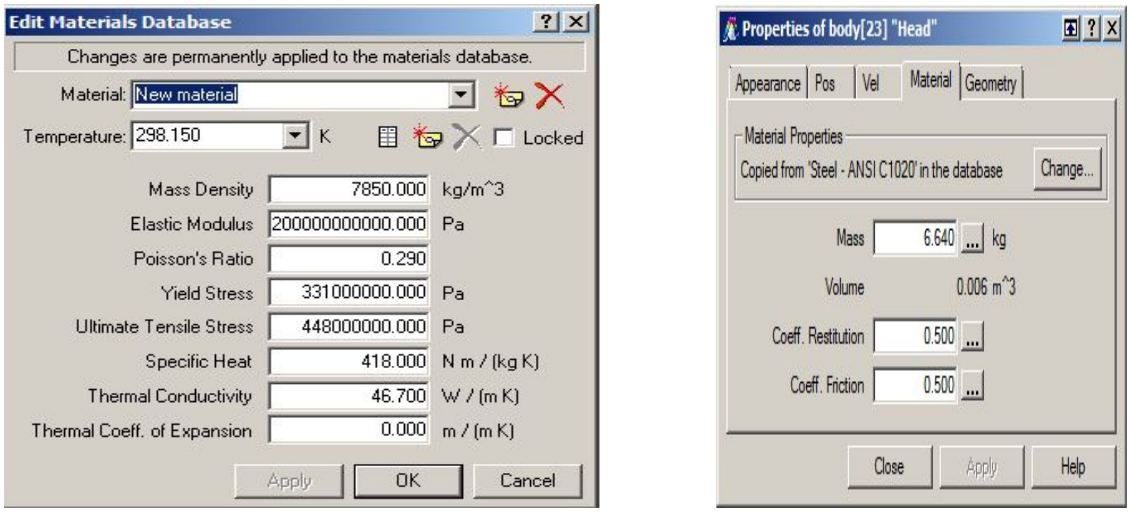

(a) New material (b) Properties of body

Figure 3.2: Dialog box to adjust own material

The software tools permit integration with 3D CAD design softwares such as SolidWorks, Catia, Solid Edge and Autodesk, as SimWise has only simple shapes. In this project the CADs were imported from SolidWorks software into the system. The constrains connect all the segments together via joints to generate maneuver through the actuators. This is done by choosing by default constrains between two segments or locate a frame coordinate on each segment by cord function. Many types of constrains can be select based on system movement as illustrated in Figure 3.3.

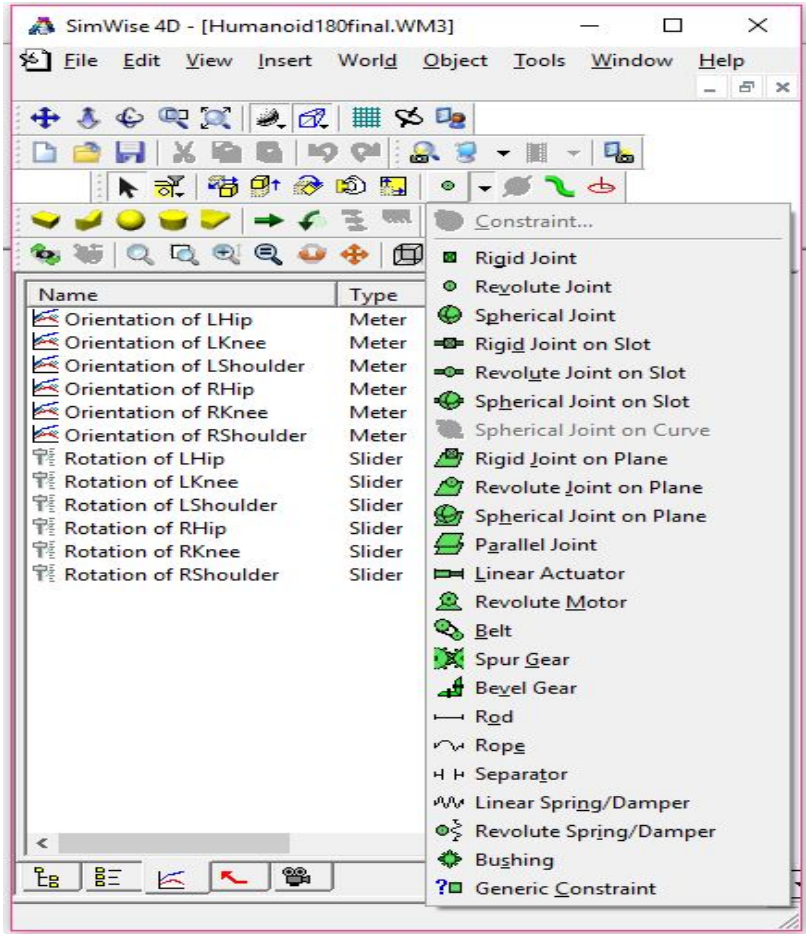

Figure 3.3: Dialog box for constraints selection

Furthermore, the software allows to change weight and height of segments to investigate the system and create motion in any direction. The final stage is control which allows the system designed in SimWise to connect with MATLAB/SIMULINK for investigating and evaluating the developed controller. The software package has many types of input and output control signals that need to be defined by the user based on the control mechanism to integrate with MATLAB/SIMULINK. The input control signals are summarized in Table 3.1 while the output control signals are described in Table 3.2.

In this work, there are three main reasons to use SimWise. Firstly, it allows assembling the humanoid and the exoskeleton models designed in SolidWorks. Secondly, it allows measuring the torque, force, orientation, position, velocity and acceleration of joints and links. Finally, it allows visualizing the movement of humanoid and exoskeleton as in a real environment.

Table 3.1: The input signals

Generic
Force
Length
Velocity
Acceleration
Torque
Rotation
Rotation velocity
Rotation acceleration
Spring Constant
Reset Length/Angle
Damper Constant

Table 3.2: The output signals

Time
Position
Velocity
Acceleration
Orientation
Angular velocity
Angular acceleration
Constraint Tension
Constraint Length
Constraint Displacement
Constraint Force
Constraint Torque
Contact Force
Contact Impulse
Fraction Force
Closet distance
Interference
FEA Result

3.4 The human body model

Anthropometry is a measurement technique established by physical scientist for human subject to develop engineering design and evaluate engineering applications. Many researchers have studied the human physical properties and have attempted for anatomical definitions (Bjørnstrup, 1995). The body segmental parameters are required for two main areas, namely motion analysis and prosthesis design. The motion analysis refers to description and analysis of human movement, computer simulation and motion visualization due to external force. Prosthesis design is to allow the prostheses look right, for instance with the right dimension such as length, mass, and mass disturbance (Bjørnstrup, 1995). One of the most common and valid anthropometric data in motion analysis is reported by Winter(2009). Winter (2009) defines that parameters of body segments such as length, volume, centre of mass, and density can be expressed as total body fractions of height (H) and weight (M).

Three main plans and directions configure the human body with planes crossing the body gravity centre. Sagittal plane divides the body into right and left, frontal plane divides it into front and back and horizontal plane divides it into lower and upper. Figure 3.4 shows a graphical overview of segments length calculation based on average human dimension while Table 3.3 details the proportional segments length used to develop the humanoid model in this project corresponding to fraction of body height (H). Table 3.4 lists the percentage of segments mass related to the total body mass.

In this research, a humanoid of 75 kilograms weight (W) and 1.7 metres height (H) was considered. A previously designed humanoid model replicating a real physical system was adopted and modified in SolidWorks. Then the segments were imported to SimWise virtual environment. There are 15 body segments connected through 14 joints to form the humanoid model Cardero (2012). The designed humanoid moves in sagittal, y axis and frontal plan, x axis while it is blocked in transversal plane, z axis.

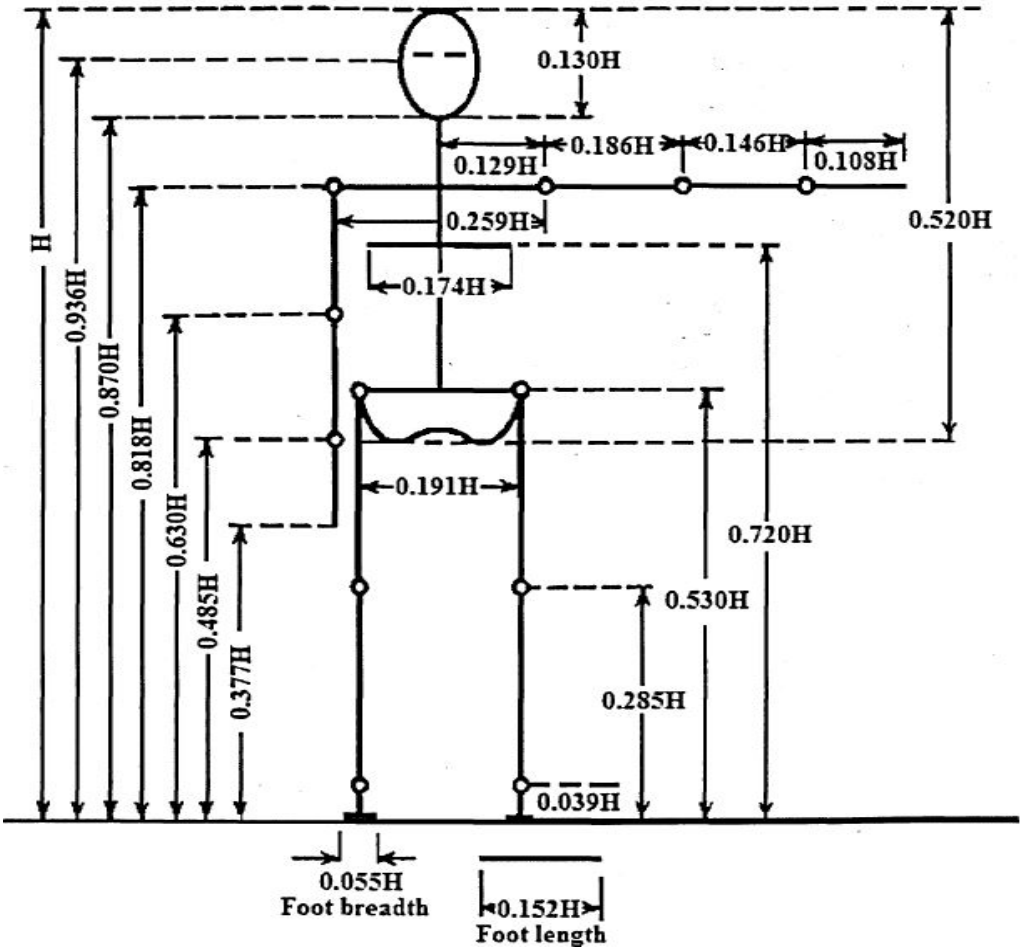

Figure 3.4: Human model associated with anthropometric dimension

Table 3.3: The length of each body segment (Winter, 2009)

Body segments	**Body Segment Height (H)**	**Body Segment length (m)**
Head	0.13H	0.221
Neck	0.052H	0.0884
Trunk	0.288H	0.4896
Upper arm	0.186H	0.3162
Lower arm	0.146H	0.2482
Hand	0.108H	0.1836
Thigh	0.245H	0.4165
Shank	0.246H	0.4182
Foot length	0.152H	0.2584
Foot height	0.039H	0.0663

Table 3.4: The mass of each body segment (Winter, 2009)

Body segments	**Body Segment weight(M)**	**Segments mass(kg)**
Head	0.0665M	4.98
Neck	0.0165M	1.237
Trunk	0.497M	37.275
Upper arm	0.028M	2.1
Lower arm	0.016M	1.2
Hand	0.006M	0.45
Thigh	0.1M	7.5
Shank	0.0465M	3.4875
Foot length	0.0145M	1.0875

Options utilised in this research to create constraint in SimWise include rigid joints, revolute joints and revolute motors. Table 3.5 shows the joints of the humanoid model, their types, rotation axes, number of segments and DOF. Hip and knee joints are the most important joints as they significantly contribute in human mobility

Table 3.5: The length of each body segment

Body segments	**Type of joint**	**Axis**	**Number of segments**	**Control parameter**	**DOF**
Head	Rigid	No	1	No	0
Neck	Rigid	No	1	No	0
Shoulder	Revolt	y	2	No	1
Elbow	Revolt	y	2	No	1
Wrist	Revolt	y	2	No	1
Waist	Revolt	y	1	No	1
Hip	Revolt	y	2	Torque	1
Knee	Revolt	y	2	Torque	1
Ankle	Revolt	y	2	No	1

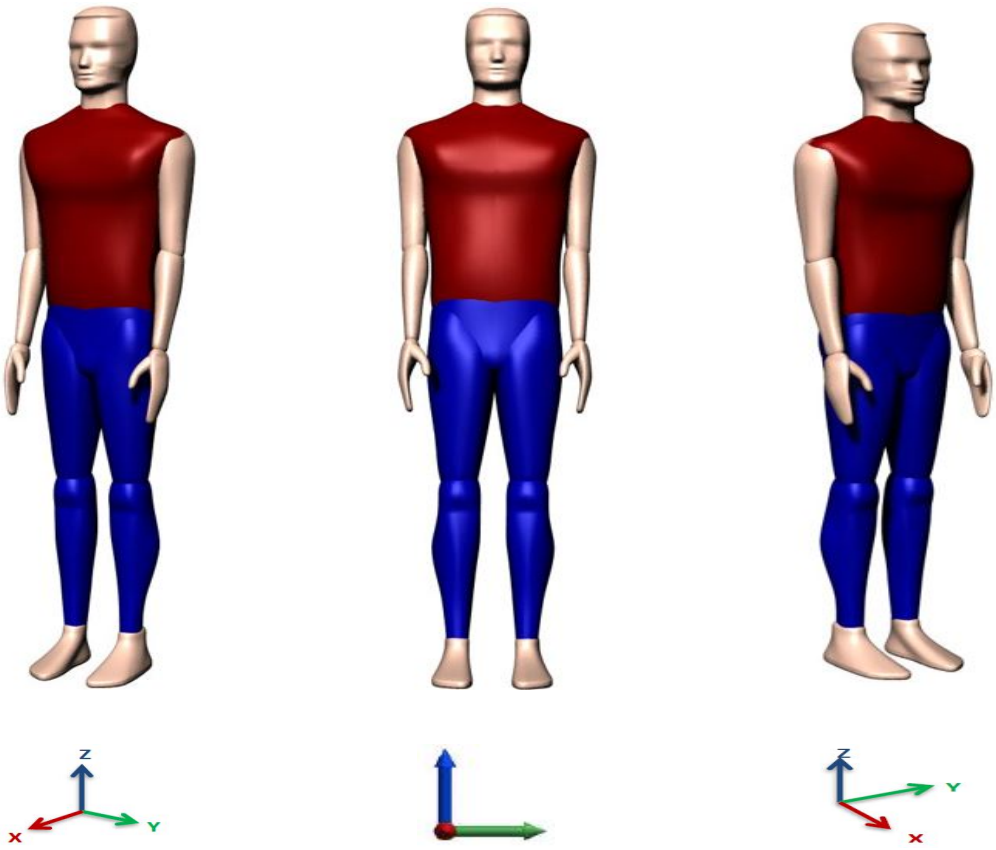

(a) Side view (b) Front view (c) Side view

Figure 3.5: Frontal and lateral views of humanoid model

The developed humanoid model considered throughout this work is shown in Figure 3.5 as frontal and lateral views. SimWise environment provides joint limits, which in this project were selected according to those provided by Low (2011).

3.5 Exoskeleton model

The main purpose of this research is to provide assistance to elderly mobility. The designed exoskeleton is to transfer the frame's weight directly to the ground by making a force track between the wearer and the ground, which releases the user from gravity effect, therefore sole segment is included (Onen et al., 2014). Thus, the mechanical design of an exoskeleton is an important task where many criteria should be taken into consideration such as lightweight, low cost material, adaptable, tracking the user motion smoothly and able to assist as needed by supplying enhanced torque.

For the aims identified previously, a lower limb exoskeleton was modelled in Solid-

Works. Three components, namely upper leg, lower leg and foot were designed for each leg. The exoskeleton components were assembled to provide modification ability for both articulation and structure. The exoskeleton is fastened to the humanoid at feet through shoes, at waist by a belt, and at thighs and calves through straps. Dimensions of the segments are selected corresponding to the humanoid and polymers and glasses comprise the material used to ensure the mass is as low as possible. Then these components were exported to SimWise software and created constraints to connect together. Revolute motors are created to actuate the hip and knee joints by torque in sagittal plan. Figure 3.6 presents graphical overview of the exoskeleton model

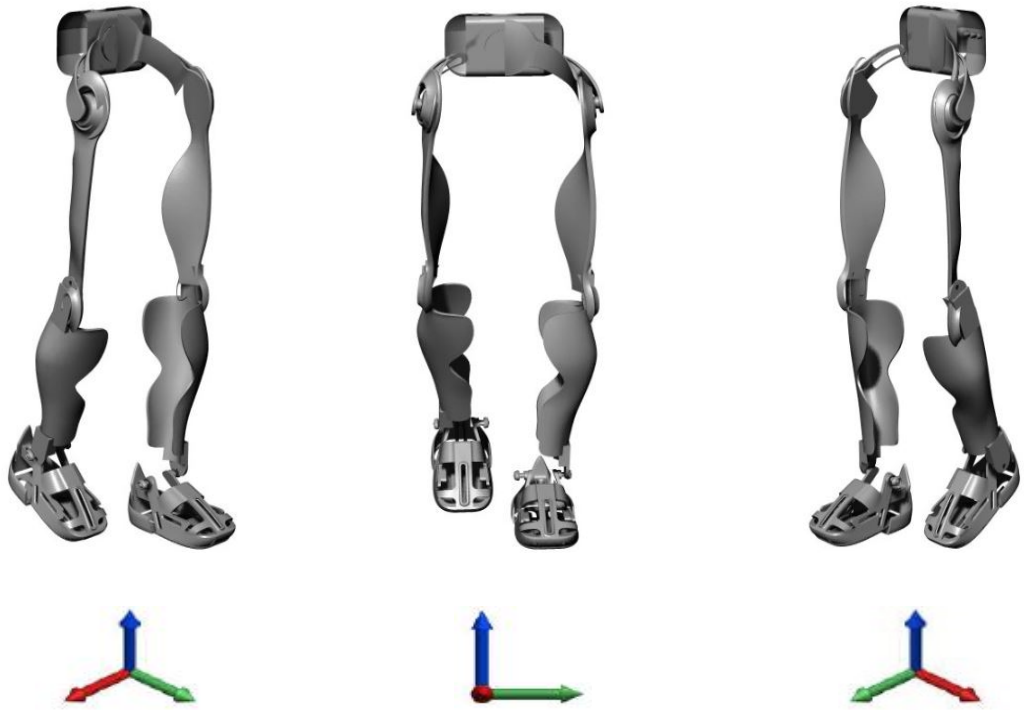

(a) (b) (c)

Figure 3.6: Frontal and lateral views of exoskeleton model

The exoskeleton model utilized for this work was upgraded to that created by PCM, Proyecto Control Montaje, S.L. as part of the EXO LEGS project (Virk et al., 2014) to devise a more advanced design. For simplicity the exoskeleton model was modified using SolidWorks. The modified model has 16 parts per leg. These parts are divided into belt 3 parts, thigh 4 parts, leg 5 parts and shoe 4 parts. The hip and knee joints are actuated in sagittal plane while the ankle has passive joints in sagittal and front plane. The mass

of each component was defined in SimWise software according to experimental prototype 15 Kg per leg. The weight of exoskeleton parts such as thigh, leg support, and shoe were specified by the designer and respected in this work, although the weights of some smaller parts were adjust as the individual weights were not stated in the initial design. The exoskeleton shown in Figure 3.7 was developed to provide assistive torque in sagittal plane for both hip and knee joints. In SimWise these motors are represented as revolute motors and the proposed exoskeleton in this work provides 40% of the total torque required (Virk et al., 2014).

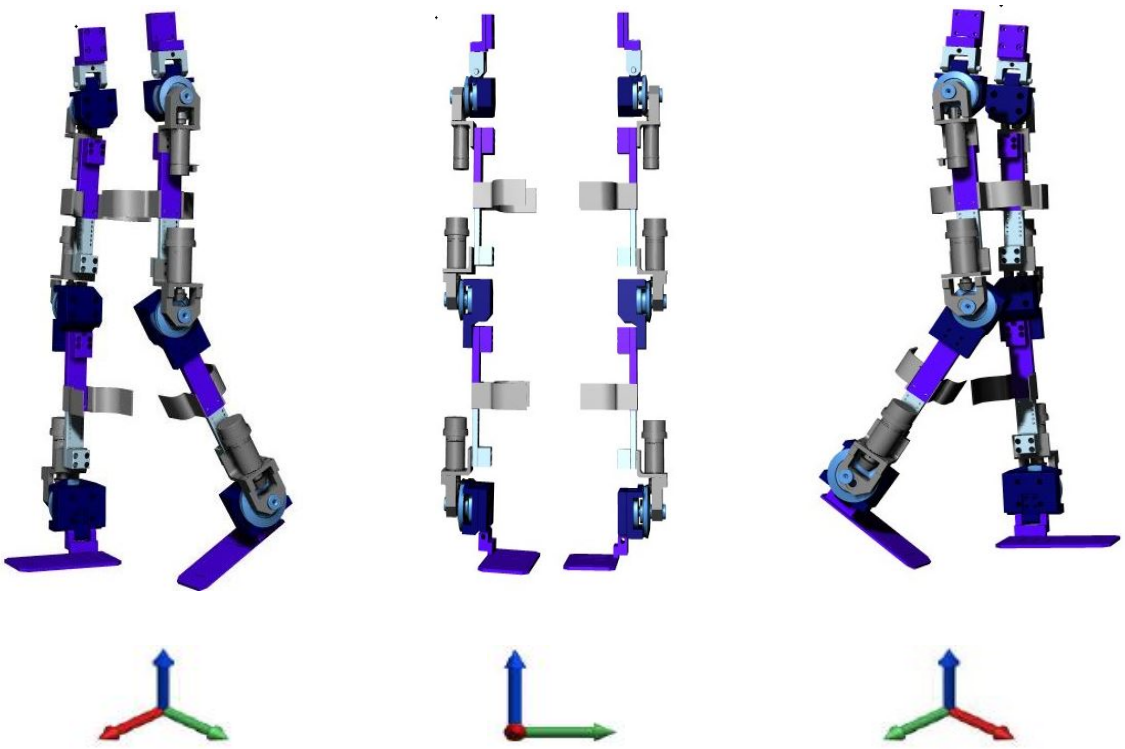

(a) Side view (b) Front view (c) Side view

Figure 3.7: The exoskeleton in different position

For the prototype the motors were considered by PCM to provide 30% of the total torque required to perform basic walking task. The hip joint is powered by DC motor (Maxon flat brushless), EC45, 70 watt and selected a gear reduction of 19:1 which supplies maximum continuous torque of 17.97 Nm. DC motor (Maxon flat brushless), EC60, 100 watt is used for knee and ankle joints with gear reduction of 53:1 and maximum torque of 20.38 Nm. MILE incremental encoder has been integrated to all motors. It has 2 channels, 1024 count per turn, 500 KHz maximum frequency and 6000 rpm maximum speed. The

system is integrated with EPOS2 50/5 controller cards to transmit and receive data from encoder and the PC by USB port to the motor. In SimWise visualization software, meters are added to the hip, knee, ankle joints to measure orientation from the SimWise plant and send as feedback to the controller. Revolute motors are considered to actuate the hip and knee joints and be driven by various quantities such as orientation, torque, angular velocity and angular acceleration.

The lower limb exoskeleton frames link to the waist and feet of the humanoid model by belt and shoe strap respectively through rigid joints, while they link to thigh and leg support by braces which are set to collide with human leg. The assembled version allows to drive the lower limb body movement in walking or sit to stand scenarios when the joint is actuated or follow the orientation in passive joint. A combination of humanoid model and the EXO-LEGS exoskeleton is depicted in Figure 3.8 in different positions

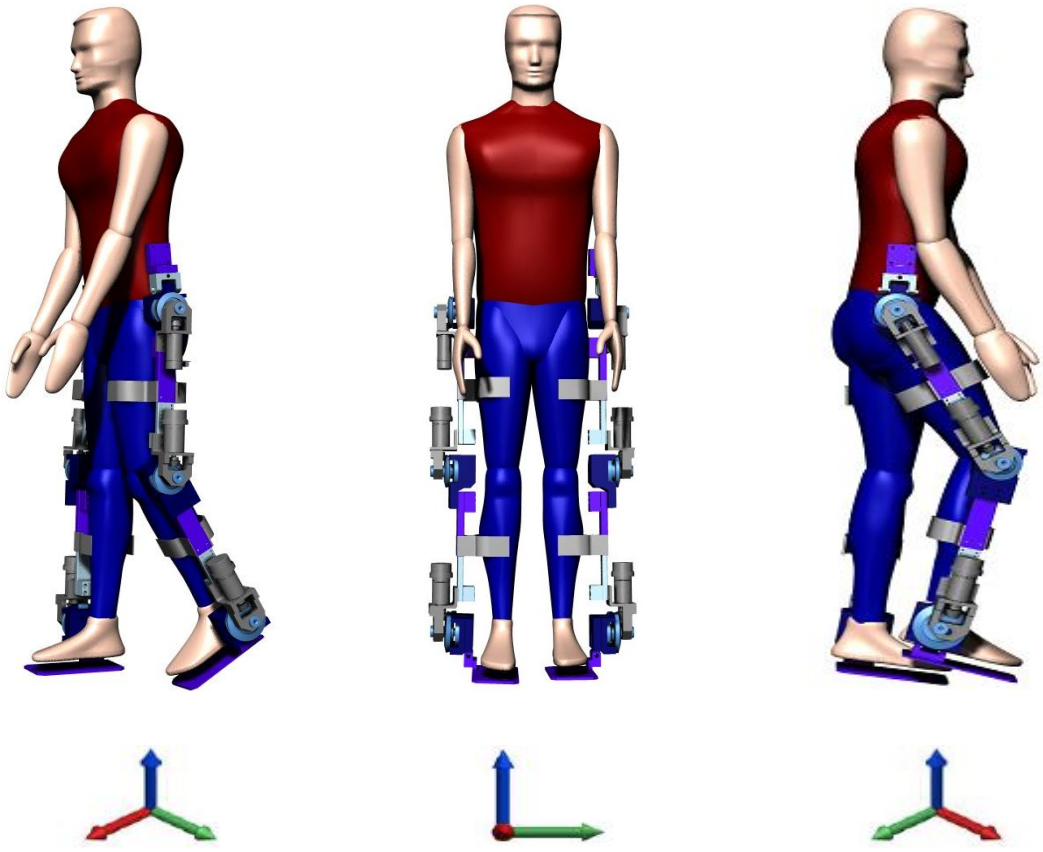

(a) Side view (b) Front view (c) Side view

Figure 3.8: A combination of humanoid and exoskeleton in different positions

3.6 SimWise integrated with Matlab/Simulink

In order to control the humanoid model and exoskeleton system in SimWise, it is important and significant to incorporate with Matlab /Simulink. Matlab provides various tools, which facilitate investigating different control strategies and validating their functionality in SimWise without building a physical prototype. The major purpose of selecting SimWise was its facility to send and receive data to and from Matlab by incorporating a block called SWPlant in the Simulink environment. This block allows searching and selecting the SimWise file with WM3 extension. The inputs and output control signals can easily selected from Matlab for instance an actuator as a revolute motor in SimWise is represented as input in Matlab and meters as sensors in SimWise are represented as outputs in Matlab. As mentioned previously, a revolute motor represents an activated joint, and it can be driven by torque, orientation, angular acceleration and angular velocity. The torque is selected to control joints for most cases in this project; torque of joint name appears as input slider in SWPlant. Correspondingly, as stated in Table 3.1 a meter of force, torque, orientation and velocity is inserted to control the joints. Table 3.2 illustrates the output control signal options. When the input and output signals are selected they connect to SWPlant block via multiplexer in input and demultiplexer at output. Figure 3.9 displays the way in which SimWise connects to Matlab in Simulink while Figure 3.10 shows the selection mechanism of SimWise file and input/output signals.

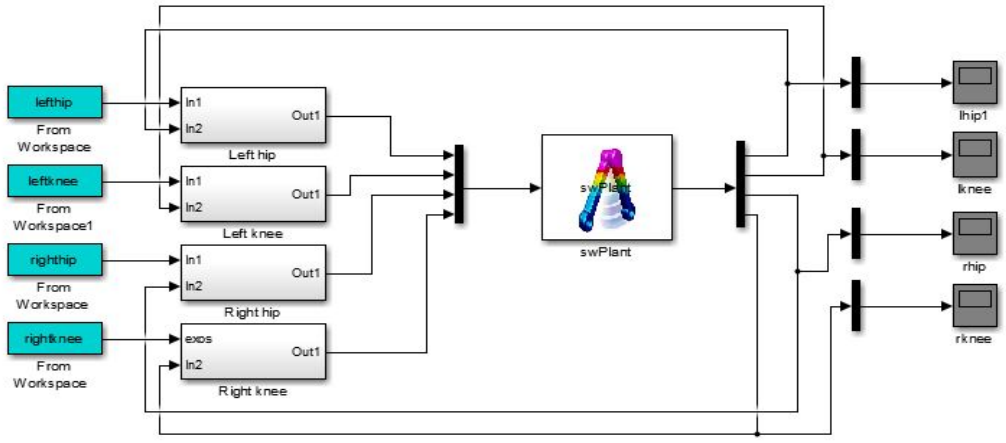

Figure 3.9: Block diagram of SWPlant in Simulink implementation

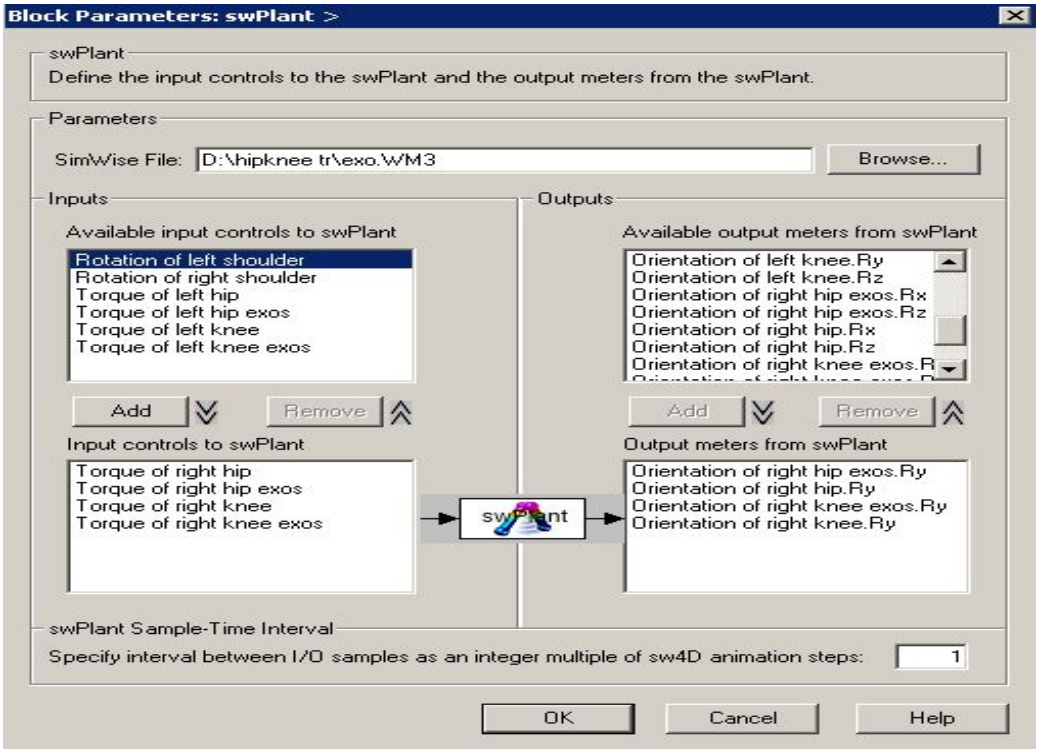

Figure 3.10: SimWise plant

3.7 Summary

The development procedure of a CAD model of humanoid and an actuated lower limb exoskeleton has been presented using vN4D and SimWise. The significant criteria in developing the model have been stated. The humanoid model has been created based on anthropometric data taken from Winter(2009).

The body segments of the model have been designed relative to full body height and weight and connected using suitable constraints. The designed models have then been simulated in virtual software environment and controlled in manner to achieve the desired objective, i.e. to provide mobility assistance to elderly people. The developed will be used in subsequent chapters to test and evaluate developed control mechanisms.

The integration methodology to incorporate SimWise virtual environment with MATLAB Simulink has been described. Such mechanism is significant in this work as it forms a platform for test and verification of the control strategies investigated in the research.

Chapter 4

Control of Lower Limb Exoskeleton

4.1 Introduction

This chapter presents development of control strategies for lower limb exoskeleton for elderly mobility assistance. Three different types of controller , namely Proportional Integral Drivative (PID), fuzzy logic control (FLC), and Fuzzy adaptive PID control. The performance of the controllers are evaluated on a comparative basis in terms of the output response trajectory.

Optimisation algorithms are further used to tune the controller parameters on basis of minimising the root mean square output error. Two types of optimisation algorithms are employed in this work. These are Spiral Dynamic Algorthim (SDA) and Invasive Weed Algorthim (IWA).

4.2 Controller theory

Controlling the exoskeleton effectively in a way to increase efficiency of the device is a significant consideration in exoskeleton system. The necessity to improve the control strategy in driving actuators of rehabilitation device will decide the growing progression of lower-limb exoskeletons. The controller types are widely varied from one type to others. The characteristics of lower extremity exoskeleton system show that it is very complex and non-linear, therefore the configurations are quit complex to represent mathematically. Based on aforementioned research, one may utilize a conventional PID controller in a feedback

loop to control the output trajectory of the system. Nevertheless, the results obtained will not be optimum for most cases, and the system may not be accurately controlled. Thus, the result of PID position control may not be impressive. For that reason, conventional PID controllers may be implemented with supplementary control strategies, such as auto tuning, and adaptive control. Moreover, intelligent algorithms, such as neural network and fuzzy logic control are able to address the complications of nonlinear systems, and do not require precise dynamical models. .

4.3 PID controller

Conventional PID control is perhaps the most popular control algorithm used in controlling industrial systems. In fact, more than 50 percent of industrial applications use PID control due to its simplicity in implementation, reliability, robustness to uncertainties as well as ease to tune. Particularly, when the mathematical representation of the plant is not available, PID control appears to be beneficial. However, the results obtained are not optimum for most cases.PID control is considered as a kind of automatic control. It measures the actual signal of the plant and the desired signal and computes the difference to generate a control action to reduce the difference to zero or close to zero (Ogata, 2010). Three main tunable parameters of thePID are proportional K_p, integral K_i and derivative K_d. These parameters are associated with the error proportion, error integration and the change of error respectively, as shown in Figure 4.1 (Ogata, 2010; Sung et al., 2009).

The proportional part (P): $up(t) = K_p e(t)$

The integral part (I): $ui(t) = K_i \int_0^t e(t)dt$

The derivative part (D): $ud(t) = K_d \frac{de(t)}{dt}$

where, e(t) is the difference between the plant output and the Reference input, and up(t), ui(t) and ud(t) represent the control output due to proportional, integral and derivative parts respectively.

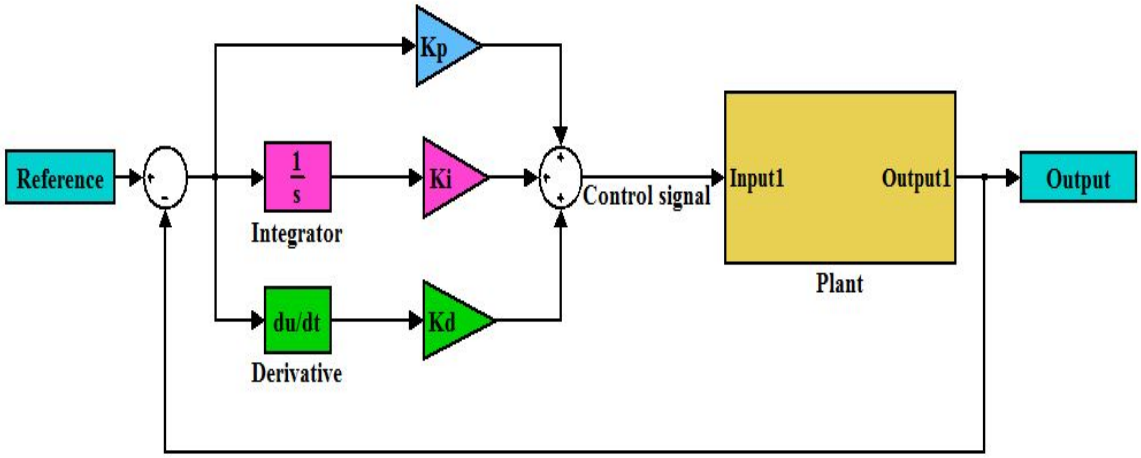

Figure 4.1: Block diagram of PID controller

The output of the PID controller is the sum of the above-mentioned three parts:

$$U(t) = K_p e(t) + K_i \int_0^t e(t)dt + K_d \frac{de(t)}{dt} \tag{4.1}$$

The integral and derivative gains are alternatively represented as Ki=Kp/Ti and Kd=KpTd, where T_i is the integral time and T_d is the derivative time Ogata (2010).

Firstly, the proportional part essentially acts as amplifier with tunable gain. It aims to maintain the system stable through regulating the control signal to diminish the error and the rise time of the output to desirable value. Secondly, the integral part tends to eliminate the steady state error by adjusting the control signal according to the accumulative error. The system order increases when adding the integral part, therefore the system might be unstable. Finally, the derivative part reduces the overshoot of the response using change of error and increases the system stability. Combination of the three terms weighted by their gains will significantly reduce the error associated with control signal (Ogata, 2010).

In practical, applications and the desired system reaction adjudicates the appearance of the three controller parts. Consequently, the controller is renamed by the employed parts such as PI, PD, P, or I controller reflecting the absence of parts. There are various methods used for tuning the controller gains such as Trial and error, Cohen-coon, Ziegler-Nichols, and software tools. Frequently, Trial and error is the most commonly used to determine the PID controller gains by investigating the dynamical behaviour of the controlled plant

output (Ogata, 2010; Sung et al., 2009).

It is extremely important to understand the effects of the parameters on the behaviour of the process output for successful tuning.

The PID controller demonstrates the following dynamic behaviour for a step setpoint change.

- If the process output shows a big oscillation, then the proportional gain K_p is too large.
- If the controlled process output shows an overdamped response, then the proportional gain K_p of the PID controller is too small.
- For a positive step setpoint change, if the process output oscillates and the process output stays above the setpoint longer than under the setpoint, then the integral time T_i is too small that means the integral control action is too strong.
- For a positive step setpoint change, if the process output oscillates and stays under the setpoint longer than above the setpoint, then the integral time T_i is too large that is, the integral action is too weak.
- If the process output shows a high-frequency oscillation from the start to the steady state, then the derivative time T_d is too large. This is due to the amplification of a high frequency signal by the strong derivative part (Sung et al., 2009).

4.4 Fuzzy logic

Lotfi Zadeh from California University proposed the concept of fuzzy set theory in 1965 for the first time (Zadeh, 1965). Fuzzy logic has characteristic attribute to incorporate the uncertainty and nonlinearity of the system (Engelbrecht, 2007). In this regard, fuzzy logic plays a crucial role in the powerful human facility of making rational decisions of uncertainty and imprecision environment by human being (Zadeh, 1988). Fuzzy logic shows significant advantages due to its capability of incorporating fuzzy linguistic information that are close to human cognition.

In 1974 Mamdani used the theory in practical implementation of a steam engine controlled by fuzzy logic (Mamdani, 1974). Fuzzy logic has greatly succeeded in most disciplines from engineering to social behaviour because it is able to create knowledge base rule similar to human thinking. Fuzzy logic control (FLC) is significantly superior in contrast to conventional methods relative to theory and practical (Wang, 1993). Moreover, it is easy to implement fuzzy logic in terms of understanding the environmental behaviour of real systems.

A considerable disadvantage of Mamdani type fuzzy logic is formal assessment of its stability because there is no standard mechanism to establish or analyse the system stability. However, many important reasons have strongly motivated the implementation of a fuzzy logic methodology in this work:

- Fuzzy logic principles are easy to understand especially for those who are not control specialists because it imitates the emulation of human control strategy.
- It is simply implemented to admit high level of equivalent implementation for hardware and software.
- The development cost is inexpensive therefore software and hardware are easy to develop.
- It is suitable for systems with difficult mathematical representation and depends on human experts to provide linguistic information for the system control directions.

- Fuzzy control is a model free technique that does not need a mathematical identification of the system under control.
- It delivers nonlinear controllers, which are suitable for nonlinear systems due to the nonlinearity components in fuzzy control.

Four vital parts constitute a fuzzy logic controller; fuzzification, rule base, inference mechanism, and defuzzification. Figure 4.2 shows block diagram of a typical fuzzy logic architecture. A brief description of each part is presented in the following sections.

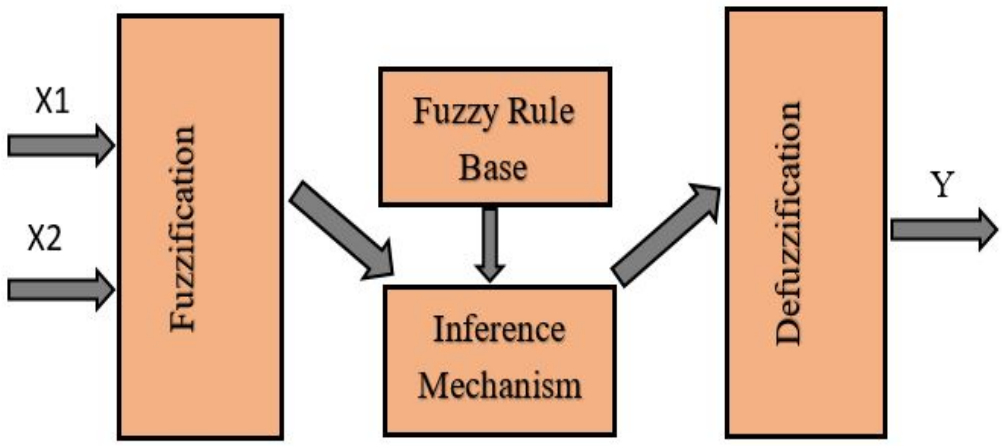

Figure 4.2: Fuzzy logic architecture

4.4.1 Fuzzy sets

A Set is a group of objects of different types such as trees, tables, names, arrays, books, etc.; known as individual elements sharing some common features. Usually a set is determined by identifying the members, each individual element in the collection is distinguished as a member, or an element, of the set. Therefore, the classical fuzzy set theory builds based on the fundamental theory of set. In general, fuzzy set involves of a membership function and universe of discourse U, which represents the range of possible numerical values defined for the fuzzy variable (Chen and Pham, 2000). If X is a set, and u is an element of set X, then the following symbol means that u belongs to set X: $u \in X$, and if u does not belong to set X then the representation would be written as: $u \notin X$.

4.4.1.1 Fuzzy set operation

Many fuzzy logic operations can be applied on fuzzy sets such as union, complement, equality, containment, and intersection (Chen and Pham, 2000; Ying, 2000). Two fuzzy sets A and B are defined in U, they are equal if and only if $\mu_A(x) = \mu_B(x)$ for all x $\in$ U where μ_A and μ_B represent degrees of certainty of set A and B in U. The set B is contained in set A, denoted by B $\subseteq$ A, if and only if $\mu_A(x) \geq \mu_B(x)$. The following membership functions represent the union, intersection and complement respectively;

$$\mu_{A\cup B}(u) = \begin{cases} max(\mu_A(u), \mu_B(u)) \\ or \\ \mu_A(u) + \mu_B(u) - \mu_A(u) \cdot \mu_B(u) \end{cases} \tag{4.2}$$

$$\mu_{A\cap B}(u) = \begin{cases} min(\mu_A(u), \mu_B(u)) \\ or \\ \mu_A(u) \cdot \mu_B(u) \end{cases} \tag{4.3}$$

$$\mu_{\overline{A}}(u) = 1 - \mu_A(u) \tag{4.4}$$

4.4.1.2 Membership function

The membership function $\mu_A(u)$ measures the fuzziness of set of element within universe of discourse, it quantifies a degree of certainty that each element belongs to the universal set U. There is a specific boundary for each membership function that begins from one point and terminates at another (Ying, 2000). On the other hand, this boundary might be on different shape such as a Triangle, Trapezoidal and Gaussian as shown in Figure 4.3, or some other type. Normally, Gausian is the widely used in most engineering applications because it gives smooth transition for good decision making process rather than other

types. Gausian MF has two important parameters m,σ which refer to the centre and width of MF respectively. However,the membership function transforms the fuzziness degree of inputs and outputs into a normalized interval [0, 1] or [-1, 1].The membership function can be represented in either continuous or discrete domain. A is a fuzzy set of ordered pairs of an element u in the Universal set U and its membership degree is denoted as:

$$A = \{(u, \mu_A(u))/u \in U\} \tag{4.5}$$

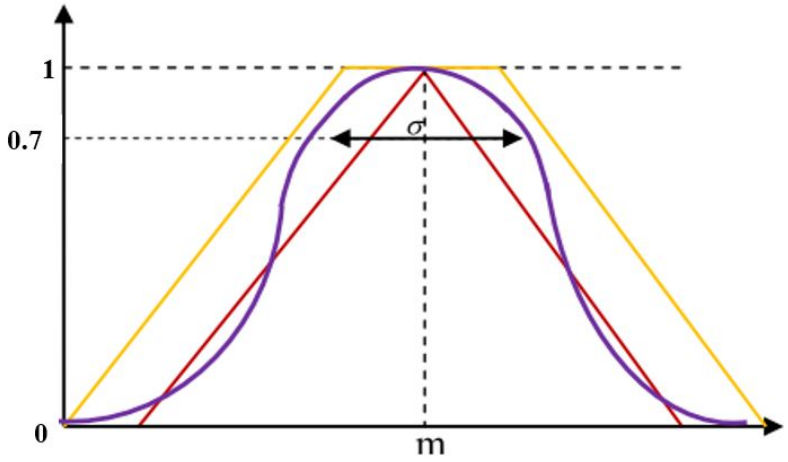

Figure 4.3: Trapezoidal, Gaussian and Triangular MF

4.4.1.3 Linguistic variables

The fuzzy set principle shows a logical approach to formulate the vague and imprecise information in linguistic variables form (Wang, 1997). In fuzzy systems, a linguistic variable defines a fuzzy variable that exists with value of words or sentences in natural language. Linguistic variables consider the essential part of writing the rules in a fuzzy system (Passino et al., 1998). The linguistic terms can be divided into three groups.

- Primary term is the simple one, which is used to characterize fuzzy sets. For example: Short, Medium, and Tall.
- Connectives: this term decides the calculation of fuzzy set output by the connection between the input variables with the operation. For instance And, Or, Not.

- The Hedge: this term is an addition to the primary terms when it is required to define more fuzzy sets , such as More, Most, Very, or Less.

4.4.2 Fuzzification

Fuzzification is a first internal block of FLC architecture , and is a mathematical process to convert a numeric value into fuzzy input. In other words, it is a procedure of transforming from a physical input variable to linguistic input variable in universe of discourse by associating one or several membership functions. Figure 4.4 illustrates an example of a traingular membership function . Generally, this conversion can be represented in two ways; singleton and non-singleton (Kovacic and Bogdan, 2005; Passino et al., 1998). Note that the singleton fuzzification is usually implemented for the noiseless case.

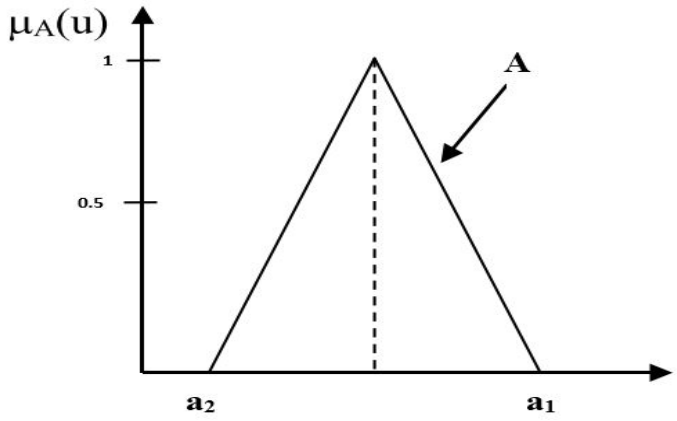

Figure 4.4: Triangular membership function

The singleton fuzzy set A_{ui} is described as :

$$\mu_{A_{ui}}(u) = \begin{cases} 1 & if \quad u = u_i \\ 0 & otherwise \end{cases} \tag{4.6}$$

The non-singleton fuzzy set A_{ui} is (triangular, trapezoidal, Gaussian MF) such that:

$$\mu_{A_{ui}}(u) = \begin{cases} \dfrac{u - a_2}{m - a_2} & a_2 \leq u \leq m \\ \dfrac{a_1 - u}{a_1 - m} & m \leq u \leq a_1 \\ 0 & a_2 \geq u \geq a_1 \end{cases} \tag{4.7}$$

4.4.3 Fuzzy inference mechanism

An inference mechanism is formulating process of a nonlinear mapping from the specified input space to an output space. The mapping has a basis from which selections could be accomplished. The fuzzy inference process needs fuzzy logic operators, membership functions and if-then rules(Wang, 1993). In most cases, there are three fuzzy inference types widely employed in control applications. These are Mamdani, Sugeno and Tsukamoto fuzzy inference. Fuzzy inference, in addition are identified as fuzzy models. The differences of their processes are the consequents of their fuzzy rules, aggregations and defuzzification techniques. Therefore selecting an alternative fuzzy inference may give different computational time (Engelbrecht, 2007).

Most approaches adopt is Mamdani fuzzy inference. In Mamdani inference the output membership functions form fuzzy sets, while in Sugeno inference the fuzzy rule Mamdani consequent is replaced by a function (Ying, 2000).

4.4.4 Fuzzy rule base

The heart of fuzzy logic system is fuzzy rule base. A collection of fuzzy If-Then rules constitute the fuzzy rule base. In general, for fuzzy systems a set of linguistic statements play a significant role in representing the dynamical behaviour of the system based on human knowledge and experience of experts and linking the fuzzy input variable to fuzzy output variable. Two main parts of a fuzzy If-Then rule are the antecedent part and consequent

part (Engelbrecht, 2007; Passino et al., 1998; Wang, 1997).

The antecedent part of the fuzzy If Then rule part, and the consequent part is the outcome part. The general form of fuzzy rule is:

If antecedent(s) Then consequent(s)

In addition, several linguistic variables might be used in the rules for condition and conclusion parts. Therefore, an FLC can be applied to multi input multi output (MIMO) problems and as well as to single input single output (SISO) problems. For typical SISO system the control signal regulates based on the error signal. Fuzzy systems can be classified into two groups depending on their fuzzy rules category.

- Standard fuzzy system: This type of fuzzy system utilises Mamdani-type linguistic fuzzy rules, which are solely formed from linguistic variables and values. They are simply abstract ideas about how to achieve good control. The general form of Mamdani rules is:

  IF $< antecedent >$ OPERATOR $< antecedent >$ THEN $< consequent >$

  This sort of fuzzy system is used for all the FLC strategies during this study. For instance:

  IF e(t) is NB AND Δe(t) is NB THEN y(t) is NB

  IF e(t) is PB AND Δe(t) is Z THEN y(t) is PS

  Where the linguistic variables e(t), Δ(t) and y(t) are the error, change of error and output of the system whereas the NB, NS, Z, PS and PB are the linguistic values linked the rules into fuzzy set which refer to negative big, negative small, zero, positive small and positive big respectively.

- Functional fuzzy system: This type of system is denoted as Takagi-Sugeno-Kang (TSK) fuzzy system, proposed as substitutional to the standard fuzzy systems. The TSK rules can be defined as follows:

  IF x_1 is ${C^1}_1$ and$\cdots$ and x_n is ${C^1}_n$, THEN Y^1 = ${c^1}_0$ + ${c^1}_1 x_1$ +.....+ ${c^1}_n x_n$

  where ${C^l}_i$ are fuzzy sets, ${c^l}_i$: are constants, and l = 1,2, ... n is the rule number. The

IF parts of the rules are the same as in the ordinary fuzzy IF-THEN rules, but the THEN parts are linear combinations of the input variables X = (x_1 ... , x_n) $\in$ U (Wang, 1997).

Standard fuzzy rules are the most widely used in many control applications. The human expert easily understands them, and the consequent parts are fuzzy sets. While in functional fuzzy rules the consequent part is a mathematical function. It is more accurate and convenient on mathematical analysis and system analysis.

4.4.5 Defuzzification

Defuzzification is an inverse procedure of fuzzification, which transforms the fuzzy output to real crisp value. The objective of this conversion is to translate the linguistic output reached by the inference mechanism into crisp value derived as actual input to the plant. It plays an important role in transforming the controller output back to crisp real signal accepted to the plant by connecting the controller rule base and the physical plant (Chen and Pham, 2000). There are several types of defuzzification strategies depending on the application such as:

- Max Membership Method
- Centre of Gravity (CoG) Method
- Mean Max Membership Method
- Middle of Maxima (MoM) Method
- Centre of Sum Method

In this study, Centre of Gravity Method is more favourable and used for most cases of implementing fuzzy logic control. In this method, the output of fuzzy inference mechanism is fuzzy set that the value of deffuzzified method lead to max MF usually close to one. Moreover, it is highly appropriate for feedback control applications because of its fine and smooth output transition. Figure 4.5 shows the CoG defuzzification method where

u_c represents the centre of gravity for the shaded area and the equations of calculation in continuous and discrete form are given as:

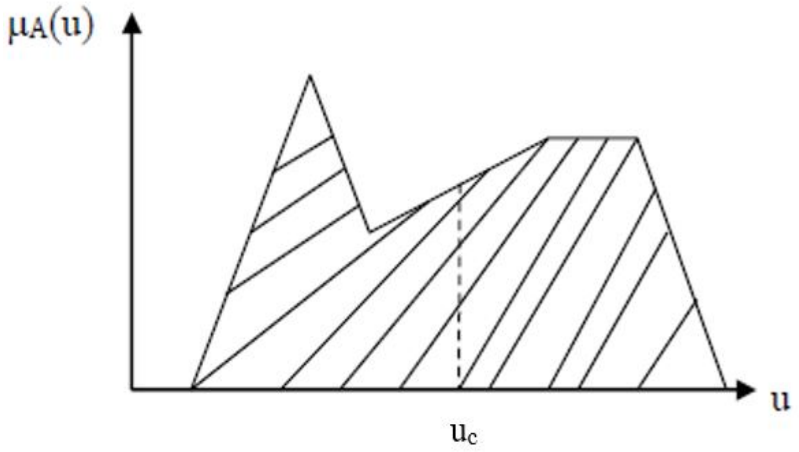

Figure 4.5: The COG defuzzification method on a fuzzy output

$$u_c = \begin{cases} \dfrac{\int \mu_A(u) \cdot u \cdot du}{\int \mu_A(u) \cdot du} & \textit{in the continous case} \\ \\ \dfrac{\sum \mu_A(u) \cdot u}{\sum \mu_A(u)} & \textit{in the discrete case} \end{cases} \tag{4.8}$$

4.5 Fuzzy PID-type control

The control efficiency and stability is play important role in achieving smooth and fast orientation tracking. A fuzzy logic adaptive PID -type controller is developed to reinforce the performance of the system and used in this work. Conventional PID is a common controller used in controlling of robotic systems. However, the limitation of PID algorithm is evident that in its poor adaptation to control nonlinear and complex systems; its parameters cannot be tuned on-line.

Therefore, a solution to deal with non-linearity and complexity of the system is to use an intelligent algorithm such as neural network and fuzzy theory (Yang et al., 2010). Such algorithms are widely used in cases where precise dynamic model of the system is not required (Yang et al., 2010; Zhao and Pan, 2010). Developing an adaptive controller by

combining fuzzy logic with PID will integrate the advantages of both controllers. Fuzzy self-tuning of PID parameters find the fuzzy relation between three parameters of PID and error e(t) and change of error ec(t). The structure of the control system design is presented in Figure 4.6. The fuzzy tuning PID controller structure consists of two inputs and three outputs. The inputs are the error and the change of error, where the outputs are the modification of PID parameters KP, KI, and KD.

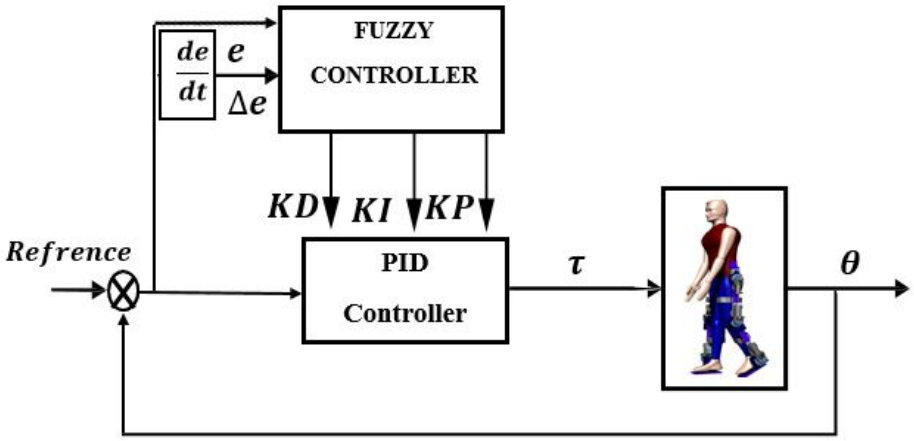

Figure 4.6: The structure of fuzzy PID controller

4.6 Optimization algorithm

Optimisation plays a significant role in addressing real world problems in various fields (Zang et al., 2010). It is one of the fast developing interdisciplinary research areas. Applying the optimum control parameters is one of the highest significant design criteria. The optimum gains improve the system response and reduce the energy consumed which lead to more efficient energy use. In this section, a brief overview of the Invasive Weed Algorthim (IWA) and Spiral Dynamic Algorthim (SDA) is presented.

4.6.1 Spiral dynamic optimisation algorithm

Spiral dynamic algorithm is a metaheuristic optimisation algorithm based on natural spiral motion, such as spiral galaxies, hurricanes, whirling currents and nautilus shells as presented in Figure 4.7. It is relatively new optimisation algorithm introduced by Tamura and Yasuda (2011a) and firstly reported in two dimension search spaces. Later, it was developed into a general model for n-dimension problems depending on the principle of two dimensional optimization design (Tamura and Yasuda, 2011b).

The shared feature of logarithmic spirals encouraged the authors in developing the algorithm, which they believed could make an effective search strategy. The algorithm was verified and compared with other proven search strategies, such as Particle Swarm Optimisation (PSO) and showing that it has effective solutions for the two-dimensional problems in three benchmark types. The SDA algorithm is simple, easy to implement with few control variables, has good local search capability, fast convergence (Benasla et al., 2014). The most important features of the SDA are the diversification and intensification occurring at the early and later phases through the search procedure respectively. Diversification is searching in exploration strategy for better solution where the search agents try to cover the global search area. While intensification demonstrates the exploitation methodology, in which the search points shift and converge toward the best global solution. A balanced combination of these techniques is crucially effective on the search strategy, which leads to accurate solution.

The searching agents in SDA move from one location to the other by dynamic step size. In SDA, all the search agents perform spiral motion from outermost layer to a centre. The step size of the spiral motion gradually decreases starting with large step and ending with small step at the centre point, Various spiral models are represented in Figure 4.7 in respect of different values of spiral radius, r and rotation angle θ ,where Case (1), Case (2) and Case (3) represent spiral forms with r = 0.9 , $\theta = \frac{\pi}{4}$, r = 0.95 , $\theta = \frac{\pi}{4}$ and r =0.95 , $\theta = \frac{\pi}{2}$ respectively.. Two important parameters directly affect the performance of SDA operation namely spiral radius, r and the displacement θ which affect the algorithm performance in

terms of accuracy and convergence speed.

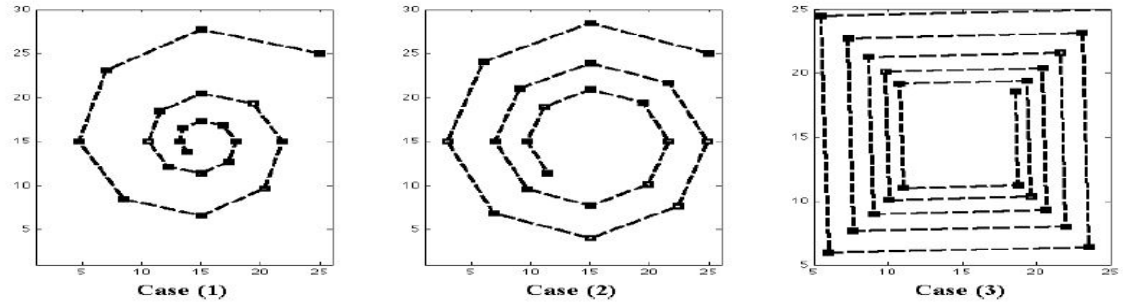

Figure 4.7: Graphical representation of spiral model
(Tamura and Yasuda, 2011a,b)

The rotation matrix for the n-dimension made of combinations of 2- axes is defined as:

$$R^n_{i,j}(\theta_{i,j}) = \begin{bmatrix} 1 & & & & & & \\ & 1 & & & & & \\ & & cos(\theta_{i,j}) & .. & .. & -sin(\theta_{i,j}) & \\ & & : & 1 & & : & \\ & & : & & 1 & : & \\ & & sin(\theta_{i,j}) & .. & .. & cos(\theta_{i,j}) & \\ & & & & & & 1 \\ & & & & & & & 1 \end{bmatrix}$$

The n-dimension spiral dynamic model is expressed using the rotational matrix as:

$$x_i(k+1) = S_n(r,\theta)x_i(k) - (S_n(r,\theta) - I_n)x^* \tag{4.9}$$

where

$$S_n(r,\theta)x(k) = (R_n n)(\theta n_i, n+1_j) \tag{4.10}$$

x is the coordinate of the point's location, and k is the number of iteration. Table 4.2 presents an explanation of parameters used in the SDA optimisation pseudo code.

Table 4.1: ASDA parameters

Symbols	Description
$\theta_{i,j}$]	Search point angular displacement on x_i-x plane around point of origin.
r	Spiral radius to be replaced by adaptive approaches as in step 2.
m	Total number of search points Maximum
k_{max}	Maximum iteration number.
x_i(k)	Position of i_{th} point generation.
R^n	Composition of rotational nxn nmatrix based on combination of all 2 axes.

A description of the n-dimension SDA optimisation pseudo code reported by Tamura and Yasuda (2011a) is as follows:

Step 0: Preparation

Select the number of search points m$\geq$ 2 , parameters 0 $\leq \theta$ <2π, 0 <r <1 of Sn (r,θ), and maximum Iteration number, kmax . Set k =0.

Step 1: Initialisation

Set initial points xi(0) in R^n i =1, 2...m in the feasible region at random and centre x as x* = $x_{ig}(0)$, ig =arg min_i f(x_i(0)), i =1, 2...m.*

Step 2: Updating xi

x_i(k+1) = S_n(r, θ) x_i (k)- (S_n (r, θ) -I_n) x , i = 1,2,...,m where spiral radius, r replaced by r_la or r_ea , and angular displacement, θ replaced by θ_{la} orθ_{ea}.*

Step 3: Updating x*

x= x_{ig} (k+1), ig =arg min_i f(x_i (0)), i =1, 2...m.*

Step 4: Checking termination criterion

If k =kmax then terminate. Otherwise set k =k +1, and return to step 2.

4.6.2 Invasive weed optimization algorithm

Invasive Weed Algorthim (IWA) is a type of ecologically inspired optimization algorithm based on colonizing of weeds, and was introduced by Mehrabian and Lucas (2006). The IWA mimics the natural behaviour of weeds in colonizing suitable place for growth and reproduction. Weeds are vigorously invasive and robust plants able to adapt to the environmental changes, posing as threat to agriculture. The robustness, adaptation and randomness of the algorithm are shown by emulating a natural phenomenon of invasive weeds. It has been used for many engineering and non-engineering fields (Nikoofard et al., 2012; Zaharis et al., 2013). In the IWA algorithm, the process simulates the survival of weeds colony, where it starts from setting the initial plant in the search area. The plant spreads randomly in the search place. Each member is able to produce seeds. However, the seeds production depends on their relative population fitness. The best member produces maximum number of seeds (s_{max}) and the worst produces minimum number of seeds (s_{min}) where the production of the weeds of each member is linearly increased (Mehrabian and Lucas, 2006; Yılmaz and Küçüksille, 2015) . After that, the seeds scatter randomly over the search space near to its parent plant. The scattering process uses normally distributed random number with standard deviation (SD) as:

$$\sigma_{iter} = [\frac{(iter_{max} - iter)}{iter_{max}}]^n(\sigma_{max} - \sigma_{min}) + \sigma_{min} \tag{4.11}$$

where $iter_{max}$ is maximum iterations, iter is current iteration, n is the nonlinear modulation index, σ_{max} is usually initial SD and σ_{min} is the final SD in the optimization process. The seeds with their respective parent plants are considered as potential solution for subsequent generations. In order to maintain the size of population in the search area, the algorithm conducts a competitive exclusion, where an elimination mechanism is employed; if the population exceeds its maximum size only the plants with better fitness can survive. Those with better fitness produce more seeds and with high possibility of survival and become reproductive. The process continues until the maximum number of iterations is reached

and the plant with best fitness is closest to the optimal solution.

Modified IWO with exponential seeds-spread factor

In order to enhance the search strategy and get desired global minimum a new modification was proposed by Kasdirin(2016). The proposed modification improves the neighbourhood search of weeds depending on their cost function. The new search mechanism has been formulated and verified by optimizing several benchmark functions in comparison with the original IWO method.The modified IWO with exponential seeds-spread factor (MIWO-eSSF) algorithm is aimed to provide better balance between global and local search as well as achieve more accurate result during the iteration process. However, variation in the SD is made exponential in the spatial dispersion process. By adding the new factor in the equation (4.11), the new SD is given as:

$$\sigma_{iter} = k[\exp\{\tau[\frac{iter_i}{iter_{max}}]^{\delta}\}](\sigma_{ini} - \sigma_f) + \sigma_f \tag{4.12}$$

where the values of σ_{ini},σ_f,and $iter_{max}$ are as described in the initial parameters setting of the algorithm. The values of τ and δ are pre-set to determine the shape of the exponential slope changes of the SD during the iteration process. It is assumed that τ = 2 and δ = 4, which are found as competitive values for MIWO-eSSF. In this work, investigations on adaptive spread factor distribution of SD of the seeds are carried out. To make the computational complexity simpler, exponential distribution was adopted. In order to control changes of SD, the following spread factor relation is used:

$$\sigma_i = \frac{\sigma_{iter} - \sigma_{final}}{\frac{|f_i| - f_{max}}{ef_{min} - f_{max}}} + \sigma_{final} \tag{4.13}$$

where σ_i is SD for every i weed,f_{min} and f_{max} are minimum and maximum fitness functions in the colony respectively, $|f_i|$ is an absolute fitness value of every weed, σ_{final} is

final SD and σ_{iter} is SD for each iteration which is calculated using equation (4.12). Using the equation (4.13), the SD will vary in the range [σ_{final} σ_{iter}] at each iteration. In this way, the exploration ability of weeds located closer to the best weed increases and allows searching around the optimal solution. It is worth mentioning that modified SD equation (4.12) with the adaptive spread factor (4.13) is necessary to handle the task from a new point of view and an original improvement may be achieved based on the proposed strategy.

4.7 Summary

A general description of the control strategy adopted in this work has been presented. The control types considered in this work include PID, FLC, and fuzzy adaptive PID-type..

A brief description of two optimisation algorithms namely Spiral Dynamic Optimisation Algorithm (SDOA),and Invasive Weed Optimisation Algorithm (IWOA) has been presented. These algorithms are used in subsequent chapters for tuning of control parameters for optimum control performance.

Chapter 5

Control of Assistive Exoskeleton in Walking Mode

5.1 Introduction

This chapter presents simulation of assistive exoskeleton for elderly people during walking function. Investigations are carried out using a humanoid model with actuated lower limb exoskeleton. Three types of controller are used for low level control of exoskeleton's knee and hip joints. These are PID, FLC and adaptive fuzzy PID-type control, designed in Matlab/Simulink to control the lower limb joins for assistance and the motion visualised in graphic animation from vN4D or SimWise dynamic simulation software. Two optimization algorithms, namely SDA and IWA are used to tune the controller parameters. The system performance with these control techniques is evaluated and assessed based on best reference tracking and minimum mean square error. In this study, predefined reference trajectories are used as reference for humanoid walking with exoskeleton.

5.2 Walking gait and predefined reference trajectories

It is important to understand the walking performance of a normal person in order to implement controllers capable of assisting the walking of elderly people. This section illustrates the principles of walking cycle, phase and duration. Walking is three dimensional but this thesis focuses only on the sagittal plane as the largest motions, torques and powers are in this plane (Raychoudhury et al., 2014; Vaughan et al., 1992).

Locomotion is one of the most common crucial daily living activities of human beings. Each person in normal life has her/his own optimised gait pattern according to their body; the resulting gait may slightly differ from one person to another. A gait cycle is a term used to define a sophisticated function of locomotion. In general, the normal walking cycle is symmetric and consists of two phases: swing and stance. The stance typically lasts about 60 percent of the cycle, therefore it is called the long phase. Swing phase is 40 percent of walking cycle, so it is referred to as short phase. In stance period, the foot is in contact to the ground, and it is divided into five sub phases:

- Initial contact (0%): it is short period and starts when the heel touches the ground.
- Loading response (0-10%): in this phase the heel contacts the ground end when the foot is flat and the toes of the opposite foot leave the ground. Here, the shift of the weight occurs from one foot to the other.
- Midstance (10-30%): this phase starts when the foot is flat on the ground and the opposite foot leaves the ground completely by the supporting limb
- Terminal stance (30-50%): in this phase, the centre of gravity is on the reference foot and the heel rises off the ground. In addition, the opposite foot touches the ground.
- Preswing (50-60%) : it begins when the heel and the toes leave the ground and the other foot takes the load of the body.

On the other hand, in swing phase the foot releases from the ground and this is divided into three stages:

- Initial swing (60-70%) : this phase begins when the toes leave the ground and the knee makes maximum flexion.
- Mid-swing (70-85%): begins when the foot remains in the air and ends when the tibia is vertical to the ground.
- Terminal swing (85-100%): it is the last phase of gait cycle starts from vertical tibia and ends when the heel touches the ground again in initial contact phase. The philosophy of the walking is shown in Figure 5.1.

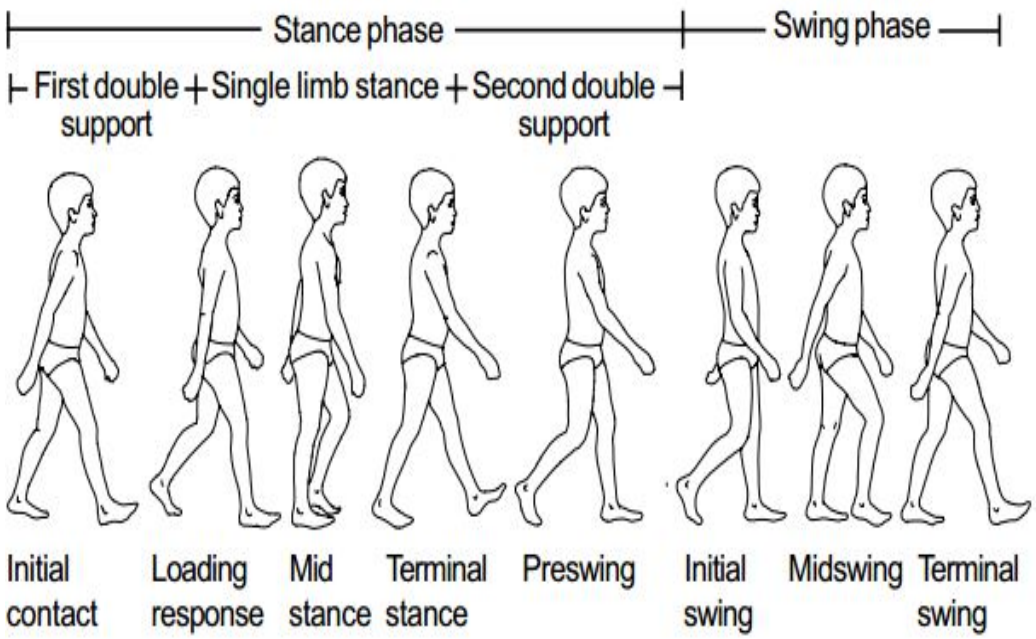

Figure 5.1: The normal gait cycle phases
(Vaughan et al., 1992)

The reference signal of human joint angles for a typical walking cycle were obtained from the Clinical Gate Analysis (CGA) with refrence to Kirtley(2006). The CGA angle data is typically collected using human video motion recording during the standard walking cycle as shown in Figure 5.2.

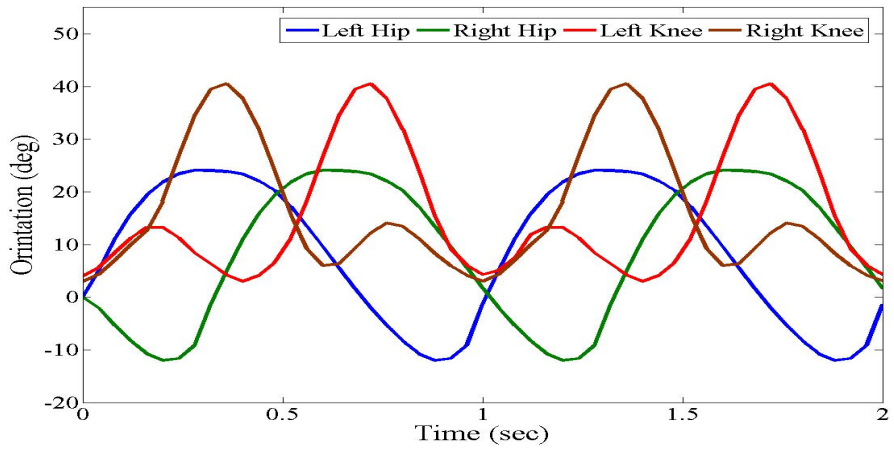

Figure 5.2: Walking reference trajectory
(Kirtley, 2006)

5.3 Implementation of PID with different gains

In this section, revolute motors are selected to actuate the humanoid lower limb model by torques, and designed PID reference tracking control for both hip and knee joints. A Simulink diagram is created in Matlab/Simulink with four PID torque controllers, two for hip (left and right) joints and two for knee (left, right) joints. Figure 5.3 shows a Simulink block diagram of the PID control structure utilised.

The input to PID controller is the difference between desired walking trajectory and the corresponding orientation measured from the plant. The controller action output is generated as torque to drive the hip and knee joints. A trial and error method was chosen to tune the controller parameters in order to obtain the best trajectory to track the predefined orientation reference.

Several PID gains were tested without saturation block in order to obtain a trajectory tracking with an acceptable torque , but the obtained torque was slightly higher than 300 Nm. Therefore, saturation blocks were added to avoid the peak in torque control signal; 200 Nm saturation block was added at the hip joints controller output and 160 N.m for knee joints. The root mean square error of the desired joint orientation and the actual joint orientation was determined according to the following equation:

$$RMSE = \sqrt{\frac{\sum_{i=1}^{n}(\theta_{reference} - \theta_{actual})^2}{n}} \tag{5.1}$$

For the first trial RMSE of 3.118 for left knee , 4.0826 for right knee , 3.3371 for left hip and 3.1965 for right hip were achieved with PID parameters shown in Table 5.1. The reference tracking and the torque profile are illustrated in Figure 5.3. Figures 5.4 and 5.5 show the performance of the predefine trajectory tracking and torque behaviour for the set of PID parameters with smallest RMSE , minimum RMSE of 3.2246 for left knee, 3.0968 for right knee, 2.7271 for left hip and 2.6219 for right hip were achieved with PID gains obtained from heurstic tuning as compared in Table 5.1.

For most testing cases with kd higher than 5 the system was unstable, while kp ,ki had larger value. The three gains were evenly set from 2 to 20 for kp, from 1 to 10 for ki and from 0.1 to 5 for kd.

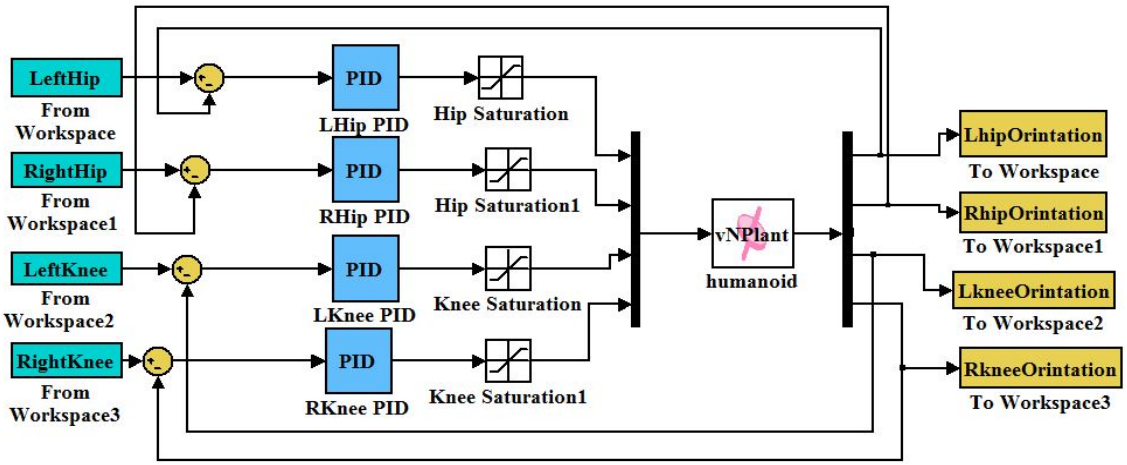

Figure 5.3: Simulink diagram to control humanoid hip and knee joints

Table 5.1: Comparison of PID parameters

Controllers	Gain Parameters	Step1	Step2
Left Hip	K1	2.17	17
	K2	4.	5.38
	K3	0.53	2.98
Right Hip	K4	8.09	14
	K5	2.	7.35
	K6	1.87	3.58
Left Knee	K7	8.47	8.2
	K8	4.57	7.67
	K9	0.21	0.28
Right Knee	K10	4.28	15.03
	K11	0.10	8.53
	K12	0.07	0.16

These parameters represent the initial condition for the PID controllers and after while the parameters will be the same for left and right knee joint and same situation for the hip joint. The RMSE values lower than 10 percent of the references amplitude is acceptable , which means less than 5 degree and 3 degree for knee and hip joints respectively. Moreover, in the second case with least RMSE value noticed that the torque profile for both lower limb joints were smoother with lower peak. It was observed that parameters with RMSE more than 10 percent gave unacceptable behaviour, with unstable trajectories.

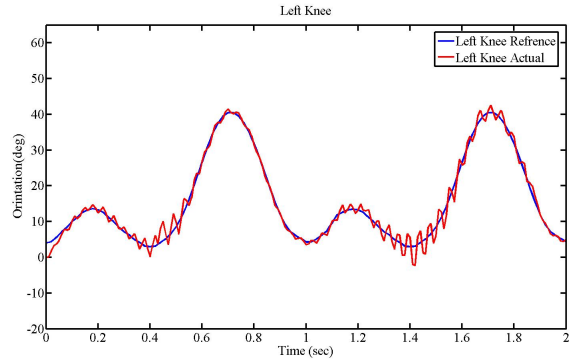

(a) Left knee orientation

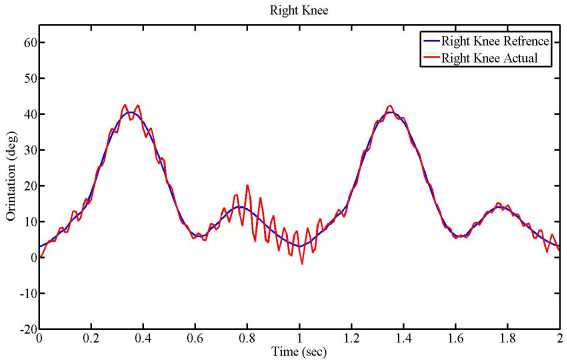

(b) Right knee orientation

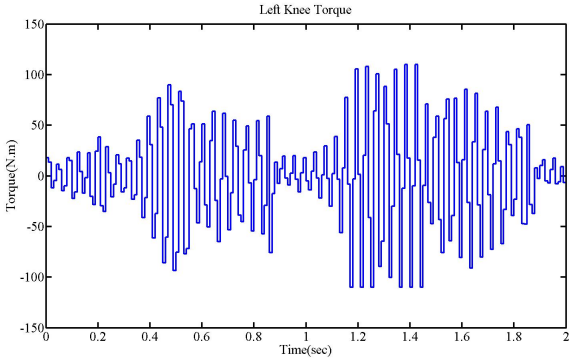

(c) Left knee torque

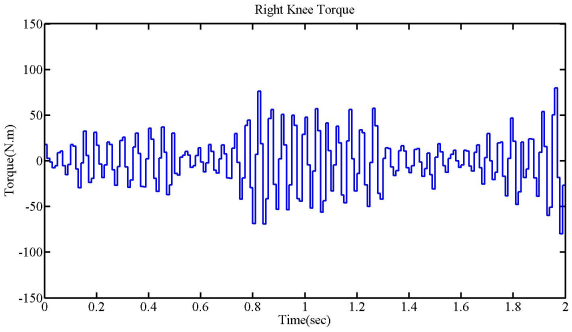

(d) Right knee torque

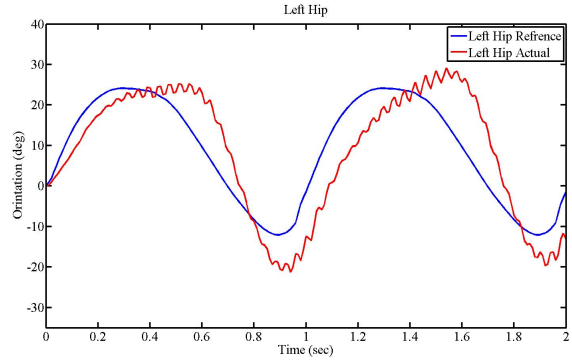

(e) Left hip orientation

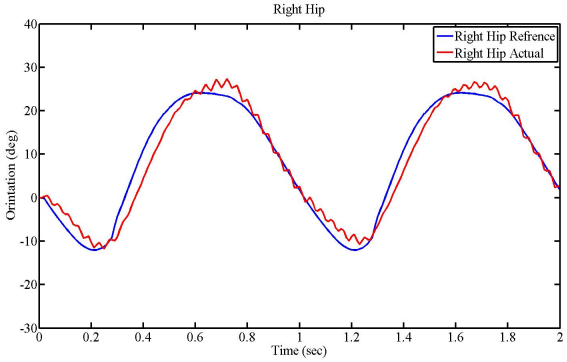

(f) Right hip orientation

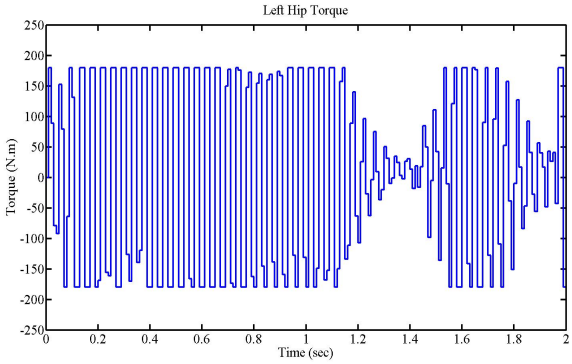

(g) Left hip torque

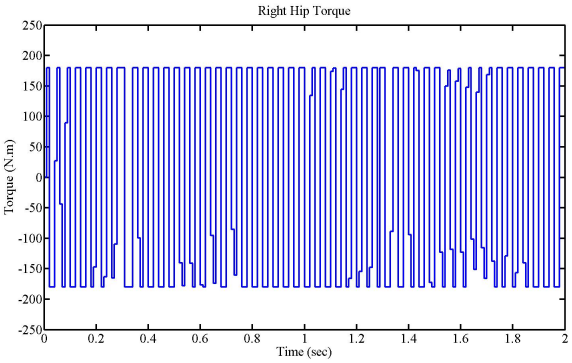

(h) Right hip torque

Figure 5.4: Orientation and torque for hip and knee joints with trial and error tuned PID

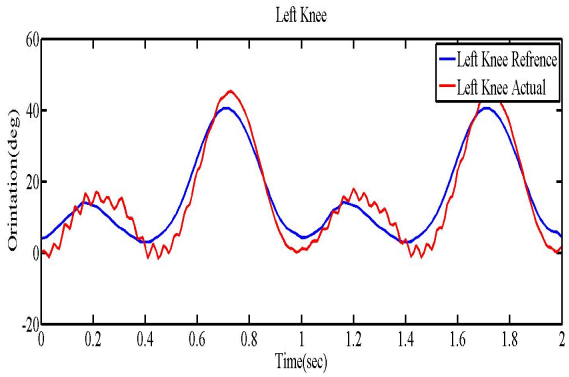

(a) Left knee orientation

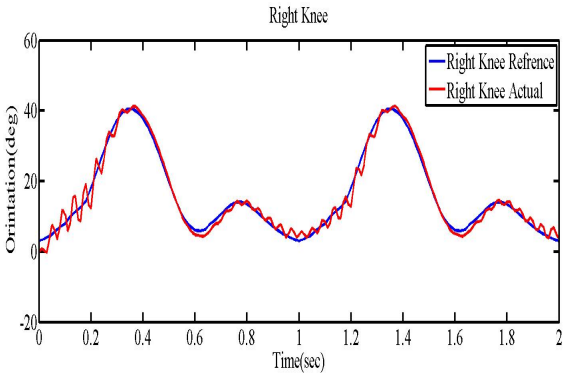

(b) Right Knee knee orientation

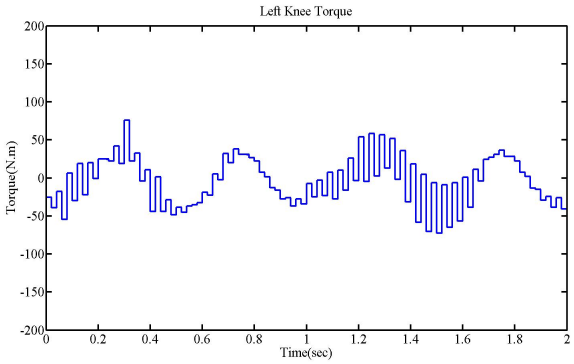

(c) Left knee torque

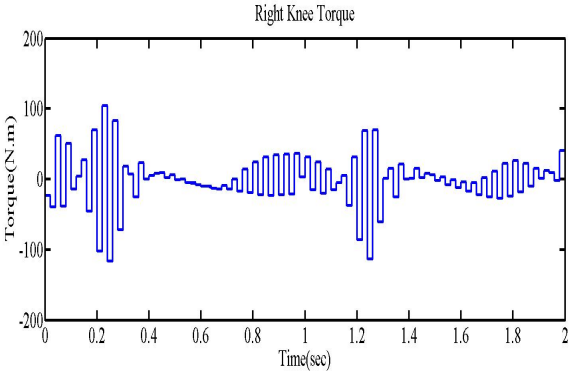

(d) Right knee torque

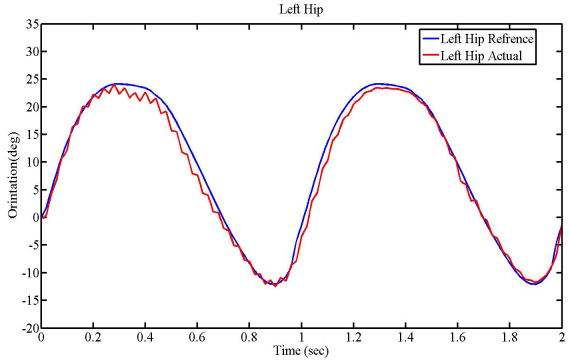

(e) Left hip orientation

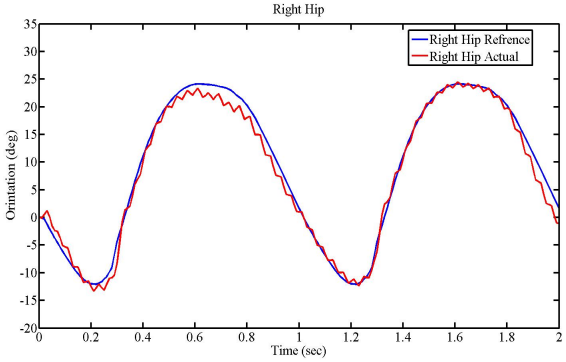

(f) Right hip orientation

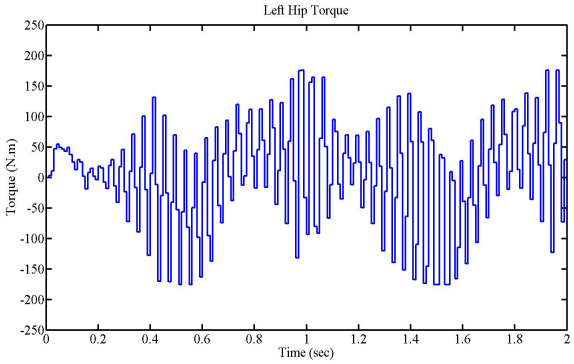

(g) Left hip torque

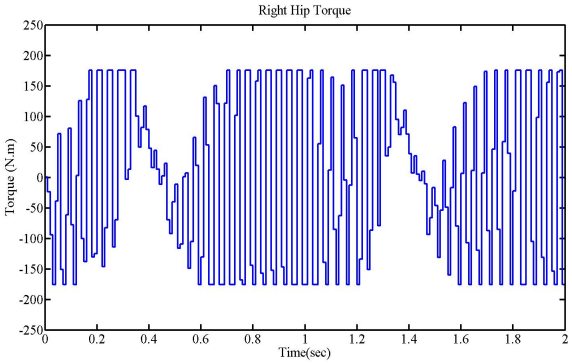

(h) Right hip torque

Figure 5.5: Orientation and torque for hip and knee joints with trial and error tuned PID

5.4 Optimizing the PID with SDA

The control scheme of humanoid lower limb is illustrated in Figure 5.3 with four feedback loops; left hip, left knee, right hip and right knee. Each loop has three parameters, which represent the PID gains. The SDA was used to tune the parameters of PID controller as shown in Figure 5.6. There were a total of 12 parameters, K1-K12 to optimise. The cost function used was sum of mean square error functions of the lower limb joints. This was formulated by their weighted sum, where the weight vector was selected as [w_1 w_2 w_3 w_4] = [0.25 0.25 0.25 0.25] providing equal weighting to all.

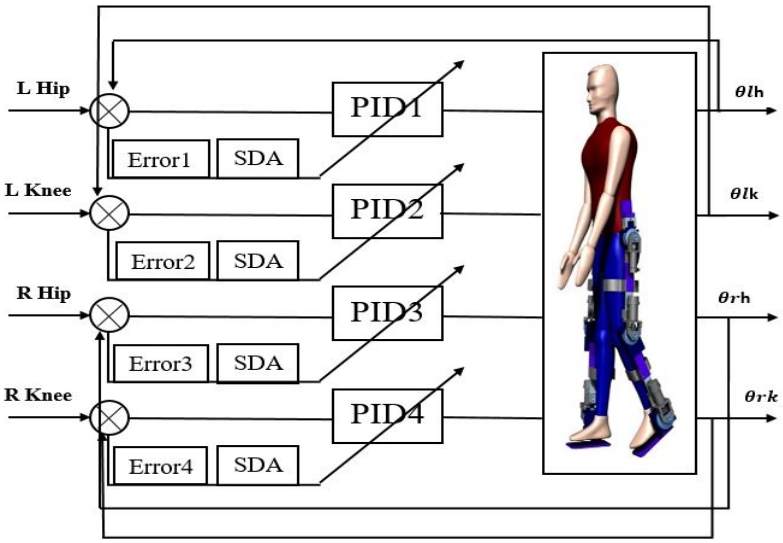

Figure 5.6: SDA tuning PID parameters

MSE of each control loop in the system was computed for the lower limb walking task as follows:

$$RMSE1 = \sqrt{\frac{\sum_{i=1}^{n}(\theta_{\text{left hip refrence}} - \theta_{\text{left hip measured}})^2}{n}} \tag{5.2}$$

$$RMSE2 = \sqrt{\frac{\sum_{i=1}^{n}(\theta_{\text{left knee refrence}} - \theta_{\text{left knee measured}})^2}{n}} \tag{5.3}$$

$$RMSE3 = \sqrt{\frac{\sum_{i=1}^{n}(\theta_{\text{right hip refrence}} - \theta_{\text{right hip measured}})^2}{n}} \tag{5.4}$$

$$RMSE4 = \sqrt{\frac{\sum_{i=1}^{n}(\theta_{\text{right knee refrence}} - \theta_{\text{right knee measured}})^2}{n}} \tag{5.5}$$

For this study, the cost function was calculated by summing the RMSE of all control loops as.

$$CostFunction = RMSE1 + RMSE2 + RMSE3 + RMSE4 \tag{5.6}$$

In the SDA process, 20 potential solutions were considered for this system with 50 iterations, and the best obtained fitness function value was 2.16 with RMSE of 2.14 for left knee , 2.16 for right knee , 2.18 for left hip and 2.16 for right hip.

Figure 5.7 shows reference tracking and the torque behaviour of the hip and knee lower limb joints. The SDA tuned parameters reduced the hip and knee joints torque as compared to trial and error method demonstrated in Figure 5.4 and Figure 5.5, where the knee torque was decreased from 120 Nm for heuristic tuning to nearly 90 Nm in SDA tuning as well as the hip torque profile reduced from 190 Nm to approximately 180 Nm. Similarly, the obtained performance was improved for the torque corresponding to the four joints (left hip, left knee, right hip and right knee) where the controller produced low torque using the optimized parameters. Table 5.2 shows the tuned parameters obtained by SDA.

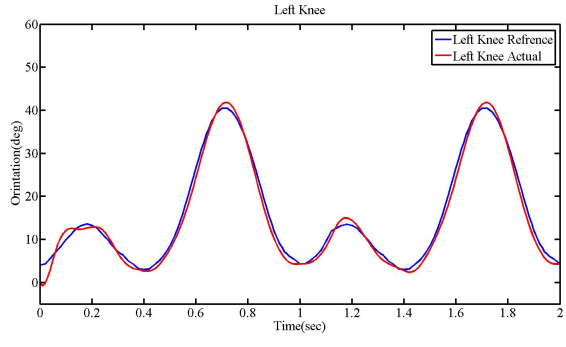

(a) Left knee orientation

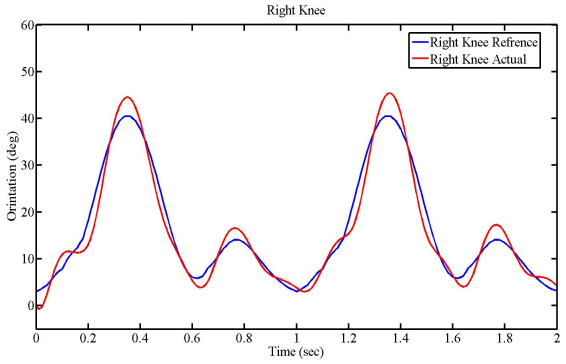

(b) Right knee orientation

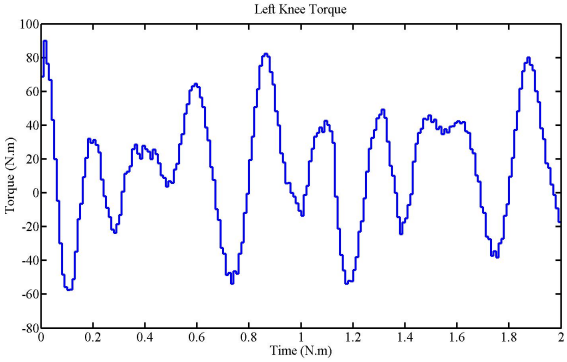

(c) Left knee torque

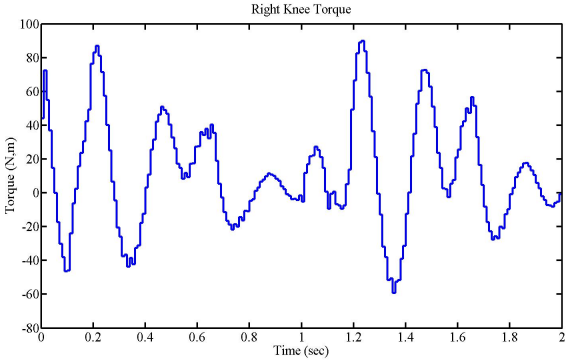

(d) Right knee torque

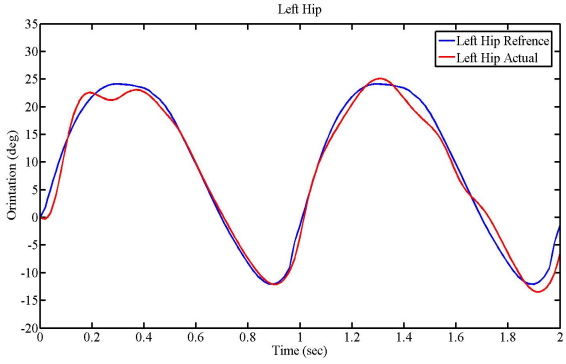

(e) Left hip orientation

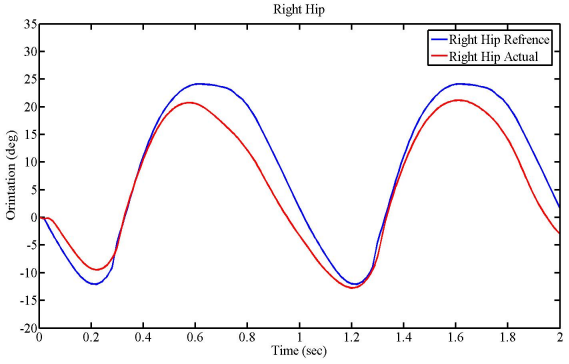

(f) Right hip orientation

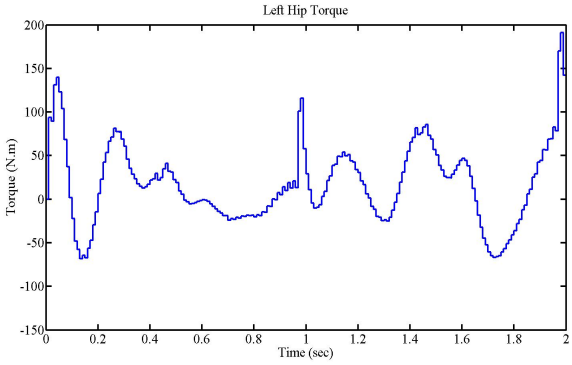

(g) Left hip torque

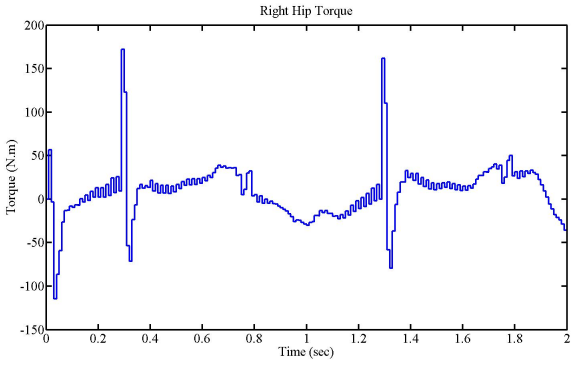

(h) Right hip torque

Figure 5.7: Orientation and torque for hip and knee joints with SDA tuned PID control

Table 5.2: SDA optimised control parameters

Joints	Gain Parameters	SDA
Left Hip	K1	16.7699
	K2	1.7042
	K3	0.3704
Right Hip	K4	14.05
	K5	1.6
	K6	0.444
Left Knee	K7	2.4565
	K8	0.3056
	K9	0.0182
Right Knee	K10	2.9447
	K11	2.6154
	K12	0.0258

5.5 Optimisation of PID with IWA

In this section, PID controllers are developed for controlling the lower limb joints movement. The IWA is used to adjust and minimise the orientation error for the hip and knee joints while the humanoid is in walking mode. The optimisation algorithm is used for best tuning of the controller gains to minimise the error between the reference trajectory and the measured joint trajectory. Moreover, the optimisation algorithm can be used to reduce RMSE further by obtaining the best trajectories to track the predefine orientation reference. The block diagram of the PID controller used is shown in Figure 5.8. The input of the PID controller is the error between the system output and the reference while the output is the joint torque.

The simulation focuses on the trajectory of hip and knee joints and the controller ability to drive the model accordingly. The controller output is the torque which is fed to the humanoid model. In Figure 5.8, the error (1-4) need to be decreased, in order to improve the system performance. The RMSE of each loop is calculated according to equations (5.2)-(5.5) and the cost function is determined as in equation (5.6). In this investigation, the

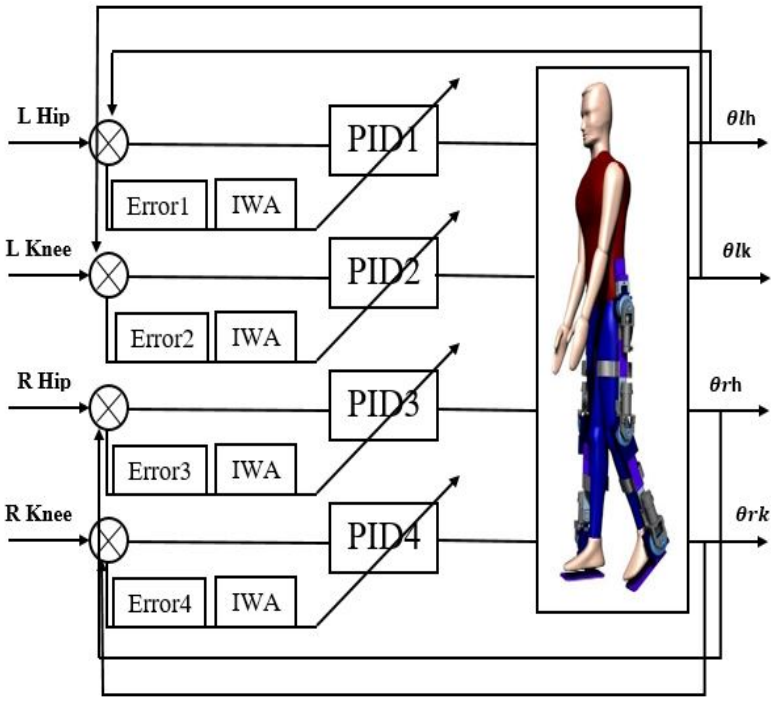

Figure 5.8: IWA tuning PID parameters

simulations were executed for two gait cycles as shown in Figure 5.9. The PID controller gains were tuned using the IWA. The algorithm performance assesses based on the RMSE value achieved and its ability of smoothly follow a pre-defined orientation. A population size of 30 with 50 iterations were considered for this problem, and the best cost function obtained was 2.075 with RMSE of 1.9 for left knee, 2.1 for right knee, 2.2 for left hip and 2.1 for right hip. The hip and knee joint torques were reduced in comparison to trial error tuning of PID, and knee torque was reduced, where the knee torque was reduced from 120 Nm for heuristic tuning to nearly 85 Nm with IWA tuning and the hip torque was reduced from 190 Nm to about 160 Nm. Figure 5.9 shows the overall system performance with IWA, which was slightly improved in comparison to that with SDA. The optimised PID gains are shown in Table 5.3.

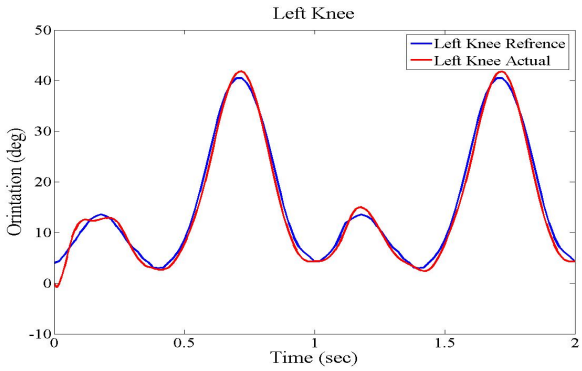

(a) Left knee orientation

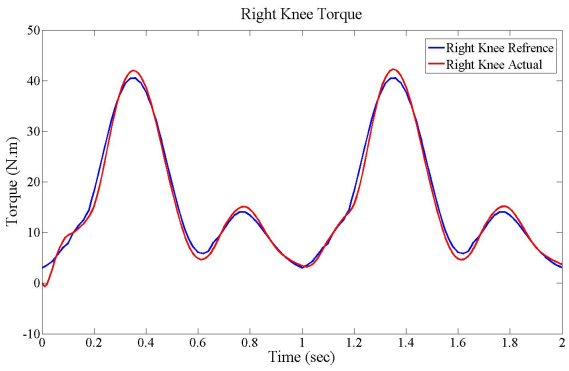

(b) Right knee orientation

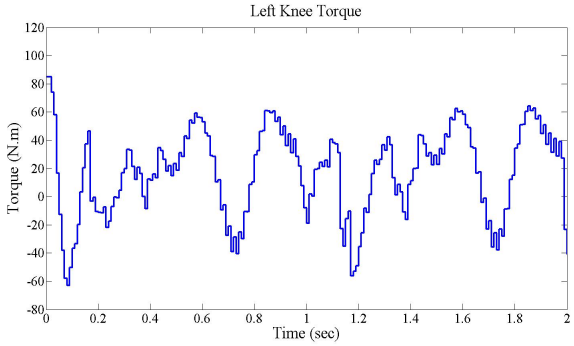

(c) Left knee torque

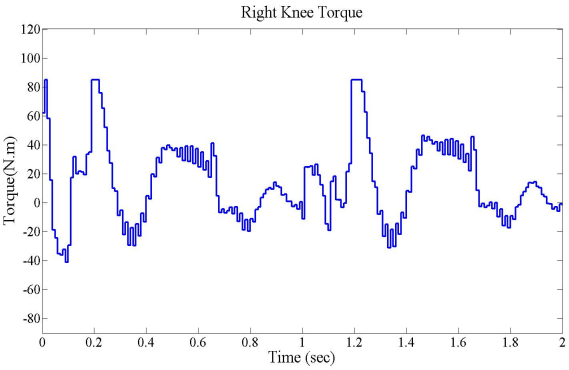

(d) Right knee torque

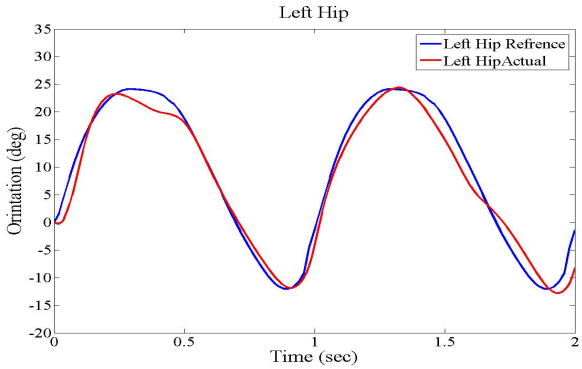

(e) Left hip orientation

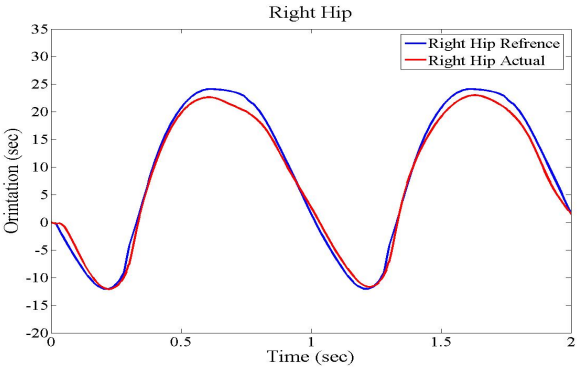

(f) Right hip orientation

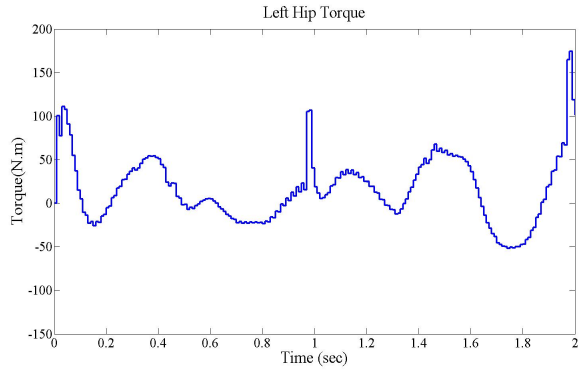

(g) Left hip torque

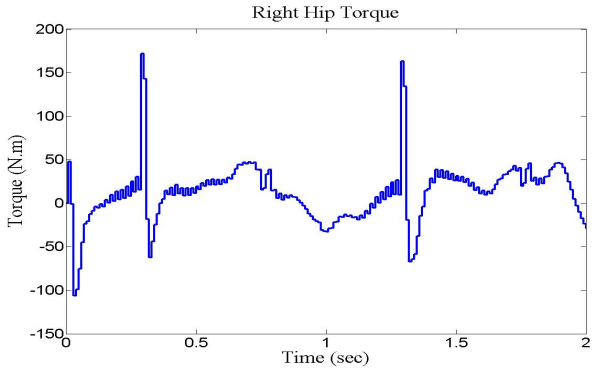

(h) Right hip torque

Figure 5.9: Orientation and torque for hip and knee joints with IWA tune PID

Table 5.3: IWA optimised control parameters

Joints	Gain Parameters	IWA
Left Hip	K1	7.4608
	K2	0.0708
	K3	0.2398
Right Hip	K4	8.3651
	K5	1.4784
	K6	0.5593
Left Knee	K7	3.1778
	K8	0.2332
	K9	0.0439
Right Knee	K10	2.7805
	K11	2.6486
	K12	0.0233

5.6 The assistive exoskeleton

The previous sections focused on developing the total torque needed for the whole system to perform the walking motion. While in this section, two separate controllers are devised, one for the humanoid model and one for the exoskeleton providing 60% and 40% of the overall torque respectively. This means 60% of power will drive the humanoid, and the other 40% of the power will drive the exoskeleton. This represents that the user is only able to supply 60% of the total torque required to perform the walking cycle and accordingly, assistance is needed to complete the function. The orientation will be controlled for the humanoid and exoskeleton lower limb joints to follow the same predefined reference trajectory although they are only "coupled" using a collision setting between exoskeleton supports at thigh, calf, and humanoids legs, and through rigid joints at belt and shoes. The high-level control is responsible of estimating the intention and sending to the exoskeleton exactly the same generated person gait to follow. Referring to the Simulink model shown in Figure 5.10, PID control is used for both the two joints of the humanoid and the exoskeleton for each leg.

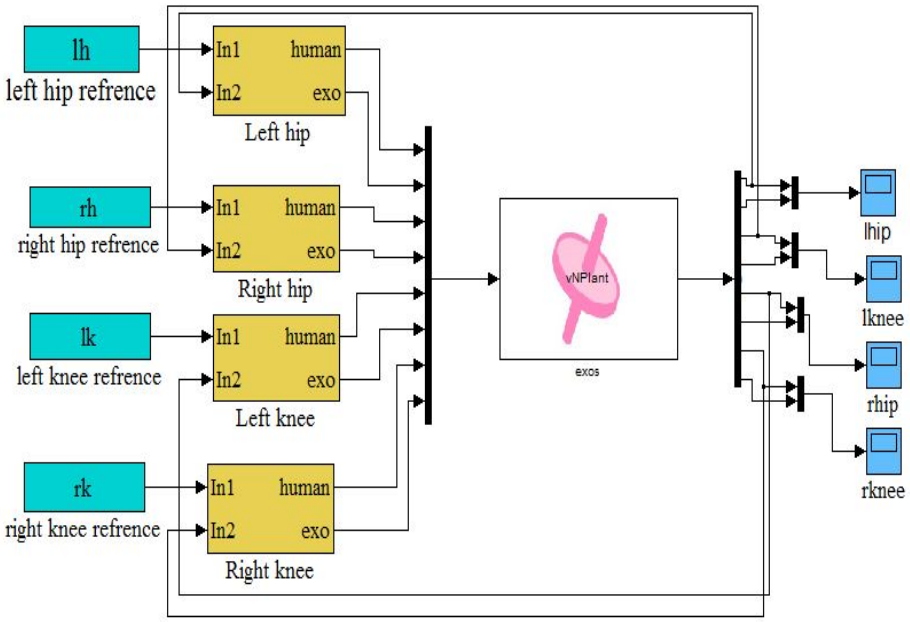

Figure 5.10: Simulink model of of PID control

Figure 5.11 shows the torque behaviour of the knee and hip joints respectively for the humanoid and exoskeleton. The saturation torque was 200 Nm for hip joints and 160 Nm for knee joints. The PID gains used were the SDA tuning parameter, which are represented in Table 5.2 of 2.16 fitness function. Referring to Figure 5.11, the red solid line is the exoskeleton torque, and blue line is the humanoid torque. It shows that the humanoid torque required to complete a walking cycle was augmented as required; the exoskeleton has provided a support torque of approximately 35 Nm for knee joint and 70 Nm for hip joint. Figure 5.12 shows the torque profile of humanoid and exoskeleton using the IWA tuning parameters shown in Table 5.3. It is noted that the cost function was slightly lower than that with SDA 2.075 where the total torque was reduced by 10% from that with SDA. Therefore, the support torque provided by the exoskeleton was approximately 30 Nm for knee joint and 60 Nm for hip joint.

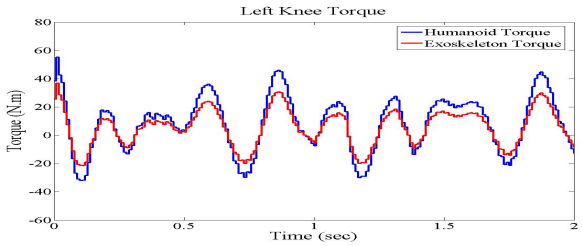

(a) Left knee torque

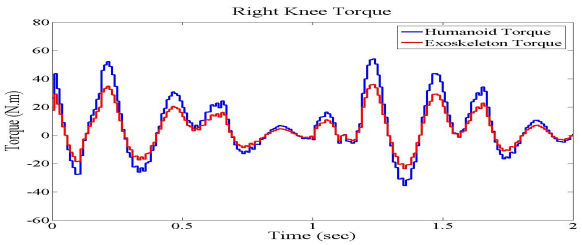

(b) Right knee torque

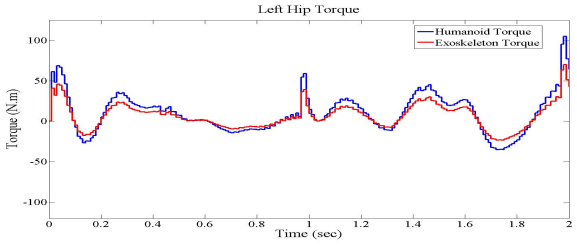

(c) Left hip torque

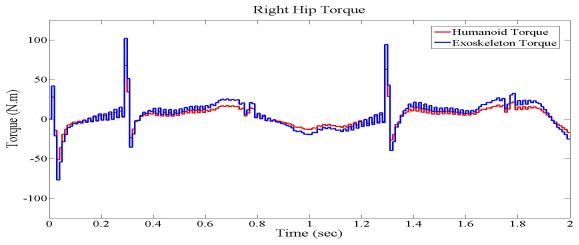

(d) Right hip torque

Figure 5.11: The torque profile for humanoid and exoskeleton using SDA

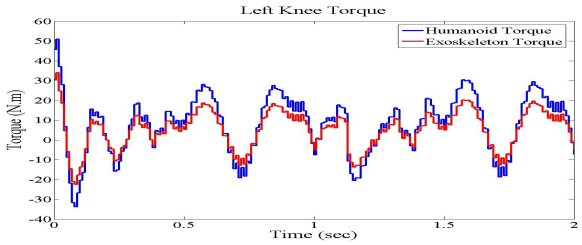

(a) Left knee torque

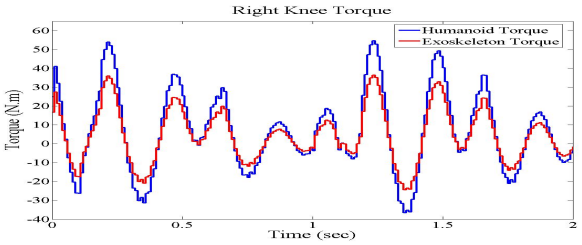

(b) Right knee torque

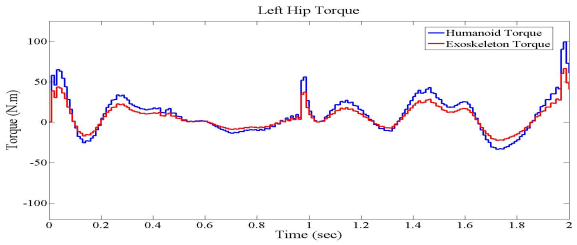

(c) Left hip torque

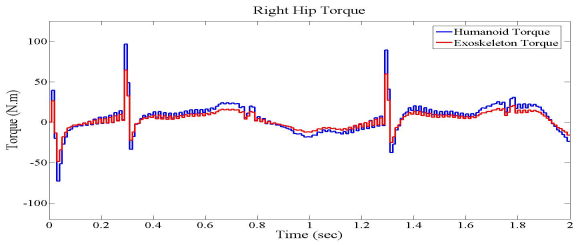

(d) Right hip torque

Figure 5.12: The torque profile for humanoid and exoskeleton using IWA

5.7 Implementation of FLC

Practically, PD-type fuzzy control is a combination of proportional and derivative gains associated with fuzzy the controller. It is most commonly used due to its ability in eliminating the steady-state error and rise time. Figure 5.13 shows the general structure of a PD-type fuzzy controller.

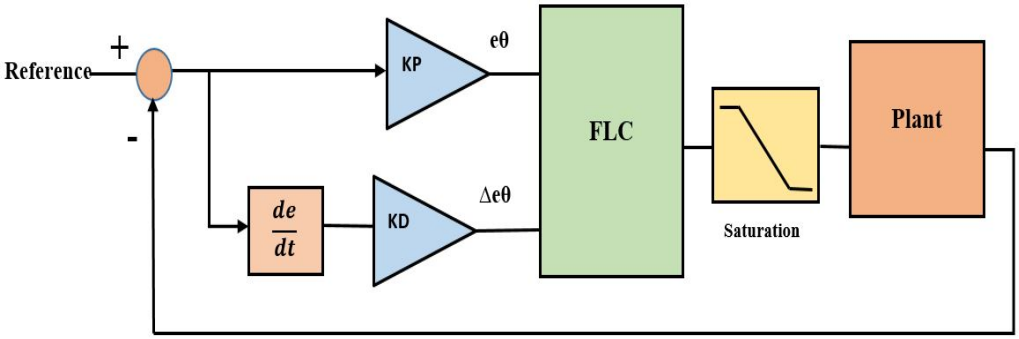

Figure 5.13: Block diagram of PD-type fuzzy control

For purposes of achieving smooth and steady response a PD-type Mamdani fuzzy controller was developed. The Mamdani inference was selected as little information is known of the system. The Sugeno type might be used if extensive information is available (Engelbrecth, 2007). Moreover, Mamdani type is simply perceived by human and the rules are easy to form.

The input and output variables can use various linguistic term levels such as 3,5,7,9 of membership functions depending on the system demand. In this work, 5 levels of membership function are used to implement all of the fuzzy controller blocks because it is appropriate for the system as labelled in Table 5.4.

Table 5.4: MFs linguistic hedges

Label	Hedge
NB	Negative big
NS	Negative big
Z	Zero
PS	Positive small
PB	Positive big

The set of fuzzy rules is developed based on particular method depending on the system performance and behaviour. Table 5.5 views the rules according to the extreme condition. Generally, if the error and the change of error both are PB then the controller generates an action of PB signal to maintain the output close to the set point as located in Group 1, the Red group region. So, a similar action applies for region within Red group. In contrast, when the error and change of error are NB, the control action produces NB signal in order to move the output back toward the reference as located in Group 2, the Blue region. Similarly, negative signal is created for the region in Blue group as shown in Table 5.5. For the other two extreme points, if the error is PB and the change of error is NB or vice versa, the Z control signal is applied to the system because it has reached a steady-state condition. The region in Group 3 the Green, Group 4 the Maroon and Group 5 the Orange same value of control signal is applied indicating that small amount is significantly required for the compensation. As the performance of the system depends on the problem, the control signal should not essentially be fixed as discussed before. However, most controllers follow the standard rule as shown in Table 5.5.

Table 5.5: The fuzzy rule base

$e/\Delta e$	NB	NS	Z	PS	PB
NB	NB	NB	NB	NS	Z
NS	NB	NB	NS	Z	PS
Z	NB	NS	Z	PS	PB
PS	NS	Z	PS	PB	PB
PB	Z	PS	PB	PB	PB

The FLC is used in this work to control the humanoid and the exoskeleton comprises a multi input single output (MISO) Mamdani type as shown in Figure.5.14. The system has two inputs; the error and change of error.

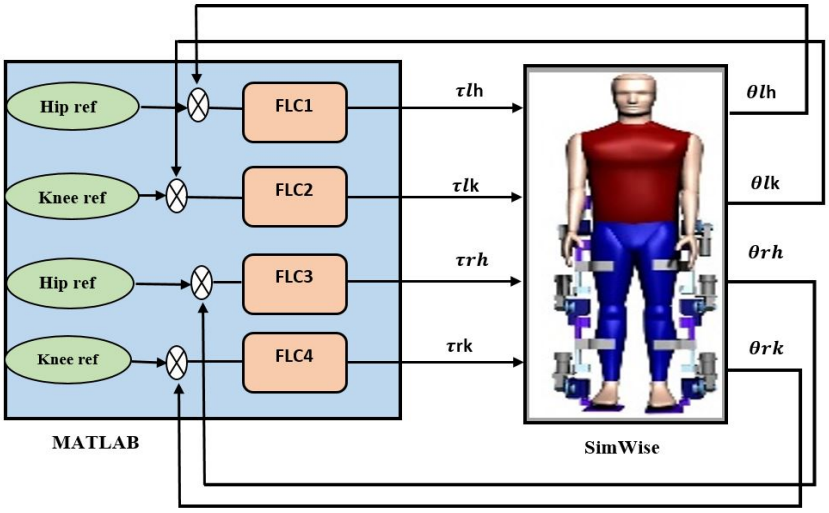

Figure 5.14: Architecture of PD-type fuzzy control

In this work, there is no coupling or interaction between all FLC subsystems while in operation. For that orientation of lower limb joints are independently controlled by PD-fuzzy logic structures. Thus, there are four independent FLC modules (FLC1, FLC2, FLC3 and FLC4), one subsystem for each joint. Normalized universe of discourse value was used for input and output within the range [-1, 1]. Five levels of Gaussian membership function (MFs) are used resulting in 5*5 = 25 rules for each fuzzy controller with fifty percent intersection between MFs as presented in Figure 5.15. The same fuzzy rule base is used for each module; FLC1, FLC2, FLC3, and FLC4, the fuzzy rules are shown in Table 5.6.

Table 5.6: The fuzzy rule base

Error e	Change of Error Δe				
	NB	NS	Z	PS	PB
NB	NB	NB	NS	NS	Z
NS	NB	NS	NS	Z	PS
Z	NS	NS	Z	PS	PS
PS	NS	Z	PS	PS	PB
PB	Z	PS	PS	PB	PB

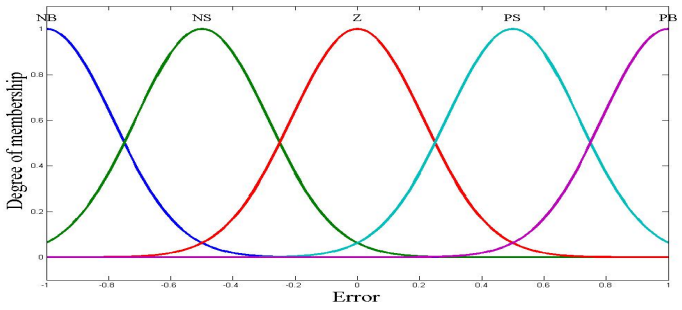

Figure 5.15: The input output membership functions

The FLCs were implemented in Matlab Simulink linked with Visual Nastran 4D environment as shown in Figure 5.16. The main advantage of this design is that each module uses the same fuzzy rule to perform the control tasks. Saturation blocks of 200Nm for hip joint and 160 Nm for knee were added after the fuzzy controller to limit the torque value sent to the system within admissible range. The reference trajectory is fed to the controller while the trajectory measured from the software fed back to the controller. The controller output is the torque required to drive the lower limb joints. These outputs control the hip and knee joints based on the corresponding references, which are sent to both the humanoid and the exoskeleton actuators in VN4D. PD gains and the fuzzy scaling factors were tuned heuristically.

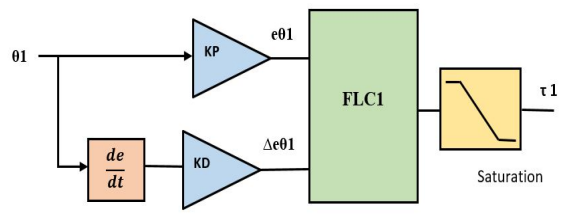

(a) Left hip

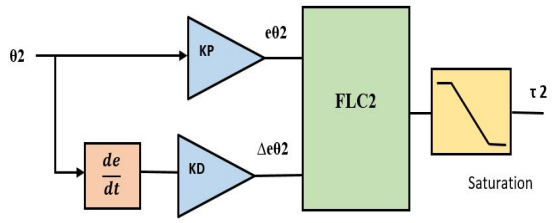

(b) Left knee

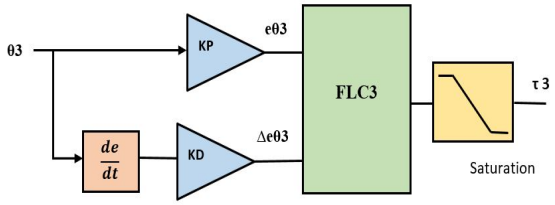

(c) Right hip

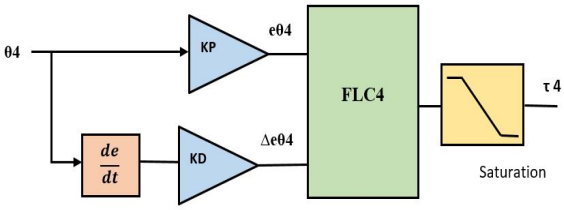

(d) Right knee

Figure 5.16: The structure of input output PD-type fuzzy controller

Reference tracking performances of the control system for hip and knee joints of humanoid model are shown in Figure 5.17. The red solid line is the actual trajectory, and the blue line is the desired trajectory. It is noted that the PD-type FLC has achieved good tracking performance than the conventional PID as presented in previous section. The system cost function was 1.7 with RMSE of 1.7 for left knee , 1.75 for right knee , 1.65 for left hip and 1.7 for right hip by tuning the fuzzy scaling parameters using trial and error method. From Figure 5.17 the maximum torques recorded were about 115 Nm for the knee joint and 180 Nm for hip joint. By using the PD-type FLC the total system cost function for reference tracking was reduced to 1.2176 and the total torque was decreased by 5% of the total torque. The scaling parameters are shown in Table 5.7.

Table 5.7: Fuzzy scaling parameters

Controllers	Gain Parameters	Heuristic
Left Hip	K1	0.5
	K2	0.052
	K3	30
Right Hip	K4	0.166
	K5	0.63
	K6	100
Left Knee	K7	0.55
	K8	0.06
	K9	75
Right Knee	K10	0.43
	K11	0.07
	K12	50

These parameters represent the initial condition for the fuzzy logic controllers and after while the parameters will be the same for left and right knee joint and same situation for the hip joint.

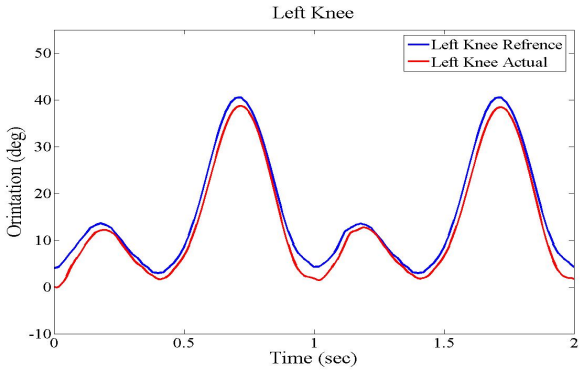

(a) Left knee orientation

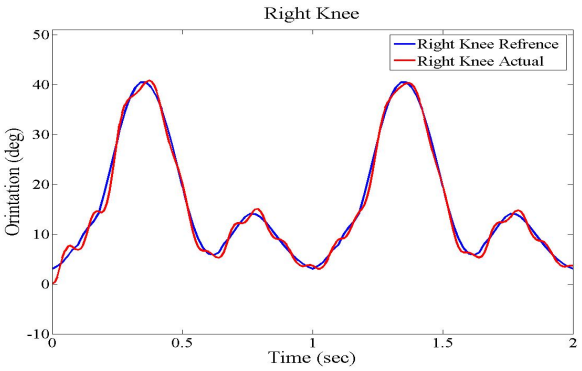

(b) Right knee orientation

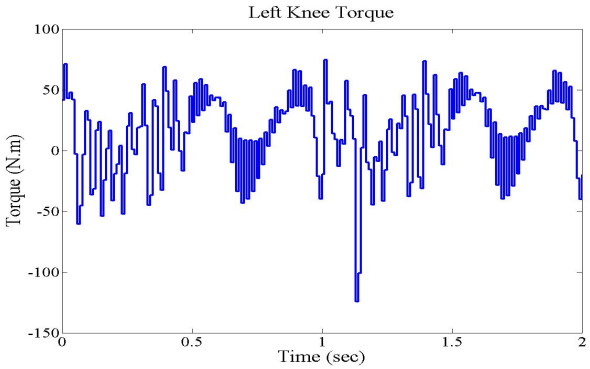

(c) Left knee torque

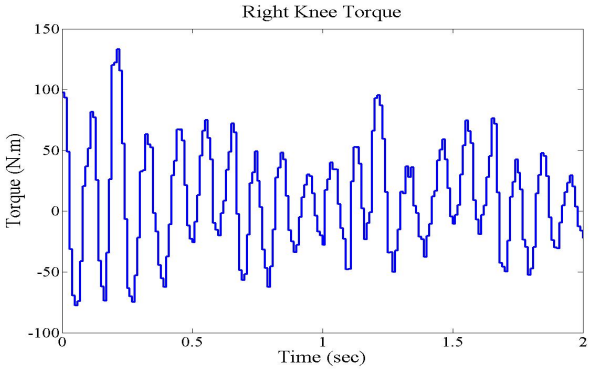

(d) Right knee torque

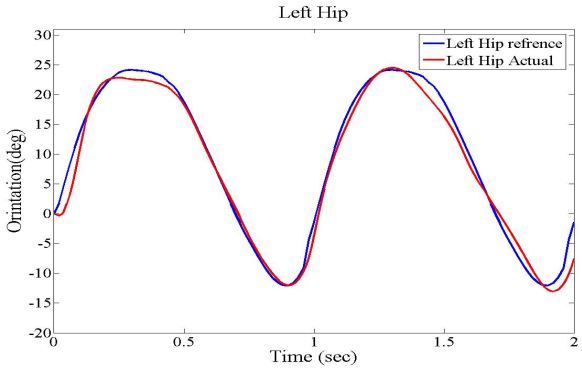

(e) Left hip orientation

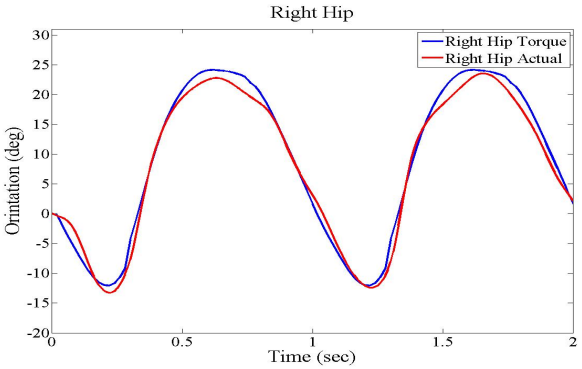

(f) Right hip orientation

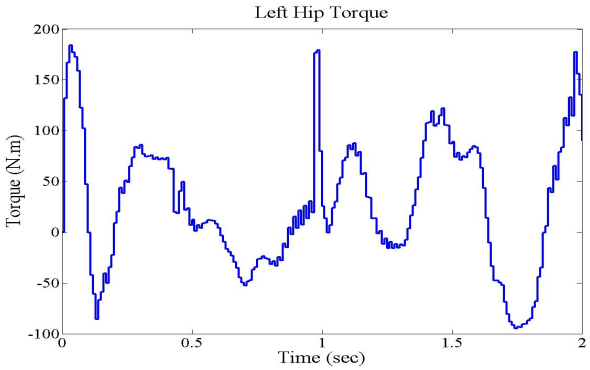

(g) Left hip torque

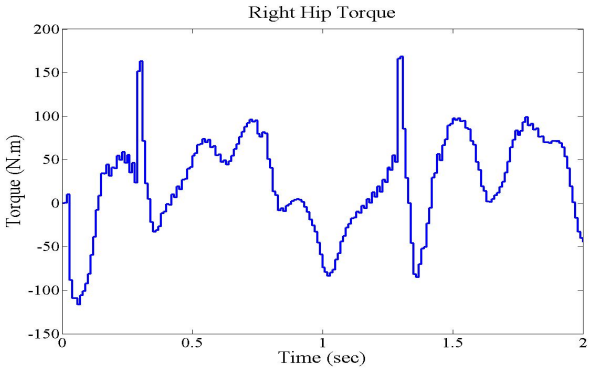

(h) Right hip torque

Figure 5.17: Orientation and torque for hip and knee joints with PD-type FLC

5.8 Optimising PD-FLC using SDA and IWA

In this work, two optimisation algorithms namely SDA and IWA are used to obtain best input output scaling factors for the fuzzy control. Choosing the fuzzy parameters carefully will provide a proper and feasible performance for the nonlinear system (Wang, 1993). The FLC structures with SDA and IWA are shown in Figure 5.18.

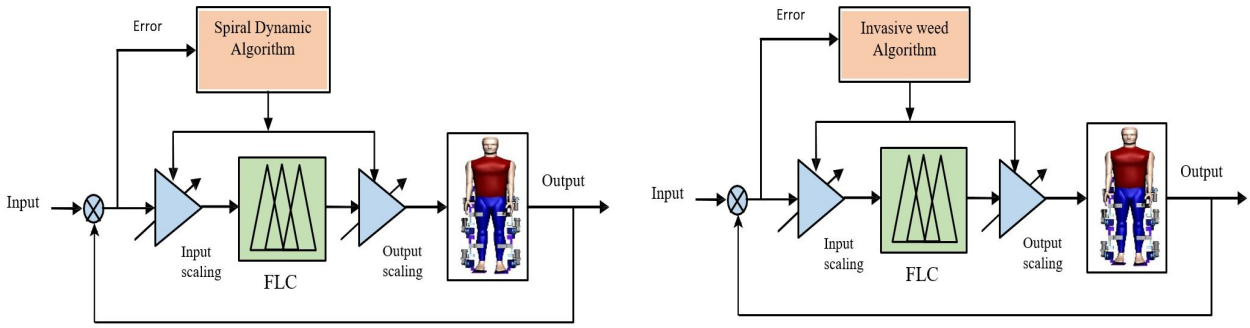

(a) Spiral Dynamic Algorthim (SDA) (b) Invasive Weed Algorthim (IWA)

Figure 5.18: Orientation and torque for knee joints

The control scheme for lower limb humanoid model is illustrated in Figure 5.19 with four feedback loops; left hip, right hip, left knee and right knee. There are two inputs and one output scaling factors for each control loop. The inputs and outputs of all controllers are normalized between [-1, 1]. Two inputs for each controller are the error (the difference between the reference trajectory and the actual trajectory measured from Visual Nastran 4D simulation output), and the change of error. The output of the controller is the torque. The objective is to minimize the orientation error for hip and knee joints while the humanoid model performs walking task. The performance index is the root mean square error (MSE) calculated as in equation (5.1). The cost function of the system is represented as equation (5.6). The vector of weight is selected as $[w_1 w_2 w_3 w_4]$ =[0.25 0.25 0.25 0.25] to give equal emphasis to the four functions. The complete control system has 12 parameters, K1-K12 to optimise.

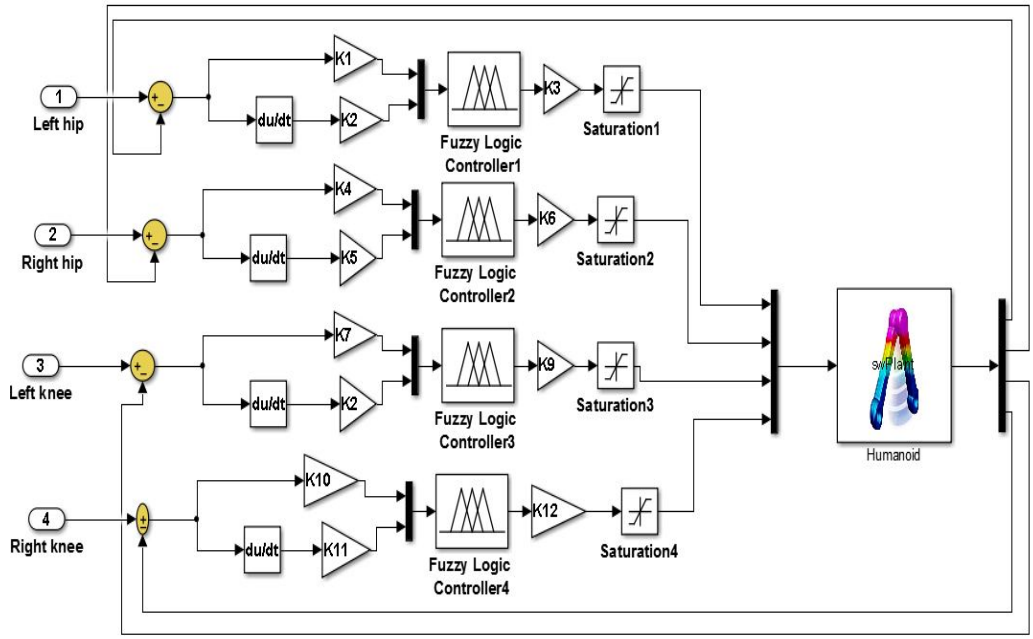

Figure 5.19: PDfuzzy controller schemes

The simulation was performed for 2 gait cycles, the results were collected from the right and left leg of the humanoid model. The angle trajectories of the hip and knee joints were measured by angle sensor attached to the humanoid in visual Nastran 4D software. In the SDA process, a population of 5 searching points for 100 iterations were used with both SDA and IWA. It was noticed that the minimum cost function for the system was 0.9384 with the SDA and 0.8356 with IWA. The scaling factor values obtained from SDA and IWA optimisation techniques are shown in Table 5.8. The reference tracking performances of the control system for hip and knee joints and the torque of humanoid measured during the walking cycle are illustrated in Figure 5.20. It is noted that the torque for the hip joints was below 160 Nm through the walking cycle and the torque for the knee joints was below 60 Nm through the walking cycle for IWA while it was for hip joints above 170 Nm and the knee joints torque was above 70 Nm for SDA. These conform to normal torque levels in practice.

Table 5.8: Fuzzy scaling parameters

Controllers	Gain Parameters	SDA	IWA
Left Hip	K1	0.48	0.3571
	K2	0.0089	0.010
	K3	80	80
Right Hip	K4	0.4763	0.6599
	K5	0.0083	0.009
	K6	80	71.429
Left Knee	K7	0.55	0.3081
	K8	0.0047	0.3081
	K9	36	34.0528
Right Knee	K10	0.5962	0.3104
	K11	0.003	0.009
	K12	24	37.9268

Figures 5.21, 5.22 show the torque profiles of the hip and knee joints for the humanoid and exoskeleton. It is noted that scaling parameters achieved by IWA have provided low torque as compare to SDA. Figure 5.21 shows that the exoskeleton provided augmentation torques for the knee joints by nearly 35Nm and 70 Nm for hip joints while in Figure 5.22 the exoskeleton has provided the necessary augmentation to the humanoid joint torques during the walking cycle by supplying 25 Nm to the knee joint and 60 Nm to the hip joint. These are within acceptable range as recommended by Low (2011); the maximum assistive torque to enhance the hip joint should be lower than 120 Nm, and for knee joint should be lower than 60 Nm.

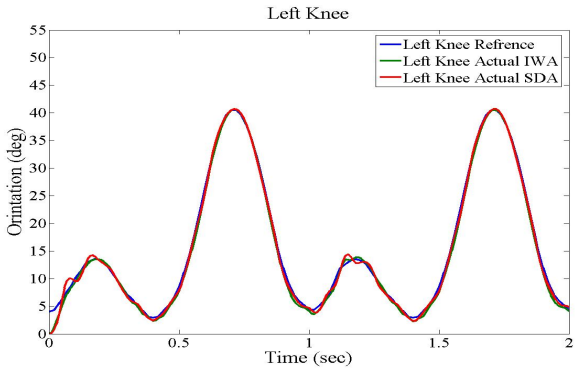

(a) Left knee orientation

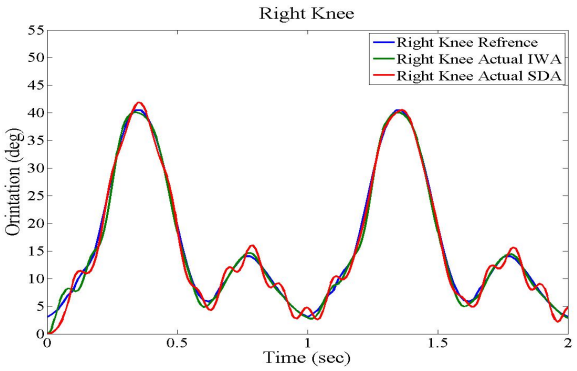

(b) Right knee orientation

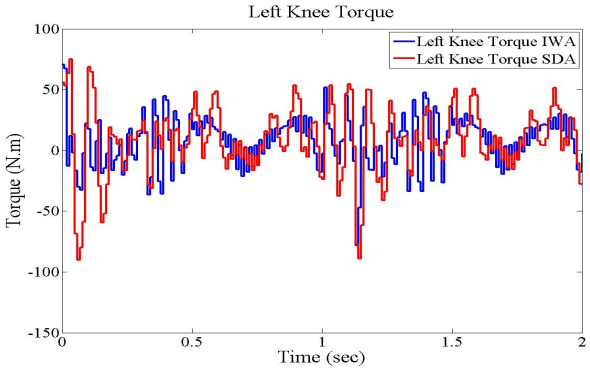

(c) Left knee torque

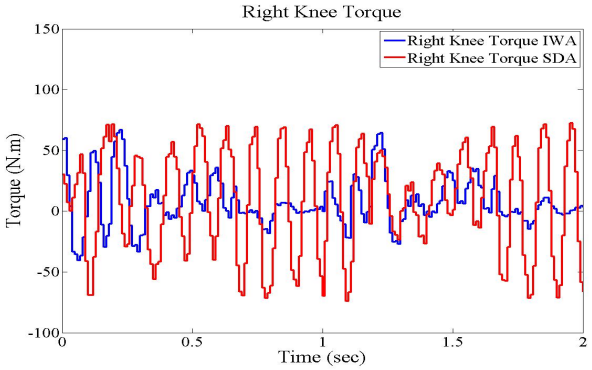

(d) Right knee torque

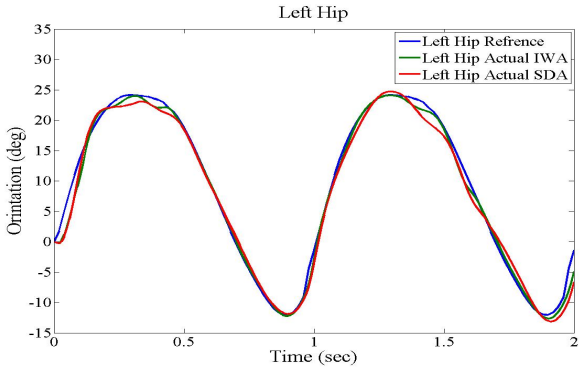

(e) Left hip orientation

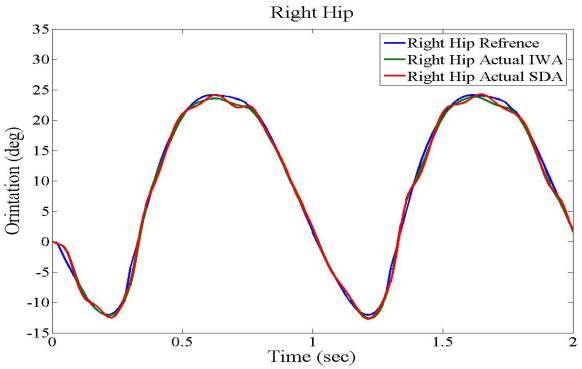

(f) Right hip orientation

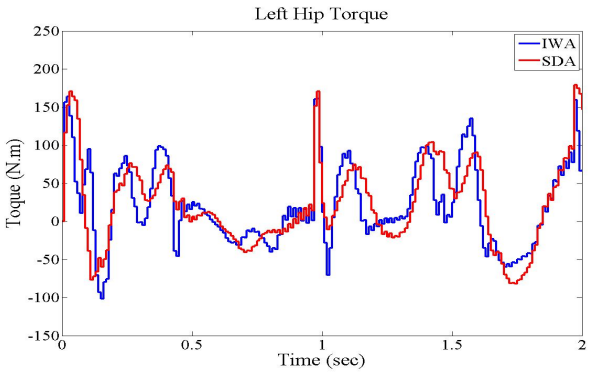

(g) Left hip torque

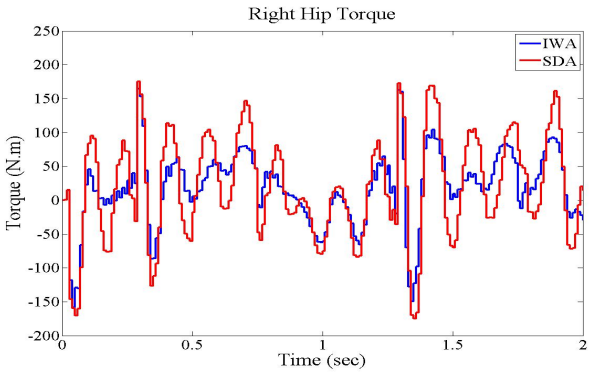

(h) Right hip torque

Figure 5.20: Orientation and torque for hip and knee joints with optimised PD-type FLC

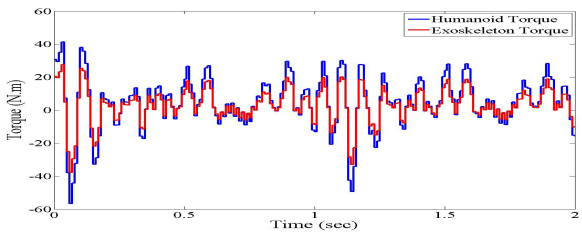

(a) Left knee torque

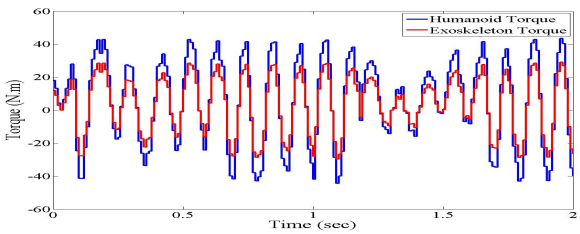

(b) Right knee torque

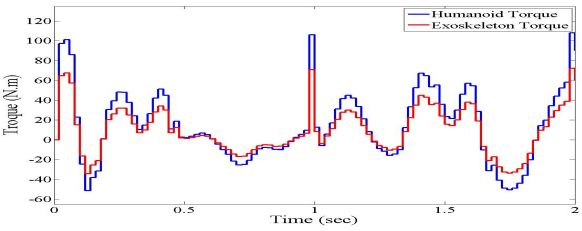

(c) Left hip torque

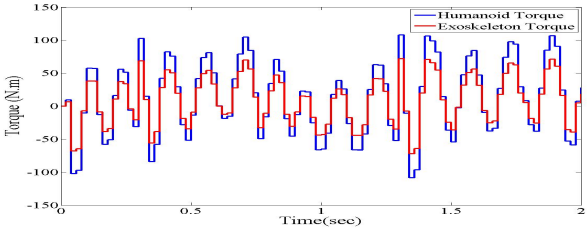

(d) Right hip torque

Figure 5.21: The torque profile for humanoid and exoskeleton using SDA tuned FLC

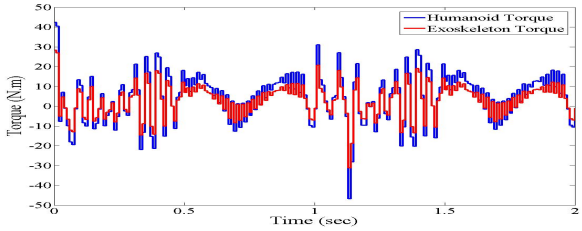

(a) Left knee torque

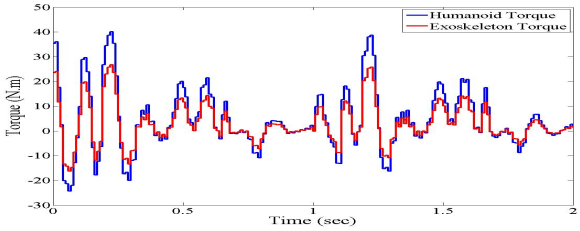

(b) Right knee torque

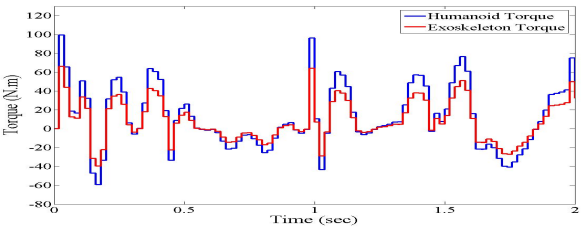

(c) Left hip torque

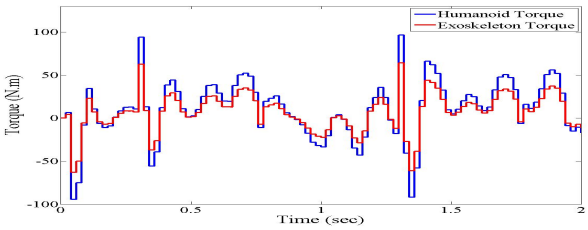

(d) Right hip torque

Figure 5.22: The torque profile for humanoid and exoskeleton using IWA tuned FLC

5.9 Implementation of PID-type FLC

The PID-type fuzzy control structure designed for controlling the humanoid lower limb model is shown in Figure.5.23.

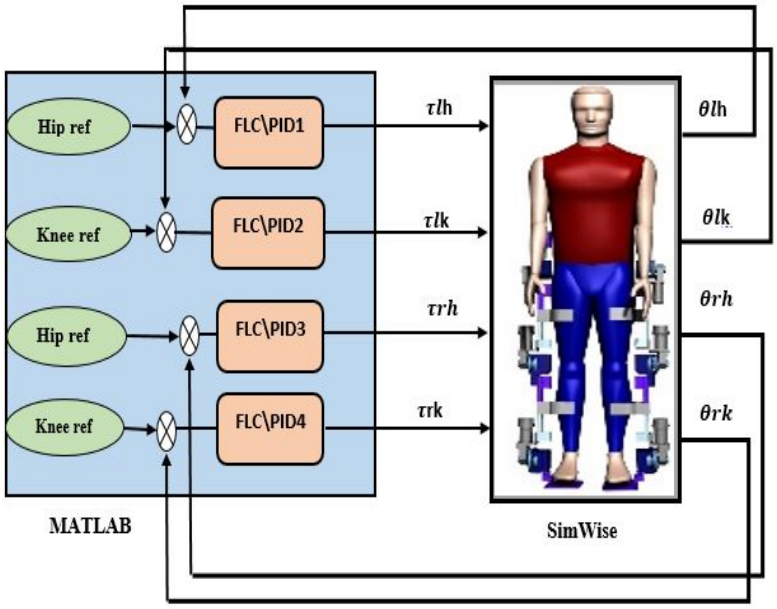

Figure 5.23: PID-type fuzzy control structure

Four Fuzzy/PID controllers are developed for hip and knee joints in each leg in this work.The Fuzzy/PID control is designed in Matlab Simulink linked with VN4D environment. The system input is the trajectory references of the lower limb joints while the output of the system is the torque (τlh,τlk,τrh and τrk) required to drive the hip and knee joints as illustrated in Figure 5.23. Figure 5.24 shows the block diagram of PID-type FLC.

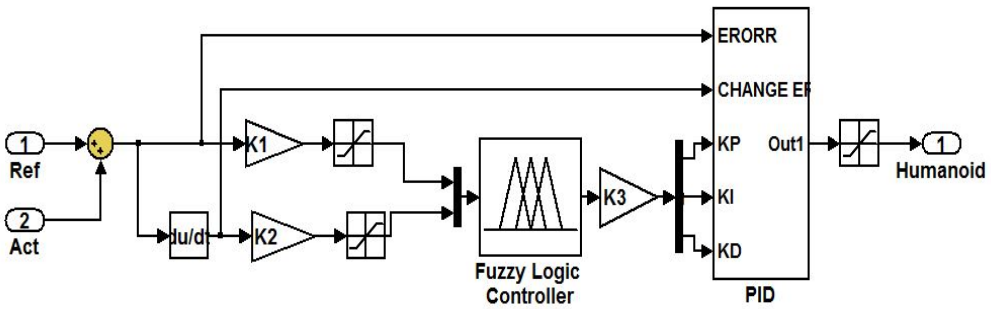

Figure 5.24: Simulink block diagram of fuzzy/PID

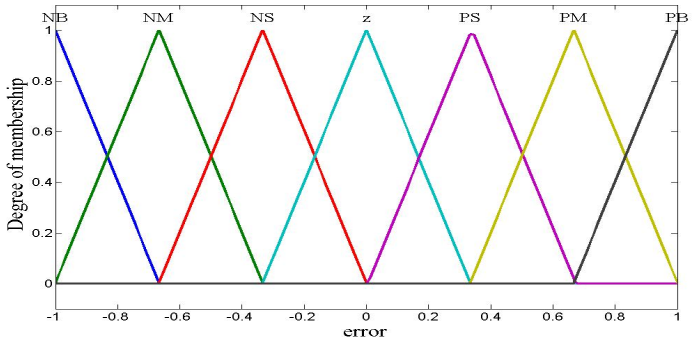

Figure 5.25: Membership function of inputs

The adaptive fuzzy controller has two inputs and three outputs, the inputs of controller are error and change of error which are normalized to [1-, 1] while the outputs are respectively kp, ki, and kd. For input the parameters K1, K2 are tuned manually in order to get optimum performance. Seven Mamdani triangular membership functions were used leading to 49 fuzzy rules, these are Positive Big (PB),Positive Medium (PM), Positive Small(PS),Zero (Z),Negative Small (NS),Negative Medium (Nm), and Negative Big (NB) as shown in Figure 5.25. The domain of error and change of error is [-1, 1] and for the output variable controller, KP = [0-20]; KI= [0-10] ;KD =[0-5]. The orientation of lower limb joints are independently controlled by Fuzzy/PID structure which have similar rule bases.

The fuzzy rules used for adaptation the PID parameters KP,KI,KD are shown in Table 5.9, Table 5.10, and Table 5.11.

Table 5.9: KP Fuzzy Inference Rule

$e/\dot{e}$	NB	NM	NS	Z	PS	PM	PB
NB	PB	PB	PM	PM	PS	Z	Z
NM	PB	PB	PM	PS	PS	Z	Z
NS	PM	PM	PM	PM	Z	NS	NS
Z	PM	PM	PM	Z	PS	NM	NM
PS	PS	PS	Z	NS	NS	NM	NM
PM	PS	Z	NS	NM	NM	NM	NB
PB	Z	Z	NM	NM	NM	NB	NB

Table 5.10: KI Fuzzy Inference Rule

$e/\dot{e}$	NB	NM	NS	Z	PS	PM	PB
NB	NB	NB	NM	NM	NS	Z	Z
NM	NB	NB	NM	NS	NS	Z	Z
NS	NB	NM	NS	NS	Z	PS	PS
Z	NM	NM	NS	Z	PS	PM	PM
PS	NM	NS	Z	PS	PS	PM	PB
PM	Z	Z	PS	PS	PM	PB	PB
PB	Z	Z	PS	PM	PM	PB	PB

Table 5.11: KD Fuzzy Inference Rule

$e/\dot{e}$	NB	NM	NS	Z	PS	PM	PB
NB	PS	NS	NB	NB	NB	NM	PS
NM	PS	NS	NB	NB	NB	NM	PS
NS	Z	NS	NM	NM	NS	NS	Z
Z	Z	NS	NS	NS	NS	NS	Z
PS	Z	Z	Z	Z	Z	Z	Z
PM	PB	NS	PS	PS	PS	PS	PB
PB	PB	PM	PM	PM	PS	PS	PB

The simulation was run for two gait cycles; the results were collected from the right and left leg of the humanoid model. The orientation trajectories of the hip and knee joints were measured by angle sensor attached to the humanoid in VN4D software. The reference tracking performances of the control system for hip and knee joints and the torque of humanoid measured during the walking cycle are shown in Figure 5.26. It is noted that the hip joint torque was below 160 Nm through the walking cycle and the knee joint torque was below 80 Nm through the walking cycle. Table 5.12 shows the scaling parameters used. The minimum cost function obtained by heuristically tuning the K1 and K2 was 0.865 with RMSE 0.823 for left hip, 0.9 for left knee,0.842 for right hip and 0.895 for right knee.

Table 5.12: Heurstic control parameters tuning

Joints	Gain Parameters	Heurstic
Left Hip	K1	0.92
	K2	0.56
Right Hip	K3	0.77
	K4	0.1
Left Knee	K5	0.84
	K6	0.33
Right Knee	K7	0.006
	K8	0.15

These parameters represent the initial condition for the PID-type FLCs and after while the parameters will be the same for left and right knee joint and same situation for the hip joint.

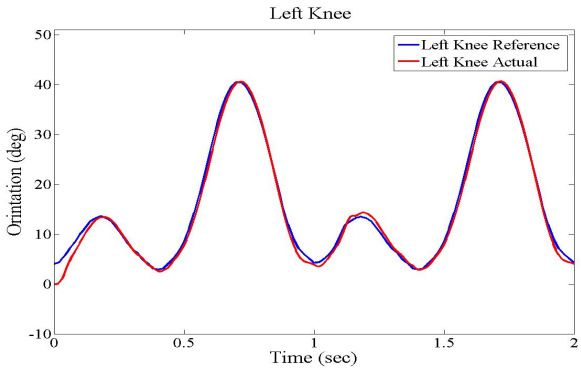

(a) Left knee orientation

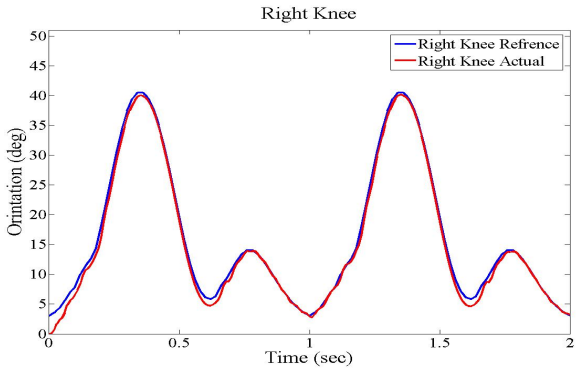

(b) Right knee orientation

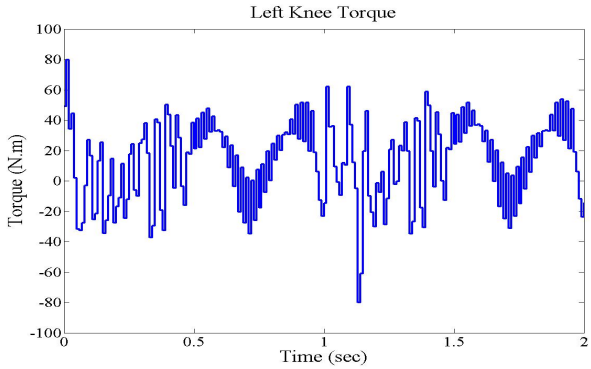

(c) Left knee torque

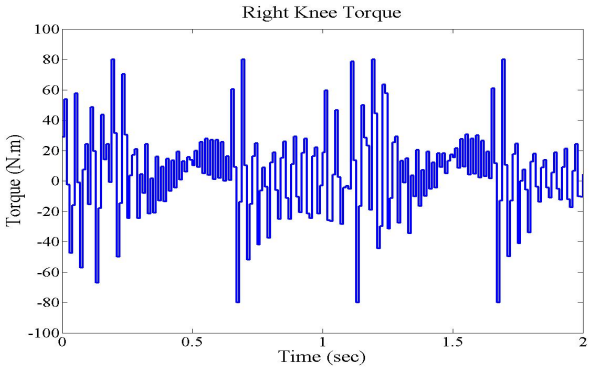

(d) Right knee torque

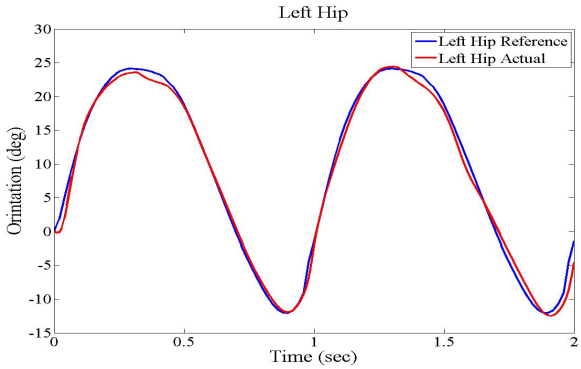

(e) Left hip orientation

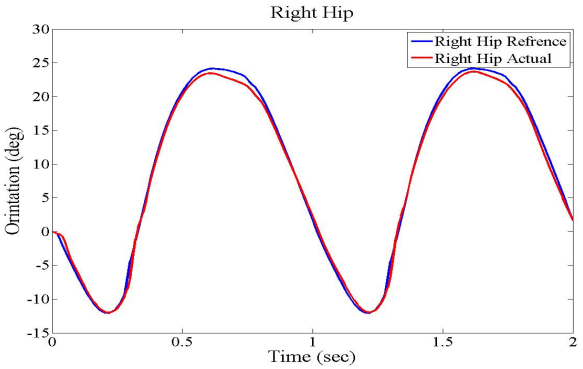

(f) Right hip orientation

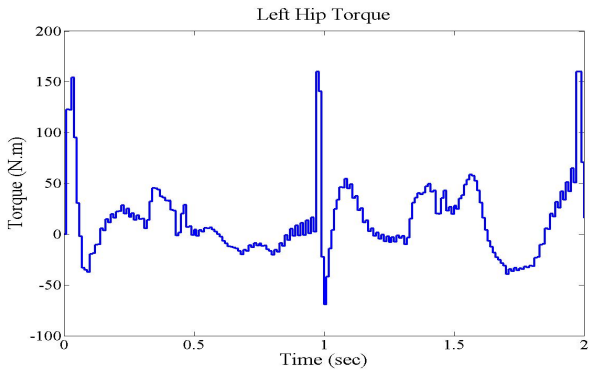

(g) Left hip torque

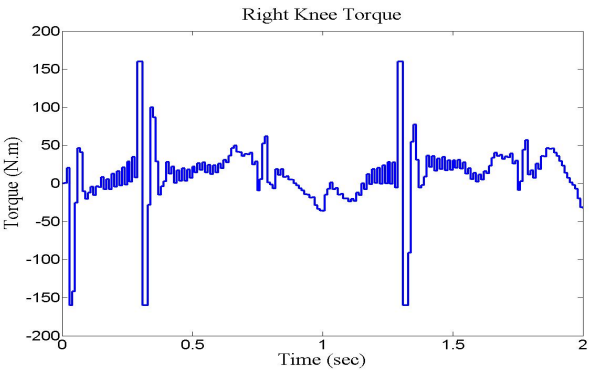

(h) Right hip torque

Figure 5.26: Orientation and torque for hip and knee joints with heuristically tuned PID-type FLC

5.10 Optimising the fuzzy/PID using SDA and IWA

In this section, the optimisation algorithms IWA and SDA are used to achieve best input scaling factors for the fuzzy control. The objective is to minimize the orientation error for hip and knee joints while the humanoid model performs walking task. A population of 5 searching points for 100 iterations were used with both SDA and IWA processes. The minimum cost function values achieved were 0.784 with the SDA and 0.556 with the IWA. The scaling factor values obtained from SDA and IWA optimisation techniques are shown in Table 5.13. The simulation was carried out for 2 gait cycles, the results were collected from the right and left leg of the humanoid model during the walking cycle. The reference tracking performances of the control loops for hip and knee joints and the torque of humanoid measured are shown in Figure 5.27 and Figure 5.28. It is noted that the torque for the hip joints was below 145 Nm through the walking cycle and the torque for the knee joints was below 60 Nm through the walking cycle with IWA tuned FLC while it was for hip joints above 150 Nm and the knee joints torque was above 70 Nm with SDA tuned FLC. The results shown in Figures 5.27 and 5.28 demonstrate that the developed PID-type FLC has successfully tracked the reference with low oscillation as compared to the conventional PID and further performed better than PD-type FLC with optimisation algorithms in term of minimising the RMSE for the system overall. The proposed controller combined the fuzzy ability dealing with nonlinear system with simple implementation of PID controller.

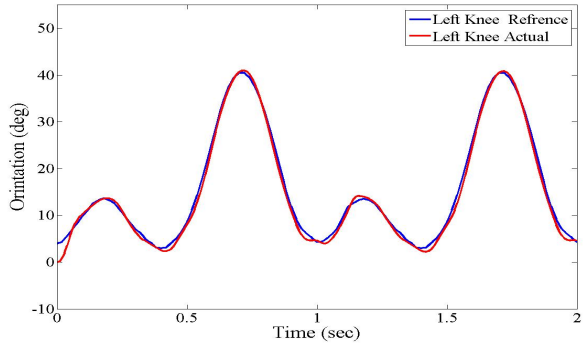

(a) Left knee orientation

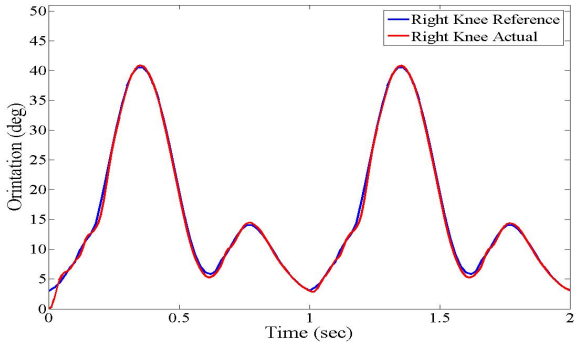

(b) Right knee orientation

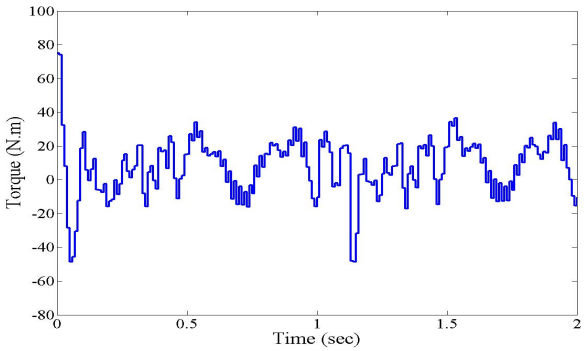

(c) Left knee torque

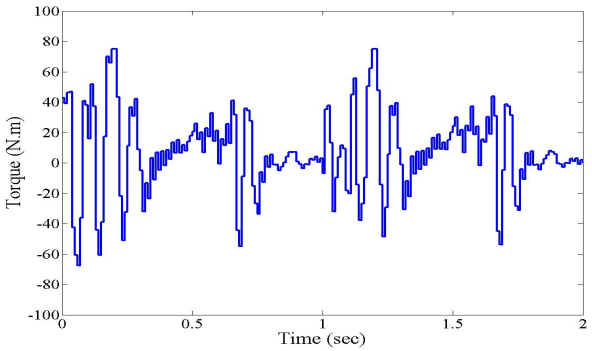

(d) Right knee torque

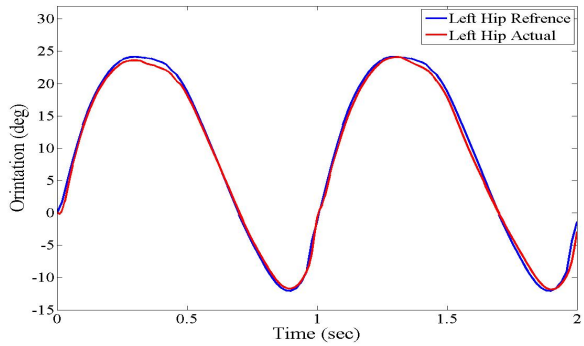

(e) Left hip orientation

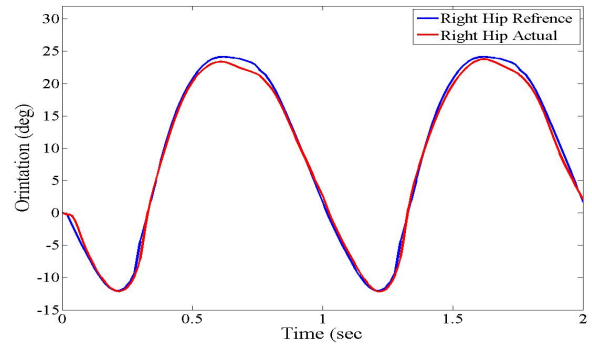

(f) Right hip orientation

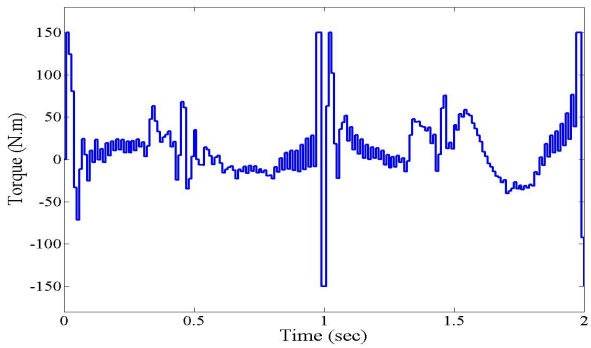

(g) Left hip torque

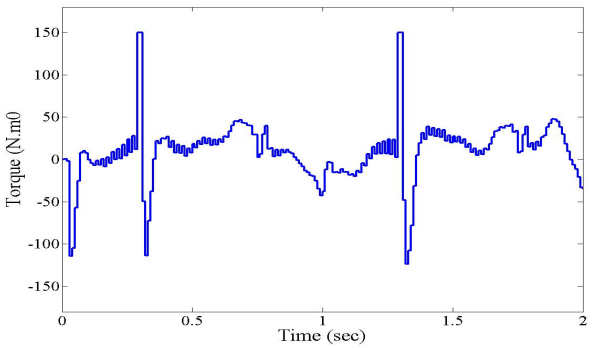

(h) Right hip torque

Figure 5.27: Orientation and torque for hip and knee joints using SDA tuned PID-type FLC

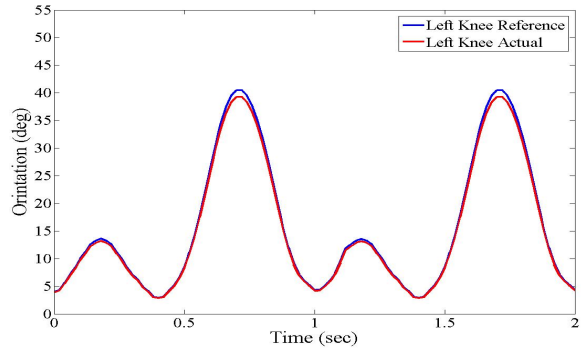

(a) Left knee orientation

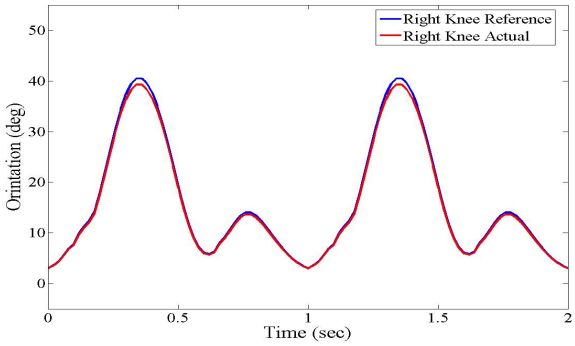

(b) Right knee orientation

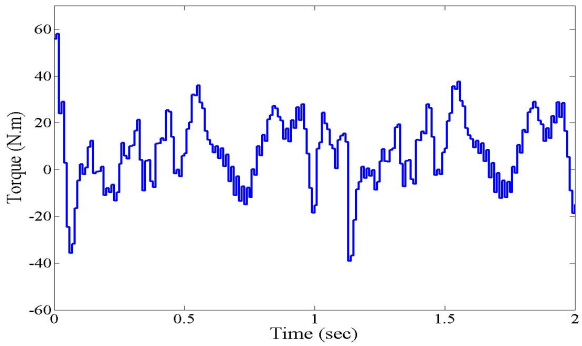

(c) Left knee torque

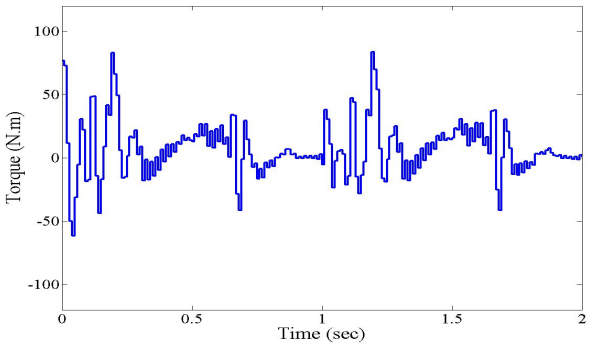

(d) Right knee torque

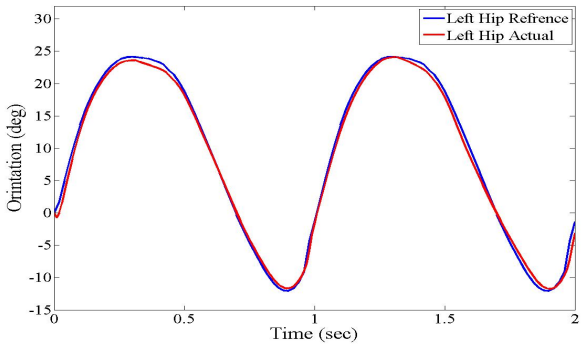

(e) Left hip orientation

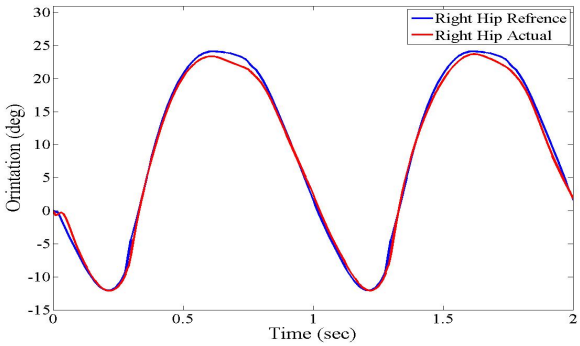

(f) Right hip orientation

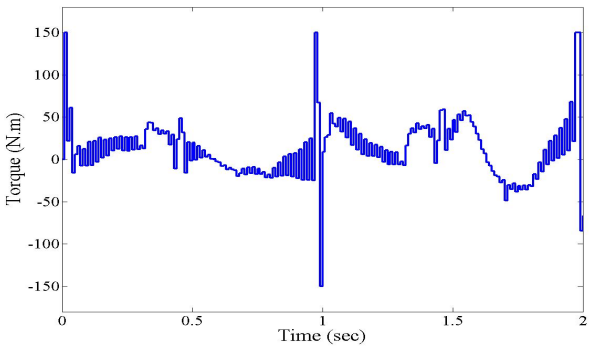

(g) Left hip torque

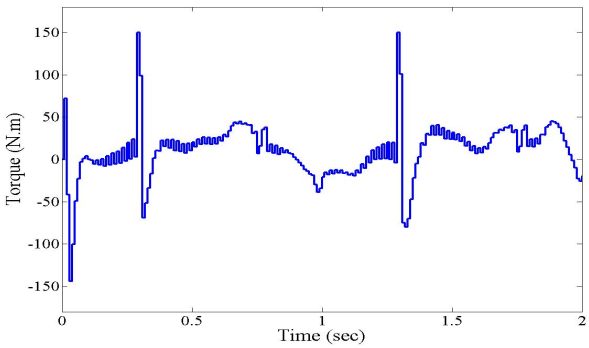

(h) Right hip torque

Figure 5.28: Orientation and torque for hip and knee joints using IWA tuned PID-type FLC

Table 5.13: IWA, SDA control parameters tuning

Joints	Gain Parameters	IWA	SDA
Left Hip	K1	0.62	0.64
	K2	0.73	0.45
Right Hip	K3	0.91	0.73
	K4	0.56	0.38
Left Knee	K5	0.19	0.28
	K6	0.004	0.005
Right Knee	K7	0.39	0.54
	K8	0.007	0.006

In case of controlling the humanoid with exoskeleton, 60 percent of the control action will drive the humanoid model while the rest 40 percent provided by the exoskeleton. Figures 5.29 and 5.30 show the torque profiles of the hip and knee joints for the humanoid wearing the exoskeleton using the scaling parameters achieved using IWA. Figure 5.29 shows that the exoskeleton augments the knee joints by nearly 30Nm and 70 Nm for hip joints. While as noted in Figure 5.30 the exoskeleton has provided the necessary enhancement to the humanoid joint torques during the walking cycle by supplying 22 Nm to the knee joint and 55 Nm to the hip joint. These are within acceptable range as recommended by Low (2011); the maximum assistive torque to enhance the hip joint should be lower than 120 Nm, and for knee joint should be lower than 60 Nm. Therefore, the exoskeleton assist the elderly by reducing the energy required to complete the walking cycle. For instance instead of the human providing about 145 Nm for hip and 60 Nm for knee wearing the exoskeleton will reduce this effort to 90 Nm for hip joint and 38 Nm for knee joint. This means nearly 40percent of the required energy has reduced by the exoskeleton.

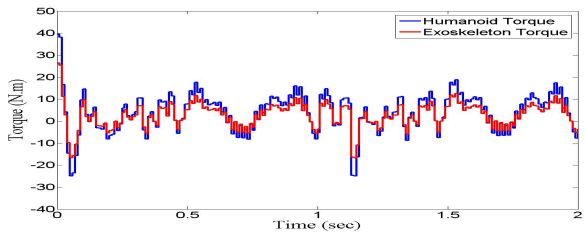

(a) Left knee torque

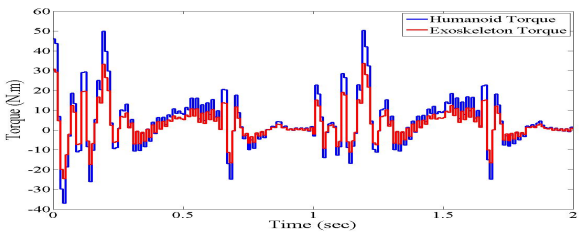

(b) Right knee torque

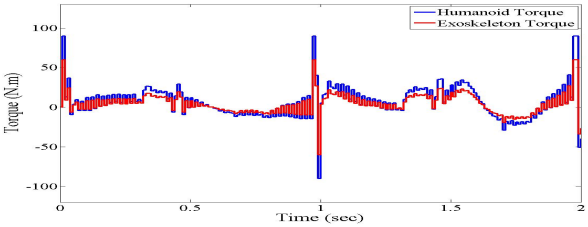

(c) Left hip torque

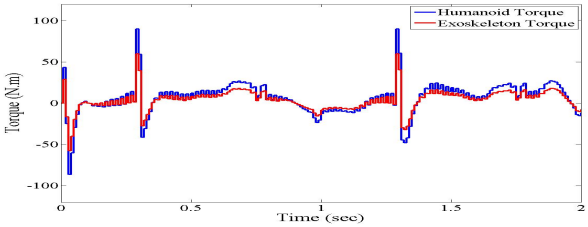

(d) Right hip torque

Figure 5.29: The torque profile for humanoid and exoskeleton using SDA tuned PID-type FLC

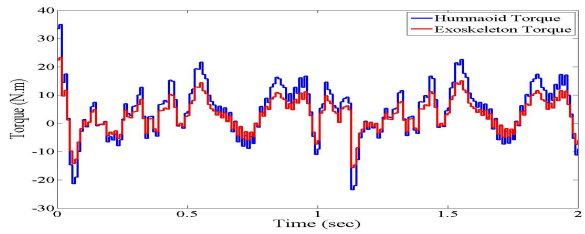

(a) Left Knee Torque

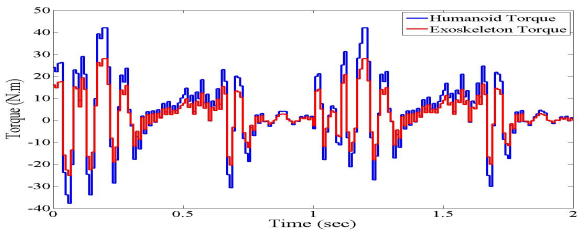

(b) Right knee torque

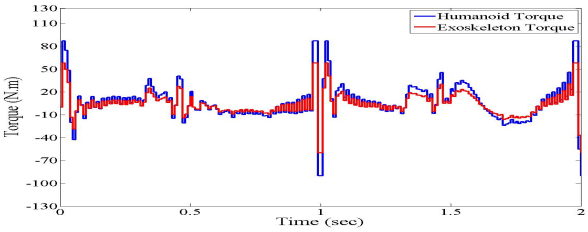

(c) Left hip torque

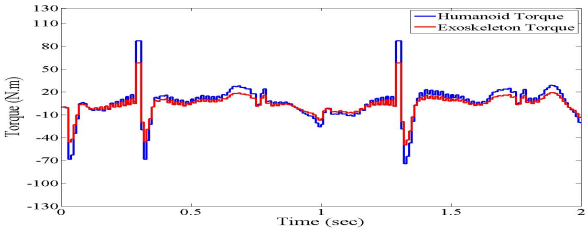

(d) Right hip torque

Figure 5.30: The torque profile for humanoid and exoskeleton using IWA tuned PID-type FLC

5.11 Summary

The main objective of the project is to assist the elderly lower extremity to perform gait task. Modelling and simulation of humanoid model and exoskeleton in Visual Nastran 4D has been carried out for theoretical investigation using different types of controllers in MATLAB environment using Simulink.

Investigations of achieving the essential torque profiles required for activating the hip and knee joint motors, to realize normal joint displacement, have been performed with the implementation of various controllers. PID control, FLC and fuzzy tune PID control.

The performances of the three proposed control methods have been evaluated using recorded trajectories from the VN4D humanoid model with exoskeleton.

A comparison of reference tracking control using the proposed controllers have shown that FLC and fuzzy PID have better performance when compared to conventional PID controller in terms of reduction of the required torque by minimising the RMSE. In addition, the optimisation algorithms used have great effect in reducing the RMSE as compared to the heuristic tuning. However, the fuzzy PID has shown better performance than FLC in terms of minimising the RMSE even with heuristic tuning and reducing the torque.

The system behaviour under the three control schemes proved that the overall references racking were acceptable. The largest mean square error among these proposed control methods during walking cycle was 2.075 belonging to the PID controller and the least mean square error of 0.556 degree for the fuzzy PID controller. The obtained result demonstrates that the torque of hip and knee joints can be controlled within admissible limits with suitable control actions of walking movement.

Comparing the results of humanoid wearing an actuated exoskeleton versus not wearing it, it has been shown that the exoskeleton decreases the required torque approximately 40% of total torque to complete walking cycle,which means it can support the users in their walking manoeuvres while reducing the energy required of them.

Chapter 6

Control of Assistive Exoskeleton in Sit to Stand Mode

6.1 Introduction

This chapter presents investigations into control of the assistive system designed for elderly people in sitting down and standing up motion. The study includes the computer aided lower limb exoskeleton attached to a humanoid model modelled in SolidWorks and visualisation in virtual environment software (SimWise).

The purpose of the assistive exoskeleton is to follow the lower limb intentions in the sagittal plane, and generate the required torque to support the hip and knee joints when performing the movement. The system is controlled using three controller types for addressing the low level control of exoskeleton's knee and hip joints. The controller types are PID control, FLC and adaptive PID-type fuzzy control designed and simulated in Matlab/Simulink.

Furthermore, nature-inspired optimization algorithms , namely SDA and IWA are used with SimWise to optimise the controllers gains. The system performance is assessed on a comparative basis in light of best reference tracking and minimum mean square error.

6.2 Sitting to standing predefined reference trajectories

Rising from sitting position to standing position is one of the most commonly performed activities of daily life. To complete the standing up motion requires about 1.5 to 2 seconds for healthy subjects (Kralj and Bajd, 1989; Nuzik et al., 1986; Schenkman et al., 1990). The whole-body posture changes through moving the segments during the movement.

Several researches are associated with the standing-up and sitting-down motions. For instance Karlj and Bajd (1989) have classified the standing-up movement into four phases as described in Figure 6.1, with a timeline for each phase.

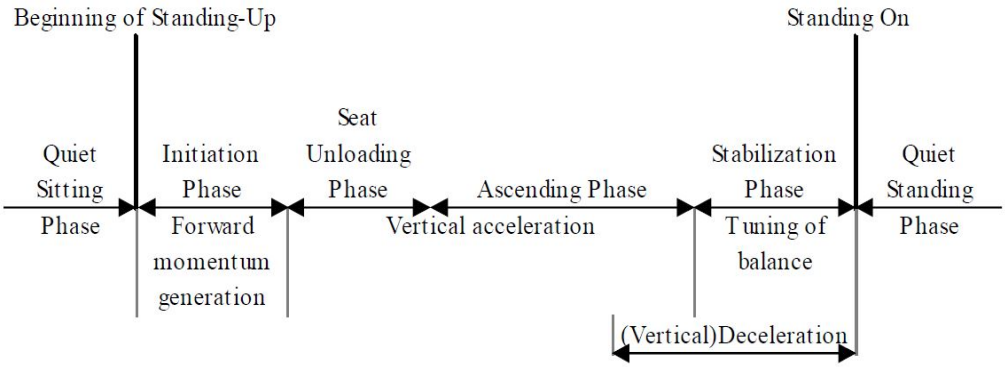

Figure 6.1: Phases of standing up movement
(Kralj and Bajd, 1989)

First phase denoted as initiation, is defined by forwarding the upper body movement during the hip flexion and generate momentum able to transmit from sitting support to leg support. During this motion, the centre of mass (COM) moves forward and slightly downward and maintains the stability to prepare for next stage while the lower body remains static.

The second phase, momentum transfer is initiated by the beginning of the vertical acceleration , and in this moment a sudden increase in body weight appears. The flexion velocity and forward momentum of upper body decrease while the hip and ankle upward momentum and extension velocity increase pushing the COM upward. It constitutes a short period but the most demanding and less stable.

Third stage, the extension phase, commences when the ankle reaches maximum flexion

and the COM attains maximum forward position. During this stage the hip and knee joints extension velocity decease and the vertical deceleration starts towards the end of this stage.

Last stage, the fourth and final phase, stabilization begins when the hip and knee joints are fully extended and attain a full upright position and the stability reaches the standard standing position. Therefore, a small anteroposterior and lateral movement is used to obtain the balance and these motions essentially include the hip and ankle joints.

A few studies have been reported regarding sitting down motions, as shown in Figure 6.2; essentially there are four phases constituting the sitting down maneuver.

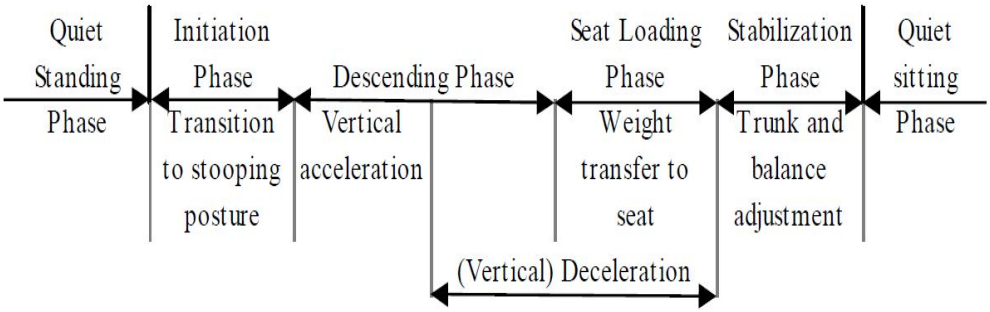

Figure 6.2: Phases of sitting down movement
Kralj and Bajd (1989)

The first phase called the initiation, occurs when the hip joint flexes. During this stage, the upper body moves forward in order to transit the standing body posture to a stooping position and lower the COM.

The second stage is vertical displacement or descending, where a vertical acceleration starts when the trunk moves down while the hip and knee joints flex.

The third stage is known as seat loading, which starts with seat contact. Then the weight transfers from leg to seat. Last stage is denoted as stabilizing or recovery, and in this stage the hip extends to acquire stable sitting position while the trunk moves backwards.

Figure 6.3 shows the orientation of the hip,knee and ankle joints to perform standing up and sitting down motions. Motion mainly consists of two different contributions. The first generates the dynamics of the motion ,and the other controls the posture.

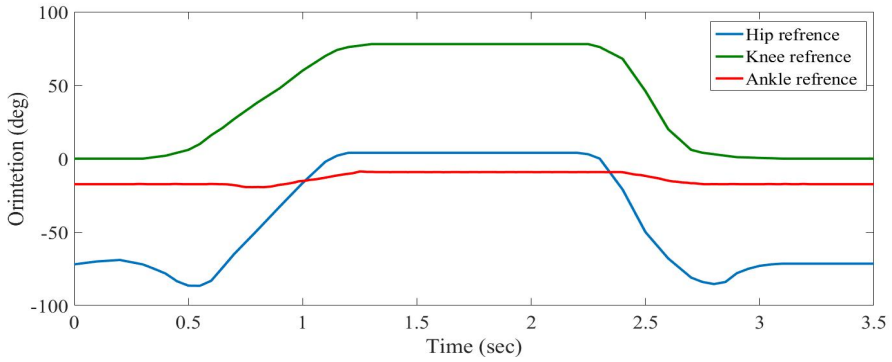

Figure 6.3: Orientation of lower limb joints during standing up and sitting down motions

6.3 PID closed loop control

This chapter aims to analyse standing-up and sitting-down movements, and develop a controllers for the exoskeleton hip and knee joints to support the elderly in their daily life activities. A significantly important goal is obtaining the torque profiles to send it to the actuator in order to ease the selection and analysis of the system when carrying out experimental trials.

Simulation of the humanoid to perform sit to stand motions was implemented in SimWise software. The data from Figure 6.3 was utilized to generate the standing-up and sitting-down references through an open loop control.

In this work, both legs receive the same references, therefore, the right and left legs are supposed to move synchronously. The second assumption is that balance is sustained throughout the motion. In SimWise simulation, feet were fixed to the ground. A saturation block of 160 Nm was placed at the output of hip joints PID controllers and of 210 Nm at the output of the knee joints PID controllers.

Revolute motors actuated by torque represented the hip and knee joints of humanoid and the exoskeleton lower limb ,and a closed-loop PID reference tracking control was implemented for these joints. Meters were attach to the hip and knee joints to monitor angular velocity, orientation and torque. Figure 6.4 shows the Simulink implementation of PID controller. In this structure, two sets of PID controllers are developed to generate the necessary torque to maintain the predefined reference signal. The first PID controller

is used for hip joint and the second PID is used for knee joint. These controllers are independently controlled to track the desired reference. A saturation block is placed at the controller output to maintain the torque within allowed limits. From the SimWise software the torque and orientation signals are monitored for both joints.

The input to the PID controller is the trajectory error which calculated from the difference between the desired reference and the actual orientation obtained from the model measured from the SimWise software. The output of the controller for hip and knee joints is the essential torque to drive the joint's motion of the lower limb humanoid model. .

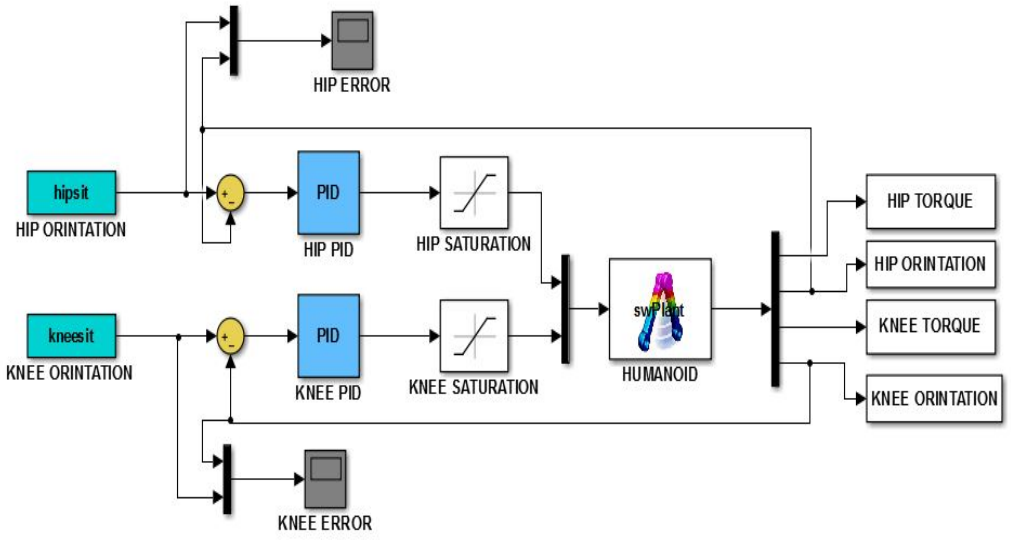

Figure 6.4: Simulink control diagram of hip and knee joints

Several PID gains were tested to evaluate the system behaviour for controlling the hip and knee revolute motors. The selected gains were varied between 2 to 20 for kp, 1 to 10 for ki and 0 to 5 for kd and for most tested cases with kd higher than 5 the system was unstable.

The RMSE values for both joints were calculated based on equation (5.2). A minimum RMSE of 7.48 for hip joint orientation and 8.21 for knee joint orientation were achieved with the set of gains presented in Table 6.1.

The orientation and torque profile for set of gains that had a smallest RMSE are illustrated in Figure 6.5 using heuristic tuning. The controller parameters were manually tuned to track the predefined reference trajectory. The tuned Kp, Ki and Kd gains for the two PID controllers are shown in Table 6.1. The achieved RMSE values for hip and knee

joints were lower than 10% of the total amplitudes of the references, therefore they were considered acceptable.

Table 6.1: PID Parameters

Controllers	Gain Parameters	Heuristic
Hip	K1	14.8
	K2	5.5
	K3	3.8
Knee	K4	9.3
	K5	4.1
	K6	0.23

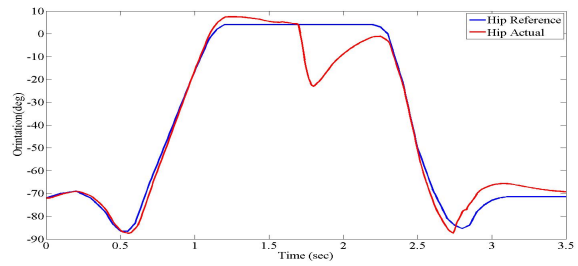

(a) Hip orientation

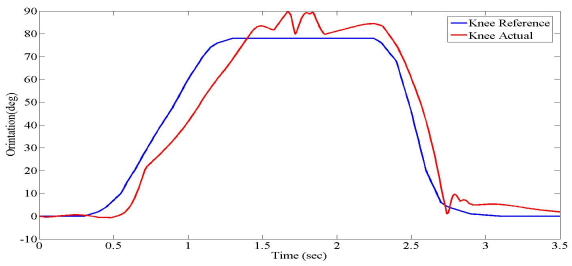

(b) Knee orientation

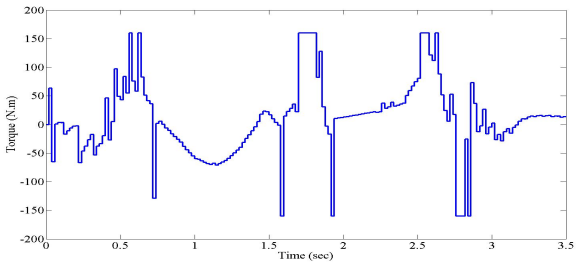

(c) Hip torque

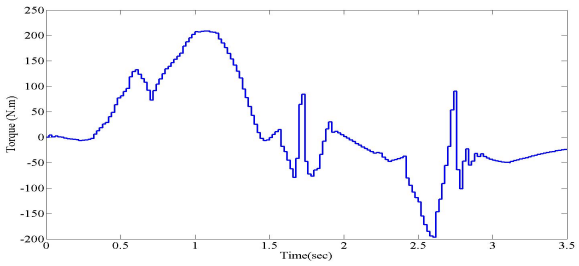

(d) Knee torque

Figure 6.5: Orientation and torque profile for hip and knee joints

As noted the system in general tracked the predefined reference well, although for 1.4 sec to 2.4 sec the tracking for both hip and knee joints was not good. Therefore, the PID gains need to be tuned using optimisation algorithms to reduce the RMSE and improve the system performance. The achieved torque was below 210 Nm approximately 208 for knee joint and 160 Nm for hip joints.

6.4 Implementation of PID controller with SDA and IWA optimisation algorithms

Investigations were carried out to tune the PID controller to determine optimised. Figure 6.6 shows the block diagram of the PID controller used for sit to stand movement.

The input of the PID controller is the error between the predefined reference trajectory and the system output while the output is the joint torque required to drive the joint to track the orientation.

For all the tests, the same population size, and the maximum number of iterations are used for comparison purposes.Table 6.2 shows the minimum cost function value and the respective desired gains achieved for each controller loop.

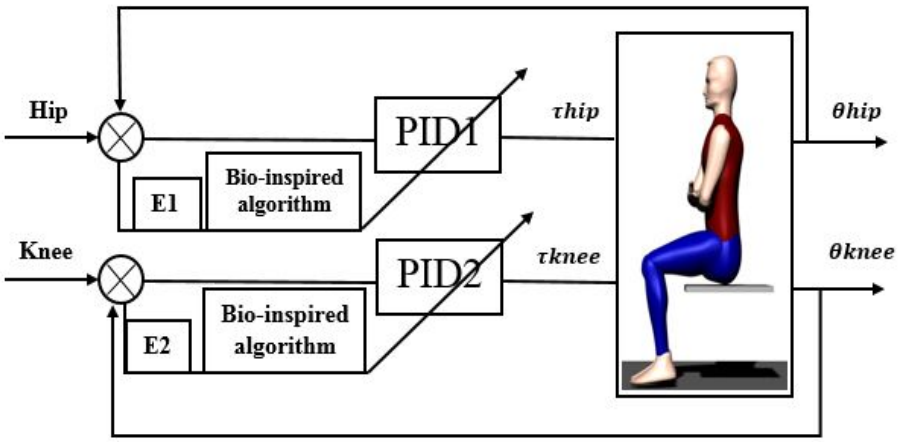

Figure 6.6: Optimizing the PID parameters

Referring to Figure 6.6, the control mechanism consists of two parts. PID 1 refers to the hip joint control mechanism and PID 2 is for the knee. E1 and E2 are the orientation errors, which are fed to the optimisation algorthim to find the best PID parameters that minimise the error. The optimisation algorithms used are the SDA and IWA.. The two inputs (τhip) and ($\tau knee$) are torque inputs to the SimWise model to activate the joints while the two outputs namely (θhip) and ($\theta knee$) represent the actual trajectories measured from the lower limb human model in SimWise visualization software. The aim of using the optimisation algorithms is to minimise the orientation error of each control loop. The MSE

represents the square of error between the reference and the actual trajectory measured from the humanoid model. The overall cost function of the system is calculated as follows:

$$Cost(x) = w1 \cdot MSE1 + w2 \cdot MSE2 \tag{6.1}$$

where cost(x) is the cost function, MSE1 is the mean square error of the hip control loop and MSE2 is for the knee joint. Therefore, the weights w1 and w2 are carefully selected so that their sum is equal to 1.

Simulation was carried out for the humanoid to perform sit to stand manoeuvre. The algorithms were used to tune the PID controller parameters. The orientation error and torque characteristics were monitored. Figure 6.7and Figure 6.8 show the trajectory with the optimised controller parameters in Table 6.2.

Table 6.2: PID Optimized Parameters

Controllers	Gain Parameters	SDA	IWA
Hip	K1	11.21	10.735
	K2	4.25	3.77
	K3	2.81	4.47
Knee	K4	7.98	7.15
	K5	1.87	1.25
	K6	4.33	4.66

In this case, the tracking was based on the hip and knee joints movement. For this experiment, the hip and knee joints follow predefined reference trajectory for sitting to standing as mentioned in Figure 6.3. With both algorithms, the PID controllers had successfully tracked the movement. The torque profiles are illustrated in Figures 6.7 and 6.8.

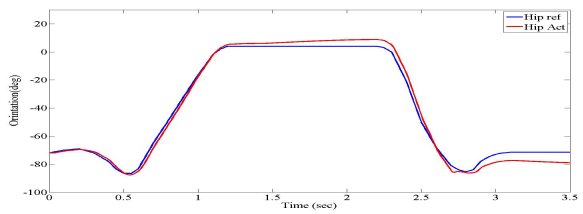

(a) Hip orientation

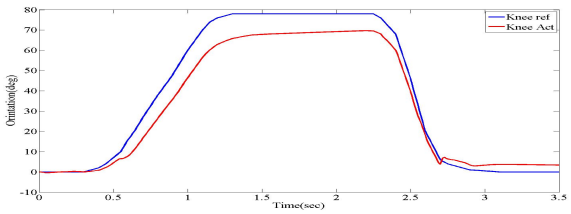

(b) Knee orientation

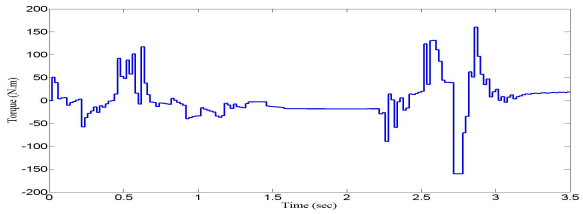

(c) Hip torque

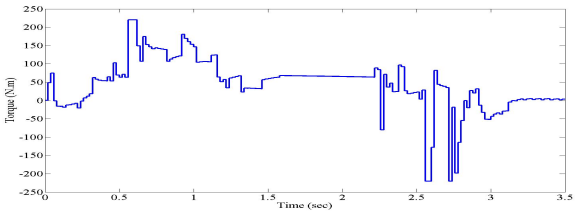

(d) Knee torque

Figure 6.7: Orientation and torque profile for hip and knee joints using SDA

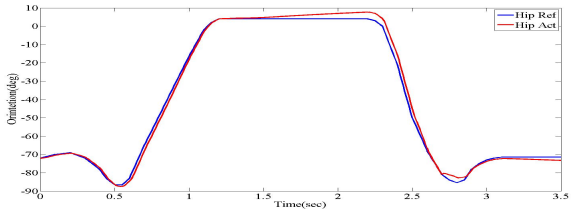

(a) Hip orientation

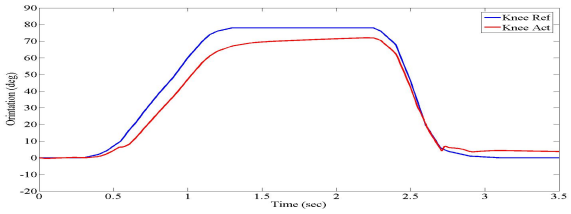

(b) Knee orientation

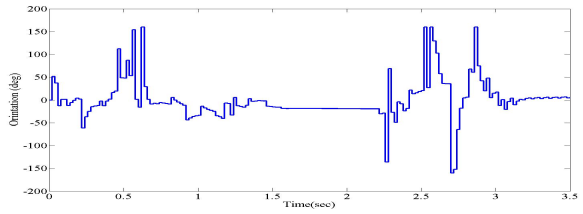

(c) Hip torque

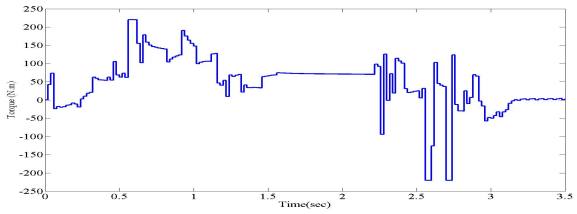

(d) Knee torque

Figure 6.8: Orientation and Torque profile for hip and knee joints using IWA

The results show that the better tuning parameters the better reference tracking. The RMSE was 3.96 for hip joint and 6.8 for knee joint using SDA algorithm. For IWA algorithm, the RMSE obtained was 3 for hip joint and 7 for knee joint. The torque was smoother with both algorithm algorithms as compared to manual tuning. The torques were within defined range. Both algorithms performed well and the results were similar.. The cost function was 5.38 with SDA tuning and 5 with IWA tuning of controller parameters.

6.5 The assistive exoskeleton

In this section, the humanoid model is combined with the exoskeleton model and visualised in SimWise software. The controller was developed in Matlab/Simulink and linked with SimWise to control the humanoid and exoskeleton model. Two separate controllers are devised, one for the humanoid model and one for the exoskeleton providing 60% and 40% of the overall torque respectively. This represents that the user is only able to supply 60% of the total torque required to perform the standing up and sitting down and accordingly, assistance needs to be provided to complete the task. The high-level control is responsible of estimating the intention and sending to the exoskeleton exactly the same generated person gait to follow. Referring to the Simulink model shown in Figure 6.4, PID controller is used for both the two joints of the humanoid and the exoskeleton for each leg.

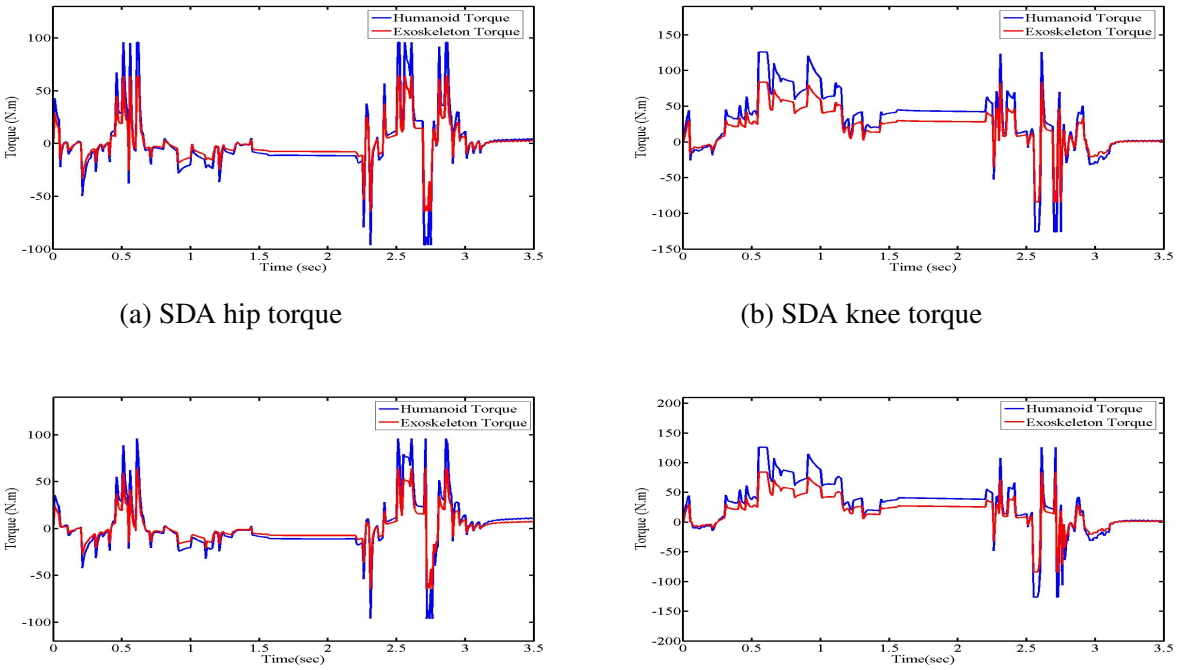

(a) SDA hip torque

(b) SDA knee torque

(c) IWA hip torque

(d) IWA knee torque

Figure 6.9: Orientation and torque profile for hip and knee joints using SDA and IWA

Figure 6.9 shows the torque profiles for hip and knee joints during the standing to sitting motion. The exoskeleton provided 60 Nm torque to assist the hip joint and 80 Nm for the joint with the optimized parameters in Table 6.2.

6.6 Implementation of FLC

In this section, PD-type fuzzy controllers are developed and implemented to control the lower limbs for sit to stand function. Figure 6.10 shows the block diagram of the control structure used in this work.The standard equation of the PD-type fuzzy control is illustrated as follows:

$$U(t) = K_P \cdot e(t) + K_d \cdot \Delta e(t) \tag{6.2}$$

Where K_P is the proportional gain and K_d is the deferential gain.

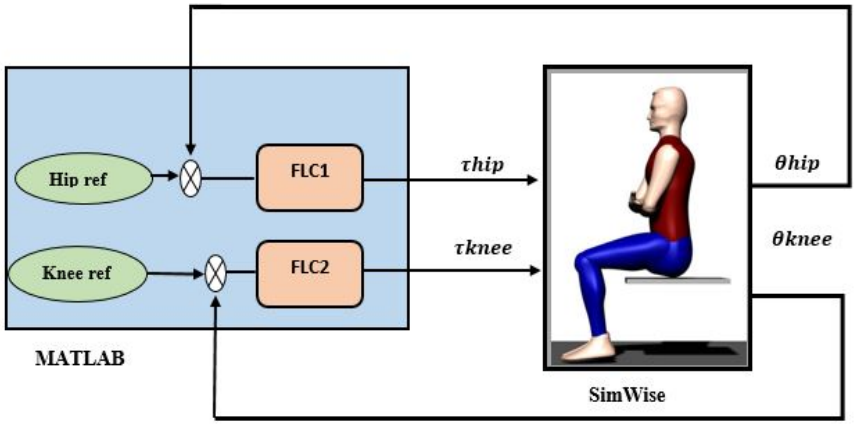

Figure 6.10: Matlab integration with SimWise

The sit to stand mechanism is initiated by driving the hip and knee joints to follow the predefined trajectory. Mamdani type fuzzy inference mechanism is selected in designing the FLCs. Two FLCs, namely FLC1 and FLC2 are developed, one for each joint with same rule bases. For each FLC there are two inputs and one output. The inputs to the controller are represented by the orientation error and the orientation change of error while the output of the controller is the torque required to actuate the joints to follow the reference. The two input are normalized between [-1, 1]. The detailed control structure is shown in Figure 6.11. Five Gaussian shape membership functions are used for each inputs and outputs as presented in Figure 6.12. It is believed that this type of membership shape gives smooth and steady response for the system.

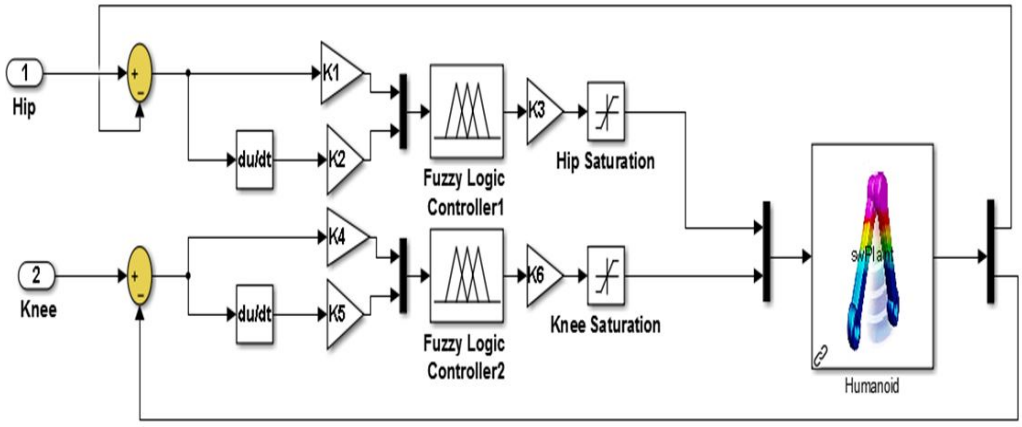

Figure 6.11: The detailed structure for PD fuzzy controller

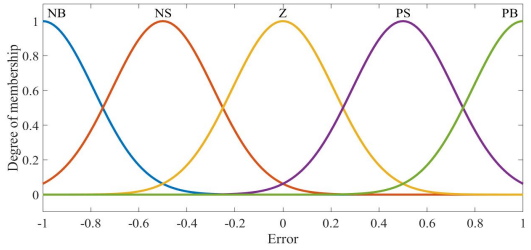

(a) Membership of error

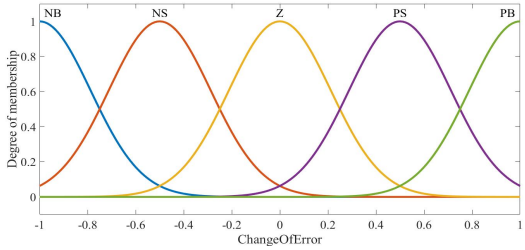

(b) Membership of change of error

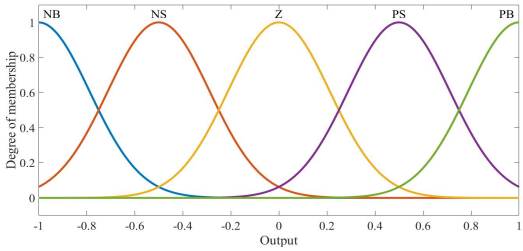

(c) Output membership function

Figure 6.12: Inputs and Output membership function

As noted in Figure 6.11 there are four input and two output scaling factors. These need to be tuned for improved system performance. The trial and error method was selected for tuning and after several attempts the system successfully tracked the desired reference. Table 6.3 shows the achieved fuzzy scaling parameters.

Table 6.3: Fuzzy scaling Parameters

Controllers	Gain Parameters	Heuristic
Hip	K1	0.124
	K2	0.83
	K3	19.6
Knee	K4	0.13
	K5	0.359
	K6	28.4

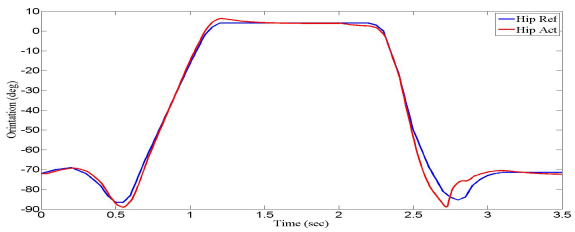

(a) Hip orientation

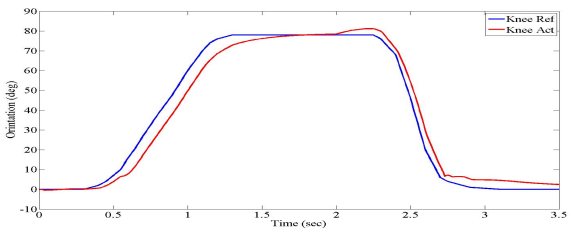

(b) Knee orientation

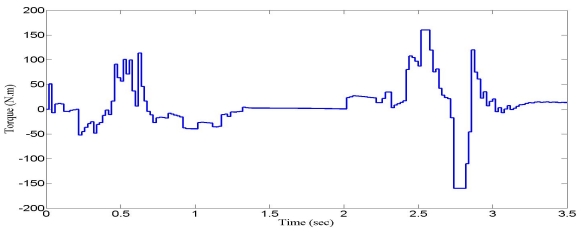

(c) Hip torque

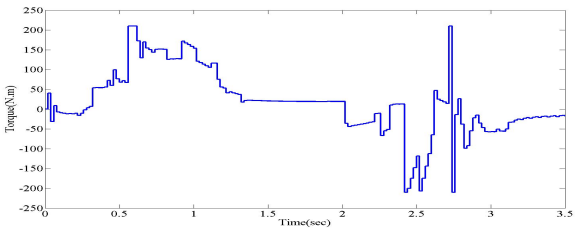

(d) Knee torque

Figure 6.13: Orientation and torque profile for hip and knee joints with heuristically tuned PD-type FLCs

Figure 6.13 presents the orientation and torque profile for heuristic tuning. Using the scaling parameters in Table 6.3, the control methodology has controlled the humanoid lower limb successfully. The obtained RMSE was 2.6 for hip joint and 5.2 for knee joint. The maximum torque value was acceptable and within admissible range. The results show that the PD-type fuzzy controller performed better than the conventional PID. However, the FLC required more calculation time as compared to PID. The PD-type FLC shows promising results but the system performance needs to be further improved by using an

optimization algorithm.

6.7 Implementation of FLC with SDA and IWA control design

In this section, SDA and IWA are used to optimise the input and output scaling factors of a FLC for sitting to stand motions of the humanoid model and exoskeleton lower limbs. Several approaches can improve the system performance such as tuning the fuzzy input output scaling factors, optimizing the fuzzy membership function and the rules , and optimizing the corresponding parameters of the constrains used in the humanoid and exoskeleton model designed in SimWise. Among all these options, optimizing the scaling factors is significantly a simple strategy. Figure 6.14 presents the structure of optimising the fuzzy scaling factors while Table 6.4 shows the optimised parameters for both algorithms.

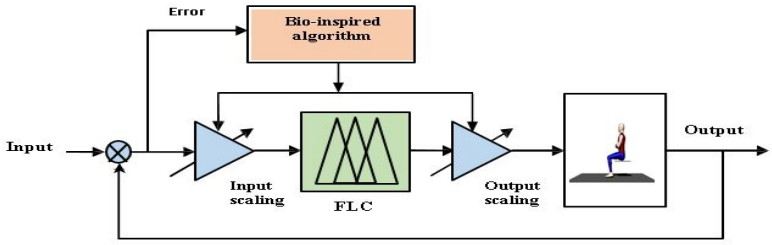

Figure 6.14: Input output of fuzzy parameters

Table 6.4: Fuzzy optimized parameters

Controllers	Gain Parameters	SDA	IWA
Hip	K1	0.5	0.15
	K2	0.425	0.87
	K3	28.1	23.7
Knee	K4	0.12	0.16
	K5	0.187	0.189
	K6	43.3	23.6

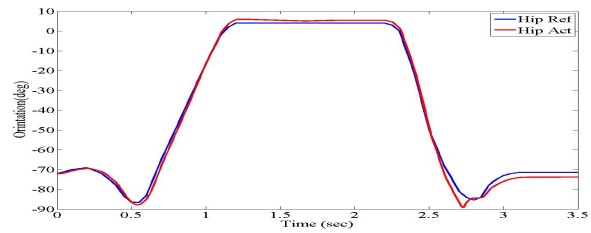

(a) Hip orientation

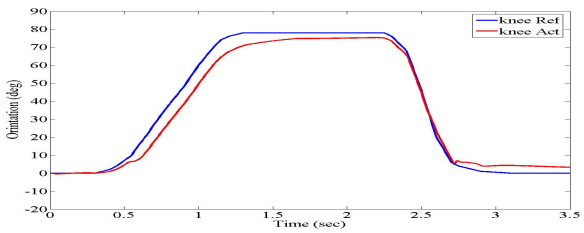

(b) Knee orientation

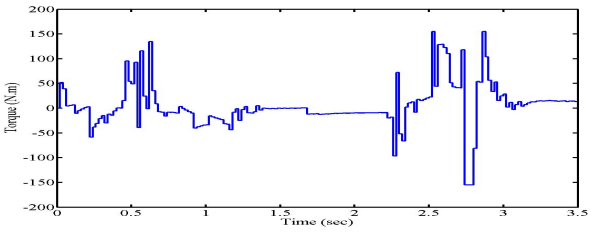

(c) Hip torque

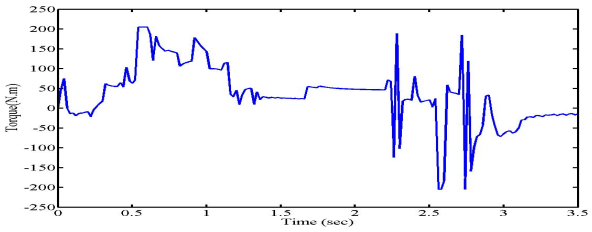

(d) Knee torque

Figure 6.15: Orientation and Torque profile for hip and knee joints with SDA-tuned FLC

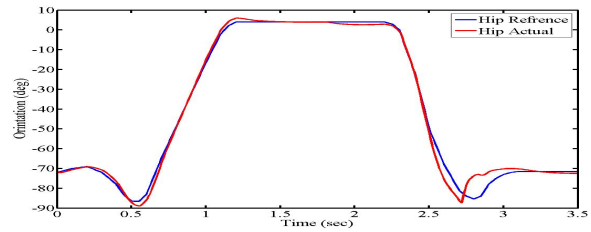

(a) Hip orientation

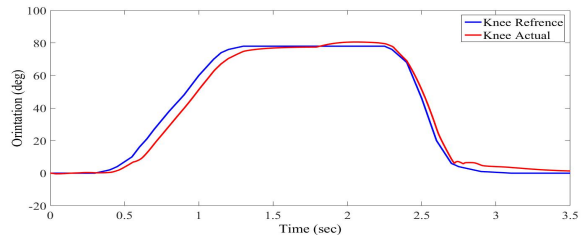

(b) Knee orientation

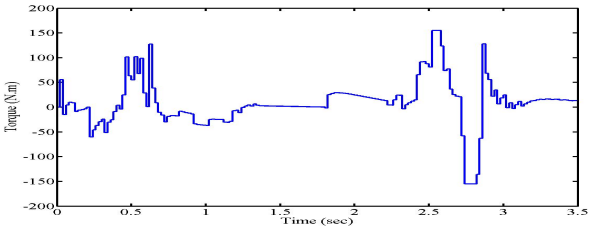

(c) Hip torque

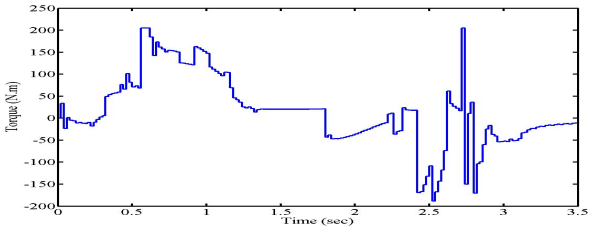

(d) Knee torque

Figure 6.16: Orientation and torque profile for hip and knee joints with IWA-tuned FLC

When optimizing the fuzzy input output scaling factors the RMSE has been reduced to 2.11 for hip joint and 5 for knee joints with SDA,as in Figure 6.15. In contrast, the archived RMSE was 2.5 for hip joint and 4.2 for knee joint with IWA as presented in Figure 6.16. Thus, both algorithms performed well;the SDA achieved better reference tracking for the hip joint while the IWA obtained better tacking for the knee joints. The torque was s slightly reduced with both algorithms to 155 Nm for hip and 205 Nm for knee joint.

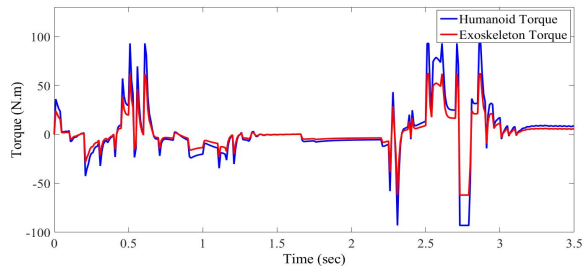

(a) SDA hip torque

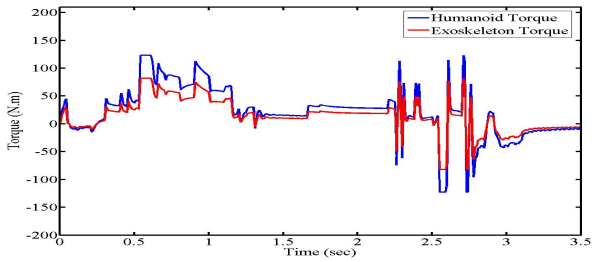

(b) SDA knee torque

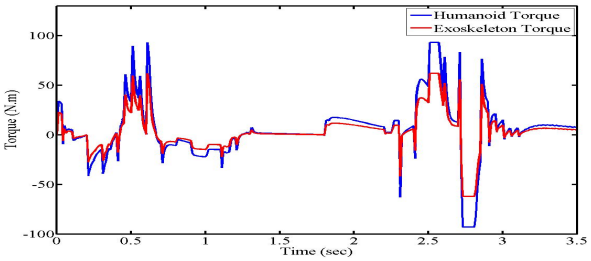

(c) IWA hip torque

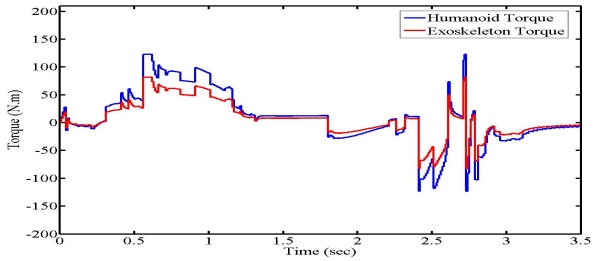

(d) IWA knee torque

Figure 6.17: Torque profile for hip and knee joints using SDA vs IWA

PD-type FLCs with the saturation level stated in the aforementioned section were used for hip and knee joints. The required torque and the RMSE were calculated after each run. In general, the results obtained with the actuated exoskeleton were satisfactory, with a MSE between 2 and 2.5 for hip joint and 4.2 and 5 for knee joint. Regarding torque, humanoid provided around 93Nm for hip joint and 123 Nm for knee joint, while the exoskeleton added 62 Nm for hip joint and 82 Nm for knee joint as shown in Figure 6.17. Without the use of the exoskeleton device, the humanoid needed about 40% more torque for hip joint ,and around 40% more for knee joint , to perform the same motions.

6.8 Implementation of FLC-PID

The characteristics of lower extremity are very complex and nonlinear, therefore its dynamic model cannot be accurately described mathematically. Thus, an intelligent control mechanism may be used for such systems. . The conventional PID control algorithm is widely usable in many control applications and plays a dominant role in the industrial control field. However, the limitation of PID algorithm is that its parameters cannot be self adjusted to control a complex and nonlinear systems well. The Intelligent algorithms have

the capability to handle the complexity of nonlinear systems, and do not require precise mathematical models. Intelligent algorithms have features to adjust their parameters during the control process. However, intelligent algorithms need more time for calculation. Developing an algorithm that combines intelligent algorithms with PID algorithms will provide the advantages of constituent components.

The first principle of fuzzy self-tuning PID controller is finding the fuzzy relationship between three gains of PID controller and the two fuzzy input error (e) and change of error (ec). Thus, the system performance will improve by combining the fuzzy logic with conventional PID. Matlab/Simulink is used to design the Fuzzy PID controller,the detailed structure of fuzzy tuning PID is illustrated in Figure 6.18

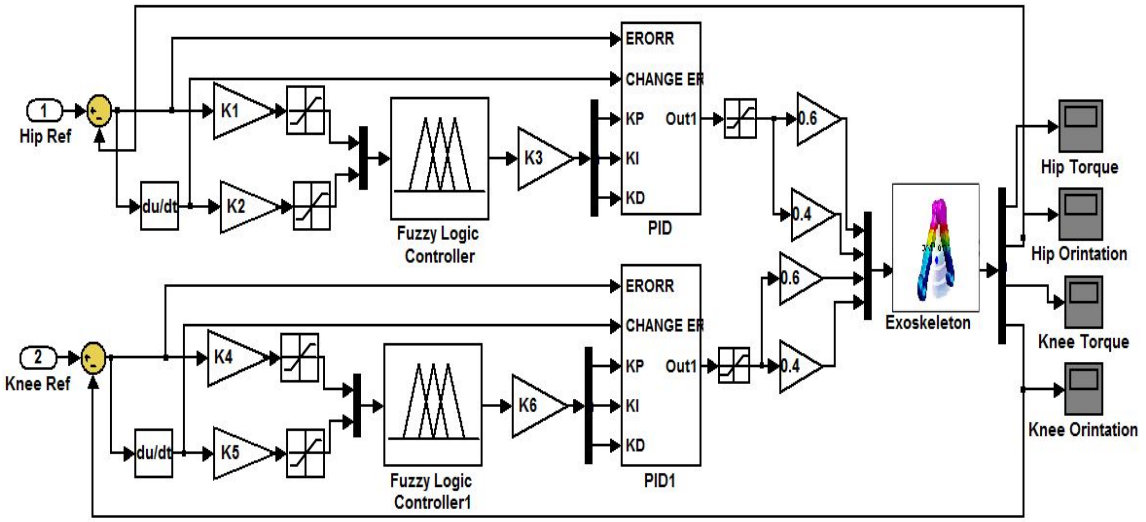

Figure 6.18: Block diagram of fuzzy PID control structure

The fuzzy PID controller is mainly constructed of two parts: adjustable gains PID controllers and fuzzy control system. The structure of the fuzzy controller consists of two inputs and three outputs, where the inputs are the orientation error and orientation change of error and the outputs are the three PID parameters.

Five Mamdani triangular membership functions were used leading to 25 fuzzy rules, these are Positive Big (PB),Positive Small(PS),Zero (Z),Negative Small (NS),and Negative Big (NB).The inputs and outputs membership function are shown in Figure 6.19 and Figure 6.20. The orientation of lower limb joints are independently controlled by Fuzzy/PID structure which have similar rule bases.The domain of error and change of error is [-1, 1]

and for the output variable controller, KP = [0-20]; KI= [0-10] ;KD =[0-5].

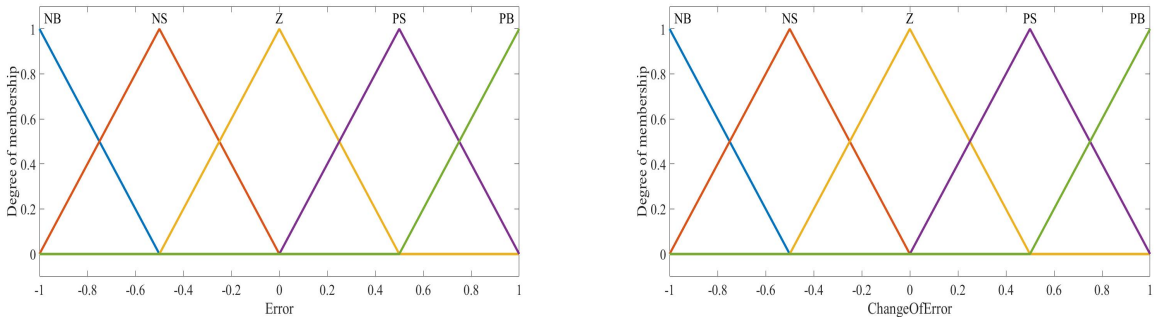

(a) Membership of error (b) Membership of change of error

Figure 6.19: Inputs membership function

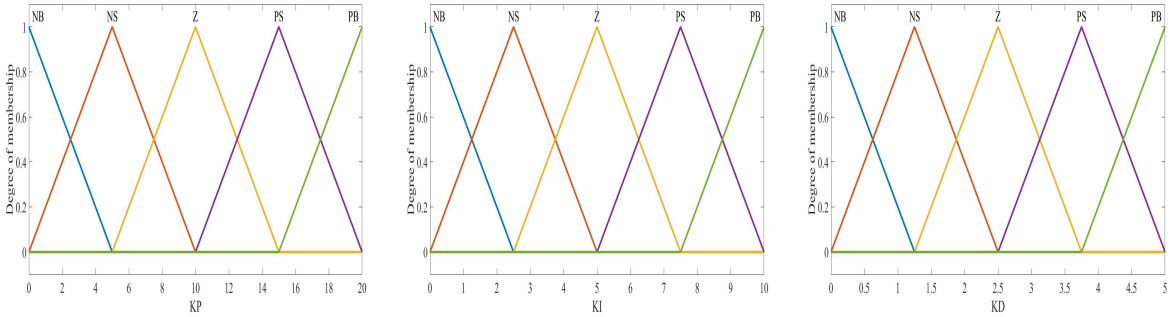

(a) Membership of KP (b) Membership of KI (c) Membership of KD

Figure 6.20: Membership functions of fuzzy PID outputs

The fuzzy rules used for adapting the PID parameters KP,KI,KD are shown in Table 6.5, Table 6.6, and Table 6.7.

Table 6.5: KP Fuzzy inference rule

$e/\dot{e}$	NB	NS	Z	PS	PB
NB	PB	PB	PS	PS	Z
NS	PB	PS	PS	Z	NS
Z	PS	PS	Z	NS	NS
PS	PS	Z	NS	NS	NB
PB	Z	NS	NS	NB	NB

Table 6.6: KI Fuzzy inference rule

$e/\dot{e}$	NB	NS	Z	PS	PB
NB	NB	NB	NS	NS	Z
NS	NB	NS	NS	Z	PS
Z	NS	NS	Z	PS	PS
PS	NS	Z	PS	PS	PB
PB	Z	PS	PS	PB	PB

Table 6.7: KD Fuzzy inference rule

$e/\dot{e}$	NB	NS	Z	PS	PB
NB	PS	NB	NB	NB	PS
NS	Z	NM	NM	NS	Z
Z	Z	NS	NS	NS	Z
PS	Z	Z	Z	Z	Z
PB	PB	PM	PM	PS	PB

The simulation was run for 3.5 seconds; the results were collected from both lower limbs of the humanoid model. Orientation sensors were attached to the humanoid to measure the trajectories of the hip and knee joints. The reference tracking performances of the control system for hip and knee joints and the torque profile are demonstrated in Figure 6.21. It is observed that the hip joint torque was below 150 Nm through the standing to sitting and the knee joint torque was below 200 Nm. The scaling parameters K1 to K6

were tuned heuristically.

The minimum cost function obtained by manual tuning was 3 with RMSE of 3 for hip joint and 2.9 for knee joint. Table 6.8 shows the scaling parameters used.

Table 6.8: Heurstic control parameters tuning

Joints	Gain Parameters	Heurstic
Hip	K1	0.125
	K2	0.747
	K3	33.5
Knee	K4	0.259
	K5	0.376
	K6	20.39

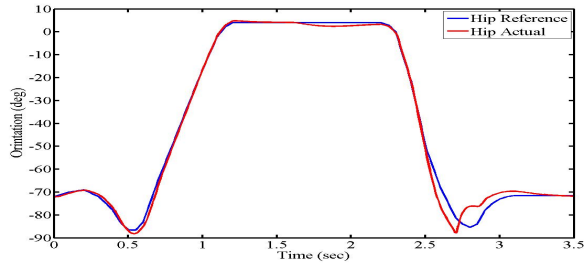

(a) Hip orientation

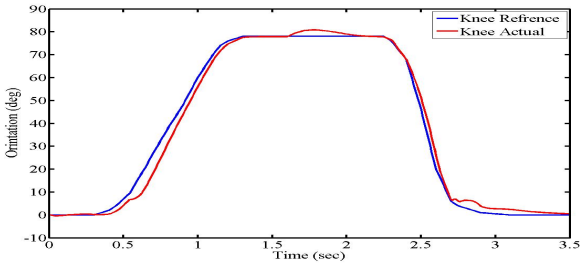

(b) Knee orientation

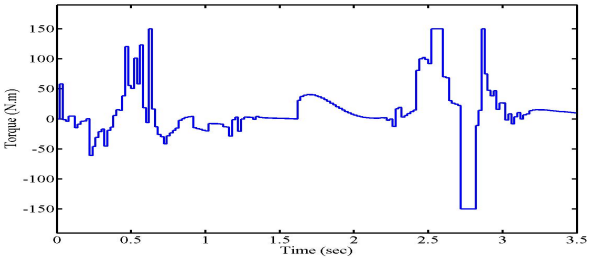

(c) Hip torque

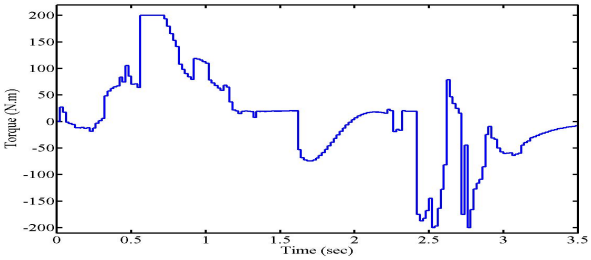

(d) Knee torque

Figure 6.21: Orientation and torque profile for hip and knee joints with heuristically tuned FLC-PID

6.9 Implementation of FLC-PID with SDA and IWA control design

In this section, SDA and IWA are used to optimise the input scaling factors of the FLC. The objective is to minimize the orientation error for hip and knee joints while the humanoid model performs the motion. A population of 5 searching points for 100 iterations were used for both SDA and IWA, with which the minimum cost function achieved for the system 2.19 with the SDA and 1.49 with the IWA. The scaling factor values obtained with the optimization techniques are shown in Table 6.9. The simulation was carried out for 3.5 seconds, the results were collected from the hip and knee joints of the humanoid model. The reference tracking performances of the control loops for hip and knee joints and the torque of humanoid measured are illustrated in Figure 6.22 and Figure 6.23. It is noted that the torque for the hip joint was below 150 Nm and below 200 Nm for knee joint with IWA while it was for hip joints above 150 Nm and the knee joints torque was above 200 Nm for SDA. The results shown in Figures 6.22, 6.23 demonstrate that the developed fuzzy/PID controller successfully tracked the reference with low oscillation as compared to the conventional PID and also performed better than PD-type FLC with optimisation algorithms in term of minimizing the RMSE for the system overall. The proposed controller combined the fuzzy ability dealing with nonlinear system with simple implementation of PID controller.

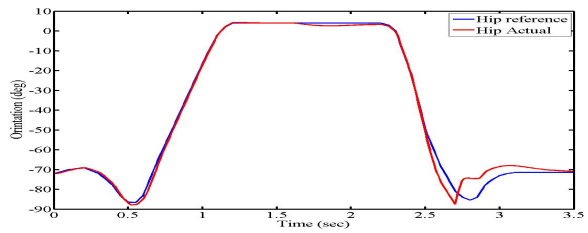

(a) Hip orientation

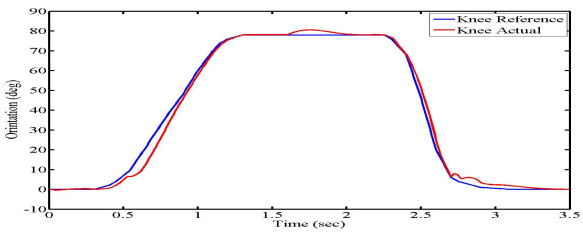

(b) Knee orientation

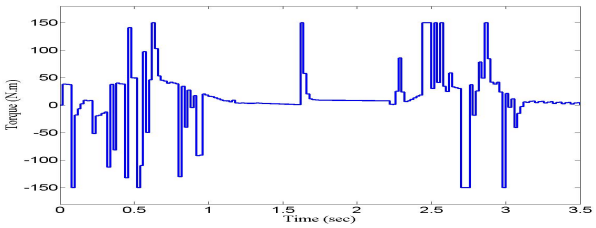

(c) Hip torque

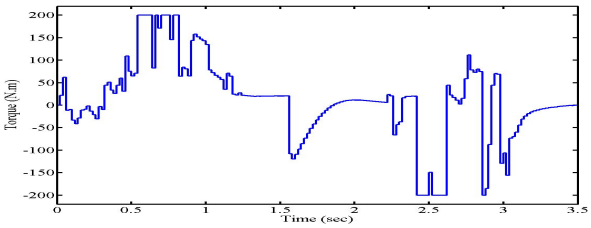

(d) Knee torque

Figure 6.22: Orientation and torque profile for hip and knee joints with SDA tuned FLC-PID

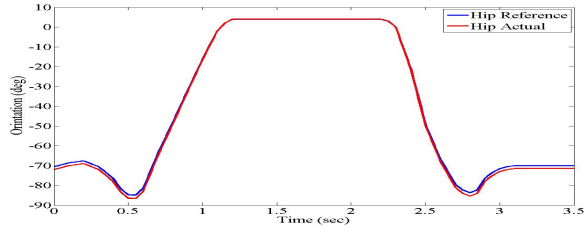

(a) Hip orientation

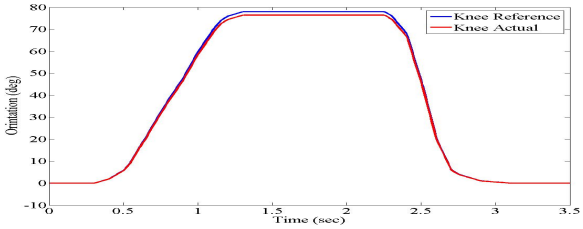

(b) Knee orientation

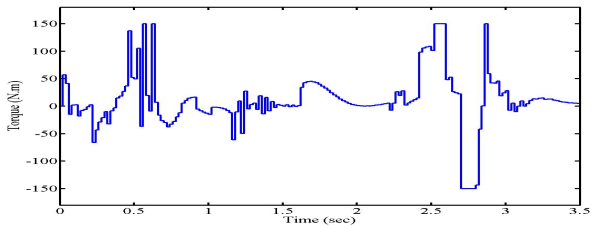

(c) Hip torque

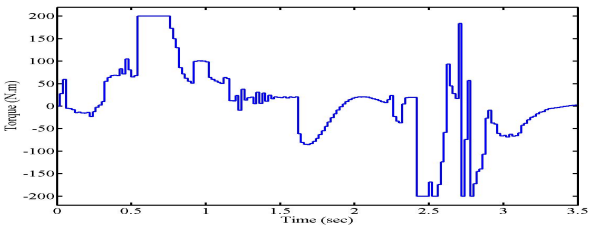

(d) Knee torque

Figure 6.23: Orientation and torque profile for hip and knee joints with IWA tuned FLC-PID

Table 6.9: Fuzzy PID optimized parameters

Controllers	Gain Parameters	SDA	IWA
Hip	K1	0.213	0.15
	K2	0.525	0.67
	K3	68	90
Knee	K4	0.19	0.36
	K5	0.487	0.589
	K6	43.3	53.6

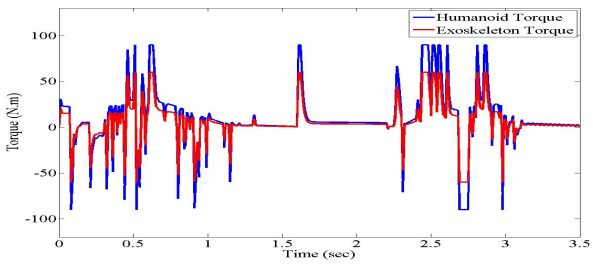

(a) SDA hip orientation

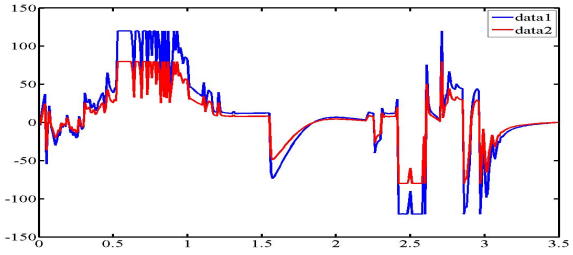

(b) SDA knee orientation

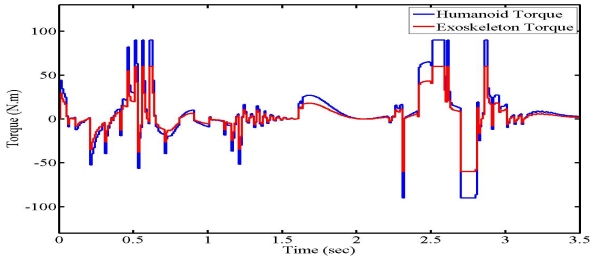

(c) IWA hip torque

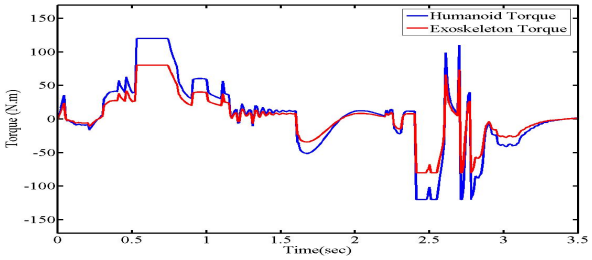

(d) IWA knee torque

Figure 6.24: Orientation and torque profile for hip and knee joints with SDA and IWA

When controlling the humanoid with actuated exoskeleton, 60 percent of the control action will drive the humanoid model while the rest will actuate the exoskeleton. Assuming the exoskeleton follows the humanoid gait trajectory and the humanoid represents an elderly with the ability to sit to stand but with weak muscles.

Figure 6.24 shows the torque profiles of the hip and knee joints for the humanoid wearing the exoskeleton. By using the same scaling parameters achieved by the proposed

algorithm, IWA provided low torque as compared to SDA. The exoskeleton augmented the knee joint by nearly 80Nm and by 60 Nm for hip joint. While the exoskeleton has provided the necessary enhancement to the humanoid joint torques during the walking cycle by supplying 76 Nm to the knee joint and 56 Nm to the hip joint. These ranges are within acceptable and recommended levels Low (2011); the maximum assistive torque to enhance the joints should be lower than 120 Nm. Therefore, the exoskeleton assists the elderly by reducing the energy required to perform the motion. For example instead of the human having to provide about 140 Nm for hip joint and 190 Nm for knee joint, wearing the exoskeleton will reduce this effort to 84 Nm for hip joint and 114 Nm for knee joint. This means nearly 40 percent of the required energy has reduced by the exoskeleton.

6.10 Summary

In this chapter, the humanoid model and the actuated exoskeleton were modeled in SimWise software. Three types of controllers namely, PID, FLC and FLC-PID have been designed in Matlab/Simulink. Investigations of controlling the humanoid model to achieve the essential torque profiles required for activating the hip and knee joint motors, to realize normal joint displacement, have been performed with the implementation of these controllers.

Comparative performance assessment of the control structures has been carried out. It has been shown that the FLC-PID control structure has performed better than PD-type FLC and conventional PID control in terms of reducing the required torque by minimizing the RMSE. In addition, the optimisation algorithms used have great effect in reducing the RMSE as compared to heuristic tuning.

The overall reference tacking has been acceptable with the three control schemes. The largest cost function among these proposed control methods was 7.845 belonging to the PID controller and the least cost function was 1.49 for the FLC-PID control.

Comparing the results of humanoid wearing an actuated exoskeleton versus not wearing it, it has been shown that the exoskeleton decreases the required torque by approx-

imately 40 % of total torque, which means it can support the users in their movements while reducing the energy requirement in part of the user.

Chapter 7

Conclusion and Future Works

7.1 Summary and conclusion

A literature review of the elderly muscle weakness, biomechanics of fundamental mobility tasks, and exoskeleton components, including control techniques engaged has been presented.

The review has revealed some gaps regarding software facilities used for early design evaluations. Few works describe the usage of virtual environments to evaluate the exoskeleton in early. This is because most of the publications related to development of lower limb exoskeleton devices have focused on prototype construction. Therefore, this research has taken advantage of available facilities of the software to develop and test the control strategies using a virtual environment of the human and exoskeletons. Moreover, publications regarding the low level exoskeleton control strategies are sparse, especially for standing-up and sitting-down motions for elderly assistance. Thus, the research has focused development of the low level controllers for exoskeletons.

Three control mechanisms have been proposed and evaluated to control a low extremity exoskeleton to assist an elderly person in upright walking and sit-to-stand manoeuvres in an augmentation manner. The main focus of the work, thus, has been to develop an assistive exoskeleton to enable an elderly to perform multitasking such as walking and sit to stand manoeuvres.

The content of this thesis can be summarised in two main applications. The first application is controlling the actuated exoskeleton adopted from the EXO-LEGS project for the

elderly. The required humanoid torque was evaluated through using three different controllers namely: PID , FLC and fuzzy PID controllers, to achieve walking function , with the lowest root mean squared error. The controller performance has been assessed using heuristic tuning versus optimised tuning.

The second application is controlling the actuated exoskeleton to perform sitting down to standing up movement by the same proposed controllers. Comparing the obtained results of the three controllers by the lowest mean square error and better reference tracking. The research has revealed that while conventional PID control can word adequately well in model-based control paradigms for systems with defined dynamic models, their performance in control of complex systems will not be adequate. Where the system is too complex to model, or is too costly to model it is found more appropriate to use a non-model based control; ie to bypass the system model determination and develop the control mechanism directly. Fuzzy logic and bio-/nature-inspired optimisation provide the potential of developing powerful and sophisticated control mechnanisms that do not require precise description of dynamic model of systems and thus are suited to control of complex systems. The research has demonstrated the design process and control mechanisms combining fuzzy logic paradigims with nature-inspired optimisation algorithms, exemplified with SDA and IWA. The results achieved have revealed the potential benefits and capabilities such approaches in the control of complex dynamic systems.

7.2 Future works

This research has embarked on evaluating the control techniques used for exoskeleton system for assisting elderly people on basic mobility tasks.

Regarding to the actuated exoskeleton used for assisting mobility such as walking and standing-up and sitting-down motions it is recommended to keep the weight as low as possible. Because the elderly people with weak muscle could not bearing to carry extra weight. In addition, it will be required to add adaptable and interface mechanisms not only for the vertical axis but also for the horizontal one as well as fitting the device to the user,

and to align the joints of the exoskeleton corresponding to anatomic position.

Investigating different combinations of assistance percentage will form the basis a scaling up design mechanism for an elderly so that the augmentation needed may be adjusted as the need arises over time..

Research may be carried out on adoption of further optimisation algorithms with the proposed control strategies for even further improved performance of the system. In terms of controller methodology, a comparison of the results obtained throughout this thesis with those of the three proposed controller show that the fuzzy tuning PID and FLC perform better than conventional PID controller. However, time consumption is an issue for real-time implementation of the approaches. Thus, research into ways of reducing the execution time by efficient coding or the algorithms may be carried out.

In terms of the software facilities, another software could be used, AnyBody, which has facilities of dynamic and kinematic calculation for both the humanoid and exoskeleton models. This software contains the calculation features for metabolic costs, estimating realistic contact forces, and calculate reacting forces to the ground while system equilibrium is considered (AnyBodyTechnology, 2016).

Lastly, system validation experiment should be implemented for controlling environment to observe the system behaviour of the suggested strategies.

References

Albertos, P. and Sala, A. (1998). Fuzzy logic controllers. advantages and drawbacks. In *VIII International Congress of Automatic Control*, volume 3, pages 833–844.

Allemand, Y., Stauffer, Y., Clavel, R., and Brodard, R. (2009). Design of a new lower extremity orthosis for overground gait training with the walktrainer. In *Rehabilitation Robotics, 2009. ICORR 2009. IEEE International Conference on*, pages 550–555. IEEE.

Ambrose, A. F., Paul, G., and Hausdorff, J. M. (2013). Risk factors for falls among older adults: a review of the literature. *Maturitas*, 75(1):51–61.

American Academy of Orthopaedic Surgeons (2014). Orthopaedics. `http://www.orthoinfo.aaos.org/topic.cfmtopic=a00523`. [Online; Accessed 01 Aug 2014].

Association, A. D. et al. (2012). Diagnosis and classification of diabetes mellitus. *Diabetes care*, 35(Supplement 1):S64–S71.

Banala, S. K., Agrawal, S. K., and Scholz, J. P. (2007). Active leg exoskeleton (alex) for gait rehabilitation of motor-impaired patients. In *Rehabilitation Robotics, 2007. ICORR 2007. IEEE 10th International Conference on*, pages 401–407. IEEE.

Banala, S. K., Kim, S. H., Agrawal, S. K., and Scholz, J. P. (2009). Robot assisted gait training with active leg exoskeleton (alex). *IEEE Transactions on Neural Systems and Rehabilitation Engineering*, 17(1):2–8.

Baumgartner, R. N., Koehler, K. M., Gallagher, D., Romero, L., Heymsfield, S. B., Ross, R. R., Garry, P. J., and Lindeman, R. D. (1998). Epidemiology of sarcopenia among the elderly in new mexico. *American journal of epidemiology*, 147(8):755–763.

Benasla, L., Belmadani, A., and Rahli, M. (2014). Spiral optimization algorithm for solving combined economic and emission dispatch. *International Journal of Electrical Power & Energy Systems*, 62:163–174.

Bjørnstrup, J. (1995). Estimation of human body segment parameters-historical background.

Blanke, D. J. and Hageman, P. A. (1989). Comparison of gait of young men and elderly men. *Physical Therapy*, 69(2):144–148.

Bogue, R. (2015). Robotic exoskeletons: a review of recent progress. *Industrial Robot: An International Journal*, 42(1):5–10.

Bortole, M. (2013). Design and control of a robotic exoskeleton form gait rehabilitation.

Bouri, M., Stauffer, Y., Schmitt, C., Allemand, Y., Gnemmi, S., Clavel, R., Métrailler, P., and Brodard, R. (2006). The walktrainer: a robotic system for walking rehabilitation. In *Robotics and Biomimetics, 2006. ROBIO'06. IEEE International Conference on*, pages 1616–1621. IEEE.

Brown, L. A., Shumway-Cook, A., and Woollacott, M. H. (1999). Attentional demands and postural recovery: the effects of aging. *The Journals of Gerontology Series A: Biological Sciences and Medical Sciences*, 54(4):M165–M171.

Buesing, C., Fisch, G., O'Donnell, M., Shahidi, I., Thomas, L., Mummidisetty, C. K., Williams, K. J., Takahashi, H., Rymer, W. Z., and Jayaraman, A. (2015). Effects of a wearable exoskeleton stride management assist system (sma®) on spatiotemporal gait characteristics in individuals after stroke: a randomized controlled trial. *Journal of neuroengineering and rehabilitation*, 12(1):69.

Byrne, D. P., Mulhall, K. J., and Baker, J. F. (2010). Anatomy & biomechanics of the hip. *The open sports medicine journal*, 4(1).

Cardero, C. (2012). Articulated human body.grabcad. `https://www.grabcad.com/library/articulated-human-body-2`. [Online; Accessed 01 Aug 2014].

Chen, B., Ma, H., Qin, L.-Y., Gao, F., Chan, K.-M., Law, S.-W., Qin, L., and Liao, W.-H. (2016). Recent developments and challenges of lower extremity exoskeletons. *Journal of Orthopaedic Translation*, 5:26–37.

Chen, B., Ma, H., Qin, L.-Y., Guan, X., Chan, K.-M., Law, S.-W., Qin, L., and Liao, W.-H. (2015). Design of a lower extremity exoskeleton for motion assistance in paralyzed individuals. In *Robotics and Biomimetics (ROBIO), 2015 IEEE International Conference on*, pages 144–149. IEEE.

Chen, G., Chan, C. K., Guo, Z., and Yu, H. (2013). A review of lower extremity assistive robotic exoskeletons in rehabilitation therapy. *Critical Reviews™ in Biomedical Engineering*, 41(4-5).

Chen, G. and Pham, T. T. (2000). *Introduction to fuzzy sets, fuzzy logic, and fuzzy control systems*. CRC press.

Chen, H.-Y. and Sung, W.-H. (2011). Comparison of the walking performance between healthy young adults and healthy elderly people: 2726: Board# 25 june 3 2: 00 pm-3: 30 pm. *Medicine & Science in Sports & Exercise*, 43(5):762.

Chenamgere, G. K., Maiya, A. G., Manjunath Hande, H., Kadavigere, V., Vidhyasagar, S., et al. (2015). Analysis of gait characteristics using a dynamic foot scanner in type 2 diabetes mellitus without peripheral neuropathy. *Journal of Exercise Science and Physiotherapy*, 11(1):58.

Colombo, G., Joerg, M., Schreier, R., Dietz, V., et al. (2000). Treadmill training of paraplegic patients using a robotic orthosis. *Journal of rehabilitation research and development*, 37(6):693–700.

Dassault Systèmes SolidWorks (2016). Solidworks standard. `http://www.solidworks.co.uk/sw/products/3d-cad/solidworks-standard.htm`. [Online; accessed 19-July-2016].

Design Simulation Technologies (2016). Simwise 4d integrated motion, stress analysis and optimization. msc software corporation. https://www.designsimulation.com/documents/simwise/simwisebrochure.pdf. [Online; Accessed 01 Aug 2016].

Díaz, I., Gil, J. J., and Sánchez, E. (2011). Lower-limb robotic rehabilitation: literature review and challenges. *Journal of Robotics*, 2011.

Donnan, G. A., Fisher, M., Macleod, M., and Davis, S. M. (2008). Stroke. *The Lancet*, 371(9624):1612 – 1623.

Drake, R. (2009). Vogl w. *Gray's Anatomy for Students*.

Engelbrecht, A. P. (2007). *Computational intelligence: an introduction*. John Wiley & Sons.

Esquenazi, A., Talaty, M., Packel, A., and Saulino, M. (2012). The rewalk powered exoskeleton to restore ambulatory function to individuals with thoracic-level motor-complete spinal cord injury. *American journal of physical medicine & rehabilitation*, 91(11):911–921.

Farris, R. J., Quintero, H. A., Murray, S. A., Ha, K. H., Hartigan, C., and Goldfarb, M. (2014). A preliminary assessment of legged mobility provided by a lower limb exoskeleton for persons with paraplegia. *IEEE Transactions on neural systems and rehabilitation engineering*, 22(3):482–490.

Fineberg, D. B., Asselin, P., Harel, N. Y., Agranova-Breyter, I., Kornfeld, S. D., Bauman, W. A., and Spungen, A. M. (2013). Vertical ground reaction force-based analysis of powered exoskeleton-assisted walking in persons with motor-complete paraplegia. *The journal of spinal cord medicine*, 36(4):313–321.

Garcia, P. A., Dias, J., Dias, R. C., Santos, P., and Zampa, C. C. (2011). A study on the relationship between muscle function, functional mobility and level of physical activity in community-dwelling elderly. *Brazilian Journal of Physical Therapy*, 15(1):15–22.

Goffer, A. (2006). Gait-locomotor apparatus. US Patent 7,153,242.

Grimaldi, G. and Manto, M. (2010). Neurological tremor: Sensors, signal processing and emerging applications. *Sensors*, 10(2):1399–1422.

Hageman, P. A. and Blanke, D. J. (1986). Comparison of gait of young women and elderly women. *Physical therapy*, 66(9):1382–1387.

He, H. and Kiguchi, K. (2007). A study on emg-based control of exoskeleton robots for human lower-limb motion assist. In *Information Technology Applications in Biomedicine, 2007. ITAB 2007. 6th International Special Topic Conference on*, pages 292–295. IEEE.

Hong, Y. W., King, Y., Yeo, W., Ting, C., Chuah, Y., Lee, J., and Chok, E.-T. (2013). Lower extremity exoskeleton: review and challenges surrounding the technology and its role in rehabilitation of lower limbs. *Australian J Basic Appl Sci*, 7(7):520–4.

Huo, W., Mohammed, S., Moreno, J. C., and Amirat, Y. (2014). Lower limb wearable robots for assistance and rehabilitation: A state of the art.

Ikehara, T., Nagamura, K., Ushida, T., Tanaka, E., Saegusa, S., Kojima, S., and Yuge, L. (2011). Development of closed-fitting-type walking assistance device for legs and evaluation of muscle activity. In *Rehabilitation Robotics (ICORR), 2011 IEEE International Conference on*, pages 1–7. IEEE.

Ikehara, T., Tanaka, E., Nagamura, K., Tamiya, T., Ushida, T., Hashimoto, K., Kojima, S., Ikejo, K., and Yuge, L. (2010). Development of closed-fitting-type walking assistance device for legs with self-contained control system. *Journal of Robotics and Mechatronics*, 22(3):380.

Jansen, E. C., Vittas, D., Hellberg, S., and Hansen, J. (1982). Normal gait of young and old men and women: ground reaction force measurement on a treadmill. *Acta orthopaedica Scandinavica*, 53(2):193–196.

Jezernik, S., Colombo, G., Keller, T., Frueh, H., and Morari, M. (2003). Robotic orthosis lokomat: a rehabilitation and research tool. *Neuromodulation: Technology at the neural interface*, 6(2):108–115.

Kasdirin, H. (2016). *Adaptive bio-inspired firefly and invasive weed algorithms for global optimisation with application to engineering problems*. PhD thesis, University of Sheffield.

Kawamoto, H., Lee, S., Kanbe, S., and Sankai, Y. (2003). Power assist method for hal-3 using emg-based feedback controller. In *Systems, Man and Cybernetics, 2003. IEEE International Conference on*, volume 2, pages 1648–1653. IEEE.

Kawamoto, H. and Sankai, Y. (2002). Power assist system hal-3 for gait disorder person. *Computers helping people with special needs*, pages 19–29.

Kawamura, T., Takanaka, K., Nakamura, T., and Osumi, H. (2013). Development of an orthosis for walking assistance using pneumatic artificial muscle: A quantitative assessment of the effect of assistance. In *Rehabilitation Robotics (ICORR), 2013 IEEE International Conference on*, pages 1–6. IEEE.

Kazerooni, H. (2008). Exoskeletons for human performance augmentation. In *Springer handbook of robotics*, pages 773–793. Springer.

Kazerooni, H., Racine, J.-L., Huang, L., and Steger, R. (2005). On the control of the berkeley lower extremity exoskeleton (bleex). In *Robotics and automation, 2005. ICRA 2005. Proceedings of the 2005 IEEE international conference on*, pages 4353–4360. IEEE.

Kazerooni, H., Steger, R., and Huang, L. (2006). Hybrid control of the berkeley lower extremity exoskeleton (bleex). *The International Journal of Robotics Research*, 25(5-6):561–573.

Kilicarslan, A., Prasad, S., Grossman, R. G., and Contreras-Vidal, J. L. (2013). High accuracy decoding of user intentions using eeg to control a lower-body exoskeleton. In *Engineering in medicine and biology society (EMBC), 2013 35th annual international conference of the IEEE*, pages 5606–5609. IEEE.

Kim, W., Lee, H., Kim, D., Han, J., and Han, C. (2014). Mechanical design of the hanyang exoskeleton assistive robot (hexar). In *Control, Automation and Systems (ICCAS), 2014 14th International Conference on*, pages 479–484. IEEE.

Kirtley, C. (2006). *Clinical gait analysis: theory and practice*. Elsevier Health Sciences.

Kong, K. and Jeon, D. (2006). Design and control of an exoskeleton for the elderly and patients. *Mechatronics, IEEE/ASME Transactions on*, 11(4):428–432.

Kopp, C. (2011). Exoskeletons for warriors of the future. *Defence Today*, 9(2):38–40.

Kovacic, Z. and Bogdan, S. (2005). *Fuzzy controller design: theory and applications*, volume 19. CRC press.

Kralj, A. R. and Bajd, T. (1989). *Functional electrical stimulation: standing and walking after spinal cord injury*. CRC press.

Kwak, N.-S., Müller, K.-R., and Lee, S.-W. (2015). A lower limb exoskeleton control system based on steady state visual evoked potentials. *Journal of neural engineering*, 12(5):056009.

Li, N., Yan, L., Qian, H., Wu, H., Wu, J., and Men, S. (2015). Review on lower extremity exoskeleton robot. *The Open Automation and Control Systems Journal*, 7(1).

Lilley, J., Arie, T., and Chilvers, C. (1995). Accidents involving older people: a review of the literature. *Age and Ageing*, 24(4):346–365.

Litwic, A., Edwards, M. H., Dennison, E. M., and Cooper, C. (2013). Epidemiology and burden of osteoarthritis. *British medical bulletin*, page lds038.

Lord, S. R., Sherrington, C., Menz, H. B., and Close, J. C. (2007). *Falls in older people: risk factors and strategies for prevention*. Cambridge University Press.

Low, K. (2011). Robot-assisted gait rehabilitation: From exoskeletons to gait systems. In *Defense Science Research Conference and Expo (DSR), 2011*, pages 1–10. IEEE.

Low, K. H. and Yin, Y. (2006). Providing assistance to knee in the design of a portable active orthotic device. In *2006 IEEE International Conference on Automation Science and Engineering*, pages 188–193. IEEE.

Malone, A., Meldrum, D., and Bolger, C. (2012). Gait impairment in cervical spondylotic myelopathy: comparison with age-and gender-matched healthy controls. *European spine journal*, 21(12):2456–2466.

Mehrabian, A. R. and Lucas, C. (2006). A novel numerical optimization algorithm inspired from weed colonization. *Ecological informatics*, 1(4):355–366.

Meng, W., Liu, Q., Zhou, Z., Ai, Q., Sheng, B., and Xie, S. S. (2015). Recent development of mechanisms and control strategies for robot-assisted lower limb rehabilitation. *Mechatronics*, 31:132–145.

Morris, M. E. (2000). Movement disorders in people with parkinson disease: a model for physical therapy. *Physical therapy*, 80(6):578–597.

Moylan, K. C. and Binder, E. F. (2007). Falls in older adults: risk assessment, management and prevention. *The American journal of medicine*, 120(6):493–e1.

Nations, U. (2013). World population ageing 2013. *Department of Economic and Social Affairs PD*.

Nikoofard, A. H., Hajimirsadeghi, H., Rahimi-Kian, A., and Lucas, C. (2012). Multiobjective invasive weed optimization: Application to analysis of pareto improvement models in electricity markets. *Applied Soft Computing*, 12(1):100–112.

Nuzik, S., Lamb, R., VanSant, A., and Hirt, S. (1986). Sit-to-stand movement pattern: a kinematic study. *Physical Therapy*, 66(11):1708–1713.

Ogata, K. (2010). Pid controllers and modified pid controllers. *Modern Control Engineering*, 5:567–641.

Oliver Jones (2014). The hip joint. `http://teachmeanatomy.info/lower-limb/joints/hip-joint/`. [Online; Accessed 01 Aug 2014].

Olivier, J. (2016). *Development of Walk Assistive Orthoses for Elderly*. PhD thesis, ÉCOLE POLYTECHNIQUE FÉDÉRALE DE LAUSANNE.

Onen, U., Botsali, F. M., Kalyoncu, M., Tinkir, M., Yilmaz, N., and Sahin, Y. (2014). Design and actuator selection of a lower extremity exoskeleton. *Mechatronics, IEEE/ASME Transactions on*, 19(2):623–632.

Passino, K. M., Yurkovich, S., and Reinfrank, M. (1998). *Fuzzy control*, volume 2725. Citeseer.

Pijnappels, M., Bobbert, M. F., and van Dieën, J. H. (2005). Push-off reactions in recovery after tripping discriminate young subjects, older non-fallers and older fallers. *Gait & posture*, 21(4):388–394.

Pons, J. L. (2008). *Wearable robots: biomechatronic exoskeletons*. John Wiley & Sons.

Pratt, J. E., Krupp, B. T., Morse, C. J., and Collins, S. H. (2004). The roboknee: an exoskeleton for enhancing strength and endurance during walking. In *Robotics and Automation, 2004. Proceedings. ICRA'04. 2004 IEEE International Conference on*, volume 3, pages 2430–2435. IEEE.

Prince, F., Corriveau, H., Hébert, R., and Winter, D. A. (1997). Gait in the elderly. *Gait & Posture*, 5(2):128–135.

Raychoudhury, S., Hu, D., and Ren, L. (2014). Three-dimensional kinematics of the human metatarsophalangeal joint during level walking. *Frontiers in bioengineering and biotechnology*, 2.

Richardson, J. K., Thies, S. B., DeMott, T. K., and Ashton-Miller, J. A. (2004). A comparison of gait characteristics between older women with and without peripheral neuropathy in standard and challenging environments. *Journal of the American Geriatrics Society*, 52(9):1532–1537.

Riener, R., Lunenburger, L., Jezernik, S., Anderschitz, M., Colombo, G., and Dietz, V. (2005). Patient-cooperative strategies for robot-aided treadmill training: first experimental results. *IEEE transactions on neural systems and rehabilitation engineering*, 13(3):380–394.

Salzman, B. (2010). Gait and balance disorders in older adults. *Am Fam Physician*, 82(1):61–68.

Sankai, Y. (2010). Hal: Hybrid assistive limb based on cybernics. In *Robotics Research*, pages 25–34. Springer.

Schenkman, M., Berger, R. A., Riley, P. O., Mann, R. W., and Hodge, W. A. (1990). Whole-body movements during rising to standing from sitting. *Physical Therapy*, 70(10):638–648.

Schultz, A. B. (1995). Muscle function and mobility biomechanics in the elderly: an overview of some recent research. *The journals of gerontology. Series A, Biological sciences and medical sciences*, 50 Spec No:60–3.

Sims, N. R. and Muyderman, H. (2010). Mitochondria, oxidative metabolism and cell death in stroke. *Biochimica et Biophysica Acta (BBA)-Molecular Basis of Disease*, 1802(1):80–91.

Slavnic, S., Ristic-Durrant, D., Tschakarow, R., Brendel, T., Tuttemann, M., Leu, A., and Graser, A. (2014). Mobile robotic gait rehabilitation system corbys-overview and first results on orthosis actuation. In *Intelligent Robots and Systems (IROS 2014), 2014 IEEE/RSJ International Conference on*, pages 2087–2094. IEEE.

Stauffer, Y., Allemand, Y., Bouri, M., Fournier, J., Clavel, R., Metrailler, P., Brodard, R., and Reynard, F. (2009). The walktrainer—a new generation of walking reeducation device combining orthoses and muscle stimulation. *Neural Systems and Rehabilitation Engineering, IEEE Transactions on*, 17(1):38–45.

Stolze, H., Klebe, S., Baecker, C., Zechlin, C., Friege, L., Pohle, S., and Deuschl, G. (2005). Prevalence of gait disorders in hospitalized neurological patients. *Movement Disorders*, 20(1):89–94.

Sudarsky, L. (1990). Gait disorders in the elderly. *New England Journal of Medicine*, 322(20):1441–1446.

Sung, S. W., Lee, J., and Lee, I.-B. (2009). *Process identification and PID control*. John Wiley & Sons.

Tamura, K. and Yasuda, K. (2011a). Primary study of spiral dynamics inspired optimization. *IEEJ Transactions on Electrical and Electronic Engineering*, 6(S1):S98–S100.

Tamura, K. and Yasuda, K. (2011b). Spiral dynamics inspired optimization. *JACIII*, 15(8):1116–1122.

Tsukahara, A., Kawanishi, R., Hasegawa, Y., and Sankai, Y. (2010). Sit-to-stand and stand-to-sit transfer support for complete paraplegic patients with robot suit hal. *Advanced robotics*, 24(11):1615–1638.

Tucker, M. R., Olivier, J., Pagel, A., Bleuler, H., Bouri, M., Lambercy, O., del R Millán, J., Riener, R., Vallery, H., and Gassert, R. (2015). Control strategies for active lower extremity prosthetics and orthotics: a review. *Journal of neuroengineering and rehabilitation*, 12(1):1.

Vandervoort, A. A. (2002). Aging of the human neuromuscular system. *Muscle & nerve*, 25(1):17–25.

Vaughan, C. L., Davis, B. L., and O'connor, J. C. (1992). *Dynamics of human gait*, volume 2. Human Kinetics Publishers Champaign, Illinois.

Veneman, J., Ekkelenkamp, R., Kruidhof, R., Van Der Helm, F., and Van der Kooij, H. (2005). Design of a series elastic-and bowden cable-based actuation system for use as torque-actuator in exoskeleton-type training. In *Rehabilitation Robotics, 2005. ICORR 2005. 9th International Conference on*, pages 496–499. IEEE.

Veneman, J. F., Kruidhof, R., Hekman, E. E., Ekkelenkamp, R., Van Asseldonk, E. H., and Van Der Kooij, H. (2007). Design and evaluation of the lopes exoskeleton robot for interactive gait rehabilitation. *IEEE Transactions on Neural Systems and Rehabilitation Engineering*, 15(3):379–386.

Virk, G. S., Haider, U., Indrawibawa, I. N., THEKKEPARAMPUMADOM, R. K., and Masud, N. (2014). Exo-legs for elderly persons. In *17th International Conference on Climbing and Walking Robots (CLAWAR), JUL 21-23, 2014, Poznan, POLAND*, pages 85–92. World Scientific.

Viteckova, S., Kutilek, P., and Jirina, M. (2013). Wearable lower limb robotics: A review. *Biocybernetics and Biomedical Engineering*, 33(2):96–105.

Walsh, C. J. (2006). *Biomimetic design of an under-actuated leg exoskeleton for load-carrying augmentation*. PhD thesis, Massachusetts Institute of Technology.

Wang, L.-X. (1993). Stable adaptive fuzzy control of nonlinear systems. *Fuzzy Systems, IEEE Transactions on*, 1(2):146–155.

Wang, L.-X. (1997). A course in fuzzy systems and control, prentice-hall ptr. *Englewood Cliffs, NJ*.

Wang, P., Low, K., and McGregor, A. (2011a). A subject-based motion generation model with adjustable walking pattern for a gait robotic trainer: Nature-gaits. In *Intelligent Robots and Systems (IROS), 2011 IEEE/RSJ International Conference on*, pages 1743–1748. IEEE.

Wang, P., Low, K., Tow, A., and Lim, P. (2011b). Initial system evaluation of an overground rehabilitation gait training robot (nature-gaits). *Advanced Robotics*, 25(15):1927–1948.

Winfree, K. N., Stegall, P., and Agrawal, S. K. (2011). Design of a minimally constraining, passively supported gait training exoskeleton: Alex ii. In *Rehabilitation Robotics (ICORR), 2011 IEEE International Conference on*, pages 1–6. IEEE.

Winter, D. A. (2009). *Biomechanics and motor control of human movement*. John Wiley & Sons.

Yamamoto, K., Ishii, M., Hyodo, K., Yoshimitsu, T., and Matsuo, T. (2003). Development of power assisting suit. *JSME International Journal Series C Mechanical Systems, Machine Elements and Manufacturing*, 46(3):923–930.

Yan, T., Cempini, M., Oddo, C. M., and Vitiello, N. (2015). Review of assistive strategies in powered lower-limb orthoses and exoskeletons. *Robotics and Autonomous Systems*, 64:120–136.

Yang, J., Wang, J., and Wang, L. (2010). Self-tuning-parameter fuzzy pid control in fresh air system. In *Intelligent Control and Information Processing (ICICIP), 2010 International Conference on*, pages 566–569. IEEE.

Yılmaz, S. and Küçüksille, E. U. (2015). A new modification approach on bat algorithm for solving optimization problems. *Applied Soft Computing*, 28:259–275.

Ying, H. (2000). *Fuzzy control and modeling: analytical foundations and applications*. Wiley-IEEE Press.

Young, A. and Ferris, D. (2016). State-of-the-art and future directions for robotic lower limb exoskeletons.

Zadeh, L. A. (1965). Fuzzy sets. *Information and control*, 8(3):338–353.

Zadeh, L. A. (1988). Fuzzy logic. *Computer*, 21(4):83–93.

Zaharis, Z. D., Skeberis, C., Xenos, T. D., Lazaridis, P. I., and Cosmas, J. (2013). Design of a novel antenna array beamformer using neural networks trained by modified adaptive dispersion invasive weed optimization based data. *Broadcasting, IEEE Transactions on*, 59(3):455–460.

Zang, H., Zhang, S., and Hapeshi, K. (2010). A review of nature-inspired algorithms. *Journal of Bionic Engineering*, 7:S232–S237.

Zeilig, G., Weingarden, H., Zwecker, M., Dudkiewicz, I., Bloch, A., and Esquenazi, A. (2012). Safety and tolerance of the rewalk™ exoskeleton suit for ambulation by people with complete spinal cord injury: A pilot study. *The journal of spinal cord medicine*, 35(2):96–101.

Zeni, J. A. and Higginson, J. S. (2009). Differences in gait parameters between healthy subjects and persons with moderate and severe knee osteoarthritis: a result of altered walking speed? *Clinical Biomechanics*, 24(4):372–378.

Zhao, Y. and Pan, Y. (2010). The design and simulation of fuzzy pid controller. In *Information Technology and Applications (IFITA), 2010 International Forum on*, volume 3, pages 95–98. IEEE.

Zhiqiang, L., Hanxing, X., Weilin, L., and Zheng, Y. (2014). Proceeding of human exoskeleton technology and discussions on future research. *Chinese Journal of Mechanical Engineering*, 27(03):1.